

Electronic Thesis and Dissertation Repository

10-15-2020 10:00 AM

Investigating Cognitive Impairment in TDP-43 Mouse Models of FTD-ALS Using Automated Touchscreens

Keon Coleman, *The University of Western Ontario*

Supervisor: Bussey, Timothy J., *The University of Western Ontario*

A thesis submitted in partial fulfillment of the requirements for the Master of Science degree in Neuroscience

© Keon Coleman 2020

Follow this and additional works at: <https://ir.lib.uwo.ca/etd>



Part of the [Behavioral Neurobiology Commons](#), and the [Cognitive Neuroscience Commons](#)

Recommended Citation

Coleman, Keon, "Investigating Cognitive Impairment in TDP-43 Mouse Models of FTD-ALS Using Automated Touchscreens" (2020). *Electronic Thesis and Dissertation Repository*. 7430.
<https://ir.lib.uwo.ca/etd/7430>

This Dissertation/Thesis is brought to you for free and open access by Scholarship@Western. It has been accepted for inclusion in Electronic Thesis and Dissertation Repository by an authorized administrator of Scholarship@Western. For more information, please contact wlsadmin@uwo.ca.

Abstract

TAR-DNA-binding protein 43 (TDP-43) misfolding and aggregation is a major pathological hallmark of frontotemporal dementia-amyotrophic lateral sclerosis (FTD/ALS). FTD/ALS is characterized by motor and cognitive impairment, with cognitive impairment frequently reported before the onset of classical motor symptoms. Yet, treatment for cognitive decline in FTD/ALS is lacking, and robust cognitive phenotypes related to TDP-43 proteinopathy have not been established for most mouse models of FTD/ALS. Herein, we used automated touchscreen technology to assess executive function (affected in FTD/ALS) in male TDP-43^{Q331Klow} and ^{-G348C} FTD/ALS transgenic mice. The touchscreen pairwise visual discrimination task revealed impairments in 4-5-month-old TDP-43^{Q331Klow} and ^{-G348C} mutants during acquisition and reversal phases. These cognitive impairments manifested prior to motor symptoms. This pattern of results is highly similar to observations in human FTD/ALS. Together, these findings identify the combination of TDP-43 mouse models and touchscreen tests as potentially useful tools for understanding and developing cognitive therapies in FTD/ALS.

Keywords:

TDP-43, ALS, FTD, BPSD, touchscreen, cognition, mouse, executive function, neurodegenerative disease

Summary for Laypersons

Amyotrophic lateral sclerosis (ALS) and fronto-temporal dementia (FTD) are interconnected and incurable progressive neurodegenerative diseases. ALS is characterized by brain and spinal cord neuronal death leading to loss of control over voluntary movement, consistently resulting in paralysis. Eventually, respiratory failure ensues from involuntary muscles becoming affected (e.g., diaphragm), with patients succumbing to the disease within 3-5 years. Those afflicted by FTD experience cognitive dysfunction (e.g., attention and memory), which negatively impacts their personality and social and professional behaviours. The cause of FTD is unknown; however, in 45% of cases functional alterations of a protein called TDP-43 is detected during autopsies. Intriguingly, aggregated TDP-43 is detected in 95% of ALS cases, irrespective of mutations related to ALS. Furthermore, ALS symptoms (e.g., motor impairments) are detected in FTD (~15%), and FTD symptoms (e.g., cognitive impairments), are frequently detected in ALS (~60-70%). Moreover, cognitive impairment is often reported before detection of motor dysfunction symptoms in ALS. Replicating key human FTD/ALS features in TDP-43 mouse models is essential for understanding and developing treatments for FTD/ALS. We explored whether we could detect cognitive alterations and/or motor impairments caused by the insertion of human TDP-43 protein into mice. We utilized a touchscreen system adapted for mice, which allows us to assess cognition in mice in the same way as in humans, facilitating cross-species comparisons. During testing we observed FTD/ALS-like cognitive deficits in TDP-43 mutant mice, consistent with cognitive deficits prominent in human FTD/ALS. Furthermore, the cognitive deficits observed in TDP-43 mutant mice manifested before the onset of any motor impairments related to FTD/ALS. Together these findings suggest that the TDP-43 mutant mice are able to recapitulate some key features of human FTD/ALS, showing that such models may be very useful for the development of cognitive therapies and drug treatments for human FTD/ALS.

Co-Authorship Statement

I was the primary contributor for all conducted experiments included in my thesis, and manuscript preparation. All statistical analyses prepared for this manuscript were personally conducted by me. All attempts have been made to ensure proper referencing for findings, ideas and concepts that are not my own. In very limited instances I did receive assistance with experiments. These contributions came from:

- Roseanne Franco: Performed peak grip force analysis with a single TDP-43^{Q331K}low cohort.
- Chris Fodor: Assisted with running a TDP-43^{G348C} cohort for two days (May 22-24th, 2019).
- Matt Cowan: Assisted with running TDP-43^{G348C} and TDP-43^{Q331K} cohorts for a single day on two separate occasions (January 13th, 2020, and February 22nd, 2020).

Acknowledgements

I would like to thank Dr. Tim Bussey and Dr. Flavio Beraldo for giving me an opportunity to challenge myself in new ways and learn so much during my time under your supervision. Furthermore, for always allowing me to be myself without worry or concern. I would also like to give a special thank you to Drs. Marco Prado and Vania Prado for always answering any questions I may have raised, and encouraging me to attend the Prado lab meetings. Truly, I am grateful to all of you.

Additionally, I would like to thank all of the Translational Cognitive Neuroscience Lab, the entire Rodent Cognition Core and all of the Prado Lab. I would like to extend a special thanks Dr. Sara Memar for always being willing discuss any issues I had working with the R-script and PR rate analysis, there was a lot! I also want to extend a big thanks to Matt Cowan, Chris Fodor and Mei-Peng Lim for always lightening the mood in the behaviour facility.

Finally, I would like to extend a special thank you to Dr. Jean-Pierre Julien from Laval University for graciously providing the TDP-43^{G348C} mouse line used in this project.

Table of Contents

Abstract.....	<i>i</i>
Summary for Laypersons.....	<i>ii</i>
Co-Authorship Statement.....	<i>iii</i>
Acknowledgements.....	<i>iv</i>
Table of Contents	<i>v</i>
List of Abbreviations	<i>xv</i>
1. Introduction.....	<i>1</i>
1.1 General Introduction.....	<i>1</i>
1.2 Amyotrophic Lateral Sclerosis	<i>2</i>
1.3 Fronto-Temporal Dementia and Fronto-Temporal Lobar Degeneration.....	<i>4</i>
1.4 FTD and FTLD Presentation Variations	<i>5</i>
1.5 FTD Clinical Identification	<i>7</i>
1.6 FTD/ALS Exist on a Single Spectrum	<i>8</i>
1.7 FTD/ALS Genetic Mutations.....	<i>9</i>
1.8 TDP-43 Proteinopathy	<i>11</i>
1.9 TDP-43 Propagation, Aggregation and Phase Transitions.....	<i>13</i>
1.10 Mutant TDP-43 Mouse Models.....	<i>16</i>
1.11 The TDP-43^{Q331Klow} Mouse Model of FTD/ALS.....	<i>17</i>
1.12 The G348C Mouse Model of FTD/ALS.....	<i>19</i>
1.13 Automated Touchscreens and Translation	<i>20</i>
1.14 Touchscreen Evaluation of Cognition in Mice	<i>21</i>
1.15.1 Pairwise Visual Discrimination (PVD) Task and reversa	<i>21</i>
1.15.2 Different Paired Associates Learning Task (dPAL).....	<i>22</i>
1.15.3 5 Choice Serial Reaction Time Task (5-CSRTT).....	<i>22</i>
1.15.4 Progressive Ratio Fixed Ratio Task (PRFR)	<i>23</i>
1.15 Investigation Objective.....	<i>23</i>
2. Materials and Methods.....	<i>24</i>

2.1 Q331K Low Mice	24
2.2 G348C Mice	25
2.3 Ethics	25
2.4 Housing, Food Restriction	25
2.5 Locomotion Apparatus.....	26
2.6 Grip Force Apparatus	26
2.7 Wire Hang Apparatus	27
2.8 Touchscreen Apparatus	27
2.9 Rodent Shaping.....	28
2.10 5-CSRTT Shaping	28
2.10.1 Stage 1:.....	28
2.10.2 Stage 2:.....	28
2.10.3 Stage 3:.....	29
2.10.4 Stage 4:.....	29
2.10.5 Stage 5:.....	30
2.10.6 Stage 6:.....	30
2.10.7 Stage 7:.....	30
2.11 5-CSRTT Training	31
2.11.1 Stage 8:.....	31
2.11.2 Stage 9:.....	32
2.12 5-CSRTT Probe Trials	32
2.13 Investigation Time Points	33
2.14 PRFR Shaping.....	33
2.15 PRFR Training.....	33
2.15.1 Stage 9a:.....	33
2.15.2 Stage 9b:.....	33
2.15.3 Stage 9c:.....	34
2.15.4 Stage 9d:.....	34
2.15.5 Stage 10:.....	34
2.15.6 Stage 11:.....	34
2.15.7 Stage 12:.....	34
2.15.8 Stage 13:.....	35
2.15.9 Stage 14:.....	35
2.15.10 Stage 15:.....	35
2.16 PVD Shaping.....	35
2.16.1 Stage 1:.....	35
2.16.2 Stage 2:.....	35
2.16.3 Stage 3:.....	35
2.16.4 Stage 4:.....	35
2.16.5 Stage 5:.....	35
2.16.6 Stage 6:.....	36
2.16.7 Stage 7:.....	36
2.17 PVD Training.....	36

2.17.1 Stage 9:.....	37
2.17.2 Stage 10:.....	37
2.18 dPAL Shaping.....	37
2.19 dPAL Training.....	37
2.19.1 Stage 8:.....	37
2.19.2 Stage 9:.....	38
2.20 Primary Touchscreen Parameters.....	38
2.21 Cohorts and Behavioural Testing Schedule.....	39
2.22 Statistical Analyses.....	40
3. Results.....	40
3.1 Motor Performance Battery: TDP-43^{Q331Klow} Mice.....	40
3.2 Motor Performance Battery: TDP-43^{G348C} Mice.....	43
3.3 PVD Task Learning and Cognitive Flexibility in 4-month-old TDP-43^{Q331Klow}.....	45
3.4. 4-month-old TDP-43^{G348C} Learning and Cognitive Flexibility in the PVD Task.....	47
3.5 dPAL Visuospatial Memory Performance of 8-month-old TDP-43^{Q331Klow}.....	50
3.6 dPAL Visuospatial Memory Performance of 8-month-old TDP-43^{G348C}.....	51
3.7 5-CSRTT Probe of Attention Performance in 4-month-old TDP-43^{Q331Klow}.....	53
3.8 5-CSRTT Probe of Attention Performance in 8-month-old TDP-43^{Q331Klow}.....	56
3.9 5-CSRTT Probe of Attention Performance in 4-month-old TDP-43^{G348C}.....	59
3.10 5-CSRTT Probe of Attention Performance in 8-month-old TDP-43^{G348C}.....	62
3.11 11-month-old TDP-43^{Q331Klow} Probe of Motivation Performance in PRFR.....	65
3.12 11-month-old TDP-43^{G348C} Probe of Motivation Performance in PRFR.....	69
4. Discussion.....	73
4.1 Age-Dependent Motor Performance Deficits in TDP-43 Mutant Mice.....	74
4.2 5-CSRTT Reveals Possible BPSD-like Behaviours in TDP-43 Mutant Mice.....	75
4.3 Limited Evidence For Motivational impairments in TDP-43^{Q331Klow} and TDP-43^{G348C} mutant mice.....	76
4.4 Evidence of Cognitive Flexibility Deficits in TDP-43 Mutant Mice.....	77
4.5 TDP-43 Mutant Mice Do Not Exhibit Any Apparent Deficits in the dPAL Task.....	78
4.6 Investigation Limitations.....	79
4.7 Future Directions – Can Cognitive Deficits be Linked to Specific Pathological TDP-43 Events?.....	80
4.8 Final Conclusions.....	81

References83

Curriculum Vitae 101

List of Figures

Figure 1. Flow chart of general shaping schedule prior to task specific training.	31
Figure 2. Experimental design outlining the sequence of behavioural testing in TDP-43 ^{Q331Klow} and TDP-43 ^{G348C} mutant mice.....	40
Figure 3. TDP-43 ^{Q331Klow} mutant mice 4-month and 8-month peak grip force performance. At 4-months no significant differences in peak grip force were observed. At 8-months TDP-43 ^{Q331Klow} mutants had lower peak grip force strength compared to controls (het n=27, wt n=18, **p<0.01).....	41
Figure 4. TDP-43 ^{Q331Klow} mutant mice 4-month and 8-month wire hang performance. No significant differences were observed at 4- or 8-months (het n=27, wt n=18).	42
Figure 5. TDP-43 ^{Q331Klow} mutant mice 4-month and 8-month locomotor behaviour.	42
Figure 6. TDP-43 ^{G348C} mutant mice 4-month and 8-month peak grip force performance. At 4-months no significant differences in peak grip force were observed. At 8-months TDP-43 ^{G348C} mutants had lower peak grip force strength compared to controls (het n=22, wt n=15, data are mean ± SEM, *p<0.05).	43
Figure 7. TDP-43 ^{G348C} mutant mice 4-month and 8-month wire hang performance. No significant differences were observed at 4- or 8-months (het n=22, wt n=15).	44
Figure 8. TDP-43 ^{G348C} mutant mice 4-month and 8-month locomotor behaviour. No significant differences were observed at 4- or 8-months. Mean locomotion in 5-minute intervals over a sustained 60-minute testing period (het n=22, wt n=15).	45
Figure 9. TDP-43 ^{Q331Klow} mutant mice 4-months, PVD task acquisition (A; learning), reversal learning performance (B), and correction trials (C).TDP-43 ^{Q331Klow} mutants required significantly more sessions to acquire the task, had significantly lower accuracy during reversal learning, and	

required significantly more correction trials (het n=12, wt n=9, data are mean \pm SEM, *p<0.05, **p<0.01)..... 46

Figure 10. 4-month-old TDP-43^{Q331Klow} mutant mice latency data. Reward collection latency (A), correct touch latency (B) and incorrect touch latency (C). TDP-43^{Q331Klow} mutants required marginally more time to collect reward, significantly more time to initiate correct responses and significantly more time to emit incorrect responses (het n=12, wt n=9, data are mean \pm SEM, *p<0.05, **p<0.01)..... 47

Figure 11. TDP-43^{G348C} mutant mice 4-month, PVD task acquisition (A; learning) and reversal learning performance (B) and correction trials (C). It was found that TDP-43^{G348C} mutants required significantly more sessions to acquire the task, had significantly lower accuracy during reversal learning and exhibited a highly similar number of required correction trials (het n=14, wt n=11, data are mean \pm SEM, *p<0.05, **p<0.01)..... 48

Figure 12. TDP-43^{G348C} mutant mice 4-month PVD task reward collection latency (A), correct touch latency (B) and incorrect touch latency (C). No significant differences were observed in reward collection latencies, correct touch latencies and incorrect touch latencies (het n=14, wt n=11, data are mean \pm SEM, *p<0.05). 49

Figure 13. Combined PVD task data from TDP-43^{Q331Klow} and TDP-43^{G348C} mutant mice (Figures 9A-B; 14A-B). TDP-43^{Q331Klow} and TDP-43^{G348C} mutants display a similar pattern of deficits during task acquisition and during the reversal learning phase. 49

Figure 14. TDP-43^{Q331Klow} mutant mice 8-month PAL task accuracy (A), reward collection latency (B), correct touch latency (C) and incorrect touch latency (D). No significant differences were observed in any of the dPAL measures (het n=12, wt n=9)..... 51

Figure 15. TDP-43^{G348C} mutant mice 8-month PAL task accuracy (A), reward collection latency (B), correct touch latency (C) and incorrect touch latency (D). No significant differences were observed among dPAL measures (het n=14, wt n=11)..... 52

Figure 16. TDP-43^{Q331Klow} mutant mice 4-month 5-CSRTT trials to acquisition 4- and 2-seconds. No significant differences were observed (het n=15, wt n=9)..... 53

Figure 17. TDP-43^{Q331Klow} mutant mice 4-month 5-CSRTT accuracy (A) and omission (B). It was found that TDP-43^{Q331Klow} mutants exhibited significantly higher accuracy and omissions in comparison to controls (het n=15, wt n=9, data are mean ± SEM, *<p=0.05, **<p=0.01). 54

Figure 18. TDP-43^{Q331Klow} mutant mice 4-month 5-CSRTT reward collection latency (A) correct touch latency (B) and incorrect touch latency (C) No significant differences were observed (het n=15, wt n=9)..... 55

Figure 19. TDP-43^{Q331Klow} mutant mice 4-month 5-CSRTT premature responses (A), perseverative post-correct responses (B) and perseverative post-incorrect responses (C) No significant differences were observed among measures (het n=15, wt n=9, data are mean ± SEM, *<p=0.05)..... 56

Figure 20. TDP-43^{Q331Klow} mutant mice 8-month 5-CSRTT accuracy (A) and omissions (B). It was found that TDP-43^{Q331Klow} mutants exhibited significantly higher accuracy in comparison to controls. Additionally, significantly higher omissions when compared to controls (het n=15, wt n=9, data are mean ± SEM, *<p=0.05, **<p=0.01). 57

Figure 21. TDP-43^{Q331Klow} mutant mice 8-month 5-CSRTT reward collection latency. No significant differences were observed (het n=15, wt n=9)..... 58

Figure 22. TDP-43^{Q331Klow} mutant mice 8-month 5-CSRTT premature responses (A), perseverative post-correct responses (B) and perseverative post-incorrect (C). No significant differences were observed (het n=15, wt n=9)..... 59

Figure 23. TDP-43G348C mutant mice 4-month 5-CSRTT trials to acquisition 4- and 2-seconds. No significant differences were observed (het n=8, wt n=4)..... 59

Figure 24. TDP-43G348C mutant mice 4-month 5-CSRTT accuracy (A) and omissions (B). No significant differences were observed (het n=8, wt n=4)..... 60

Figure 25. TDP-43G348C mutant mice 4-month 5-CSRTT reward collection latency (A), correct touch latency (B) and incorrect touch latency (C). No significant differences were observed (het n=8, wt n=4)..... 61

Figure 26. TDP-43G348C mutant mice 4-month 5-CSRTT premature responses (A), perseverative post-correct responses (B) and perseverative post-incorrect responses (C). No significant differences were observed (het n=8, wt n=4)..... 62

Figure 27. TDP-43G348C mutant mice 8-month 5-CSRTT accuracy. No significant differences were observed (het n=8, wt n=4, data are mean ± SEM, * $p < 0.05$). 63

Figure 28. TDP-43G348C mutant mice 8-month 5-CSRTT reward collection latency (A) correct touch latency (B) and incorrect touch latency (C). No significant differences were observed for reward collection latency. Both correct touch- and incorrect touch latencies were significantly different from control (het n=8, wt n=4, data are mean ± SEM, * $p < 0.05$). 64

Figure 29. TDP-43G348C mutant mice 8-month 5-CSRTT premature responses (A), perseverative post-correct responses (B) and perseverative post-incorrect responses (C). No significant differences were observed (het n=8, wt n=4)..... 65

Figure 30. TDP-43Q331K^{low} mutant mice 11-month fixed-ratio breakpoint (A) and progressive-ratio breakpoint (B). No significant differences were observed (het n=13, wt n=9). 66

Figure 31. TDP-43Q331K^{low} mutant mice 11-month progressive- and fixed-ratio target touches. No significant differences were observed (het n=13, wt n=9). 66

Figure 32. TDP-43Q331K^{low} mutant mice 11-month progressive- and fixed-ratio trials completed. No significant differences were observed (het n=13, wt n=9). 67

Figure 33. TDP-43Q331K^{low} mutant mice 11-month progressive- and fixed-ratio reward collection latency. TDP-43Q331K^{low} mutants exhibited significantly longer delays to reward collection during fixed ratio testing (het n=13, wt n=9, data are mean ± SEM, * $p < 0.05$). 68

Figure 34. TDP-43Q331K^{low} mutant mice 11-month progressive-ratio post reinforcement pause. TDP-43Q331K^{low} mutants exhibited significantly shorter post reinforcement pause delays (het n=13, wt n=9, data are mean ± SEM, * $p < 0.05$). 69

Figure 35. TDP-43G348C mutant mice 11-month progressive-ratio breakpoint. No significant differences were observed (het n=8, wt n=4). 70

Figure 36. TDP-43G348C mutant mice 11-month progressive- and fixed-ratio target touches. No significant differences were observed (het n=8, wt n=4). 70

Figure 37. TDP-43G348C mutant mice 11-month progressive- and fixed-ratio trials completed. No significant differences were observed (het n=8, wt n=4). 71

Figure 38. TDP-43G348C mutant mice 11-month progressive- and fixed-ratio reward collection latency. No significant differences were observed (het n=8, wt n=4). 72

Figure 39. TDP-43G348C mutant mice 11-month progressive-ratio post reinforcement pause. No significant differences were observed from control (het n=13, wt n=9). 72

Figure 40. Overview of TDP-43Q331Klow and TDP-43G348C mutant mouse deficits across all evaluation time points. 73

List of Abbreviations

5-CSRTT – 5-Choice Serial Reaction Time Task

AD – Alzheimer’s Disease

Cry2 – Arabidopsis cryptochrome-2 (Cry2)

ALS – Amyotrophic Lateral Sclerosis

BPSD – Behavioural and Psychological Symptoms of Dementia

C9ORF72 – Chromosome 9 Open Reading Frame 72

dPAL – Different Paired Associates Learning

DNA – Deoxyribonucleic Acid

fALS – Familial ALS

FR – Fixed Ratio

FTD – Fronto-temporal Dementia

FTLD – Fronto-temporal Lobar Degeneration

FUS – Fused in Sarcoma

ITI – Inter-trial Interval

KI – Knock In

mRNA – Messenger Ribonucleic Acid

ntg – Non-transgenic

PD – Parkinson's Disease

PR – Progressive Ratio

PRFR – Progressive Ratio Fixed Ratio

PVD – Pairwise Visual Discrimination

RNA – Ribonucleic Acid

sALS – Sporadic ALS

SG – Stress Granule

SOD1 – Superoxide Dimutase 1

TARDBP – Trans-active Response Element DNA-binding protein 43 Gene

TDP-43 – Trans-active Response Element DNA-binding Protein 43

UBQLN2 – Ubiquilin-2

WT – Wildtype

1. Introduction

1.1 General Introduction

Amyotrophic lateral sclerosis (ALS), also commonly known as Lou Gehrig's disease, is a late-onset rapidly progressive and incurable neurodegenerative disease, which features deterioration of motor neurons of the nervous system (Gao et al., 2018; J. R. Mann et al., 2019). The degeneration of motor neurons leads to muscle denervation, muscle atrophy and an eventual inability to initiate voluntary movement (Gao et al., 2018; Ling et al., 2013). Intriguingly, ALS frequently presents with symptoms of fronto-temporal dementia (FTD), another neurodegenerative disease.

FTD is the second most prevalent form of dementia following Alzheimer's disease (AD; Young et al., 2018). FTD is a consequence of fronto-temporal lobar degeneration (FTLD), a specific pattern of cortical neurodegeneration with distinct molecular signatures (Gao et al., 2018; Heyburn & Moussa, 2017; Ling et al., 2013), which is a key neuropathological feature linking FTD and ALS (Arnold et al., 2013a; Gao et al., 2018; Harrison & Shorter, 2017). FTD with FTLD is accompanied by prominent behavioural and personality changes in addition to cognitive deficits (Harrison & Shorter, 2017; Heyburn & Moussa, 2017; Ling et al., 2013). Patients with ALS presenting with cognitive deficits experience significantly worsened disease progression, which hastens terminal endpoints (Elamin et al., 2011; Giordana et al., 2011). FTD-related cognitive dysfunction is present in ~60-70% of ALS cases. Moreover, ~15% of FTD cases are complicated by motor deficits which meet the criteria for an ALS diagnosis (Elamin et al., 2011; Giordana et al., 2011; Ling et al., 2013; Woolley & Strong, 2015).

The trans-active response element DNA-binding protein (*TARDBP*; gene) 43 (TDP-43) is one of the main proteins implicated in ALS (Heyburn & Moussa, 2017). Among TDP-43 proteinopathies, TDP-43 nuclear clearance, cytosolic aggregation, detergent-resistant aggregate formation and hyperphosphorylated and ubiquitinated forms are pathological hallmarks (Gao et al., 2018; Heyburn & Moussa, 2017; Ling et al., 2013). Causative or FTD/ALS-linked mutations in *TARDBP* can produce TDP-43 proteinopathy, and TDP-43 proteinopathy not linked to

mutations can result in FTD/ALS. Additionally, TDP-43 positive inclusions have been detected in ~45 percent of FTLD cases (Banks et al., 2008; Gao et al., 2018; Ling et al., 2013). In this study the cognitive alterations resulting from FTD/ALS-linked TDP-43^{Q331K} and TDP-43^{G348C} mutations will be investigated in transgenic mouse models of FTD/ALS.

1.2 Amyotrophic Lateral Sclerosis

ALS is a rapidly progressing neurodegenerative disease characterized by a variety of canonical biological alterations related to the degeneration of motor neurons. Specifically, the upper motor neurons which descend from the brain and innervate the spinal cord degenerate and the lower motor neurons and their axons innervating skeletal muscle degenerate as well (Banks et al., 2008; Gao et al., 2018; Heyburn & Moussa, 2017). The progressive degeneration of these neurons can manifest in two different varieties early in the ALS disease time course. ALS patients can be afflicted by spinal-onset ALS (~80% of cases) producing substantial loss of limb strength, or alternatively, a bulbar-onset ALS (~20% of cases) producing dysphagia (struggling to swallow) and dysarthria (struggling to speak; Hardiman, 2010). Regardless of which type of ALS manifests, the resultant neurodegeneration invariably causes paralysis and death within a period of 3 – 5 years following diagnosis (Banks et al., 2008; Gao et al., 2018).

ALS is the most common form of motor neuron disease (Heyburn & Moussa, 2017). The onset of ALS is often around age 55, and invariably results in paralysis and death, usually 3 – 5 years following diagnosis (Banks et al., 2008; Chen et al., 2013). Nonetheless, there is quite large amount of heterogeneity amongst ALS related symptoms, time of onset, and progression of the disease (Banks et al., 2008; Chen et al., 2013; Chiò et al., 2018; Hardiman, 2010). Globally, the incidence of ALS is approximately 2 new diagnoses of ALS for every 100,000 people each year (statistic is equivalent in Canada), and between 2500 – 3000 people age 18 and above are currently living with the disease in Canada (Chen et al., 2013). Sex differences have also frequently been observed, with males being at a higher risk of ALS. Reports indicate that the male to female ratio ranges between 1 and 2 (Longinetti & Fang, 2019). Some risk factors have also been established for ALS, namely, smoking, intense physical activity and diesel exhaust fume exposure (Longinetti & Fang, 2019).

ALS is predominantly sporadic with ~90% of cases lacking a familial link. The outstanding ~10% are familial ALS (fALS ; familial history of inherited ALS with a causative mutation) cases with inherited mutations causative for ALS (Chen et al., 2013). The most prevalent of these mutations is *C9ORF72* which represents ~40% of all fALS cases, followed by *SOD1* (~12%), *TARDBP* (~4-5%), and *FUS* (~4-5%; Chen et al., 2013; Heyburn & Moussa, 2017). The remaining proportion of cases are represented by *UBQLN2*, *sequestosome 1*, *optineurin*, *profilin 1*, *valosin-containing protein*, *senataxin* and potentially other yet to be identified genes (Chen et al., 2013; Heyburn & Moussa, 2017).

Indeed, a comprehensive understanding of the pathogenesis of ALS has not yet been established, despite the clinicopathological framework of ALS first being described in the mid 19th century and the first causative mutation being discovered in the early 1990s (Mathis et al., 2019). The multifaceted nature of ALS increases the difficulty in identifying the exact mechanism(s) producing degeneration (Gao et al., 2019), and several complementary mechanisms have been proposed. The misfolding and aggregation of various proteins (e.g., FUS, SOD1 & TDP-43, discussed below) within diseased neurons and glia is one such mechanism, and is thought to induce neurotoxicity and degeneration (Gao et al., 2018; Heyburn & Moussa, 2017; Ling et al., 2013). Glutamate toxicity is another potential mechanism of toxicity, which is suggested to play a role in ALS neurodegeneration (Heyburn & Moussa, 2017). TDP-43, one of the key proteins involved in pathological changes in ALS, processes the RNA of genes encoding synaptic proteins such as glutamate transporters and receptors (Giribaldi et al., 2013; Heyburn & Moussa, 2017). Specifically, excitatory amino acid transporter-2 has been shown to be downregulated in ALS, suggesting the possibility of reduced glutamate uptake in ALS, and an excess of glutamate in the extracellular space causing excitotoxicity (Heyburn & Moussa, 2017). Oxidative stress and reactive oxygen species are also mechanisms known to contribute to FTD/ALS neurodegeneration (Gao et al., 2018; Ling et al., 2013).

Interestingly, cognitive impairment has recently become recognized as an integral component in ALS pathology, with data supporting a strong correlation between ALS and cognitive disorders (Ferrari et al., 2011; Gao et al., 2018; Heyburn & Moussa, 2017). ALS patients frequently present with frontotemporal dysfunction leading to cognitive dysfunction afflicting roughly 60 –

70% of ALS patients, even in the absence of any genetic mutations related to FTD/ALS (Elamin et al., 2011; Olney et al., 2005; Woolley & Strong, 2015). Moreover, the development of cognitive impairments significantly worsens the outcomes of ALS patients, when compared with ALS patients who do not exhibit cognitive impairments. Indeed, there is an approximately 30% reduction in survival outcomes for ALS patients with cognitive impairment following diagnosis (Elamin et al., 2011; Giordana et al., 2011; Olney et al., 2005). Executive function deficits -- an assortment of higher cognitive processes regulating mnemonic functions, which rely on attention, reasoning, planning and cognitive flexibility -- are the most pronounced cognitive aspects dysregulated in ALS disease pathology (Barber et al., 1995; Barulli et al., 2015; Kasper et al., 2015; Machts et al., 2014; Mantovan et al., 2003; Rabinovici & Miller, 2010; Watermeyer et al., 2015).

1.3 Fronto-Temporal Dementia and Fronto-Temporal Lobar Degeneration

FTD is a heterogenous neurodegenerative disease, which is clinically diagnosed based on various phenotypical alterations to temperament and cognition (Harrison & Shorter, 2017). Overall, there are approximately 1 – 17 cases of FTD per 100,000 people globally. Narrowing the scope to individuals 70 years of age or greater brings the range to 1 – 4 cases per 100,000 people. Global prevalence of FTD ranges between 2 – 31 cases per 100,000 people. A number of factors can increase the risk of FTD development; for example traumatic head injuries were found to contribute to a 3.3-fold increase in associated risk for developing FTD, and thyroid disease contributes to a 2.5 fold increase (Onyike & Diehl-Schmid, 2013). It is currently unclear whether there are sex difference associated risks for FTD due to contrasting reports (Chambers et al., 2016; Hogan et al., 2016; Onyike & Diehl-Schmid, 2013).

The aetiology of FTD is strongly linked to genetic factors, with familial mutations representing ~40% of cases (D. M. A. Mann & Snowden, 2017). Furthermore, sporadic and familial FTD presentations are linked to specific clinical phenotypes I will describe later (Van Mossevelde et al., 2018). Three mutations are currently recognized as causative for FTD. Namely, hexanucleotide repeat expansion mutations in *C9ORF72*, mutations in *MAPT*, and *GRN* mutations driving TDP-43 pathology (D. M. A. Mann & Snowden, 2017). FUS is also implicated

in FTD, though its presentation is predominantly sporadic and when mutated is associated with ALS. Other less frequent mutations have also been identified such as *UBQLN2*, *valosin containing protein*, *optineurin* and *TANK binding-kinase 1* (D. M. A. Mann & Snowden, 2017).

Interestingly, although FTD and ALS are quite distinct with regards to their disease progression, they are linked through a shared neuropathological feature, namely, FTLD (Banks et al., 2008; Heyburn & Moussa, 2017; Young et al., 2018). FTLD pathology is the underlying cause of FTD, which is clinically diagnosed through observed cognitive alterations and imaging techniques (Erkkinen et al., 2018; Heyburn & Moussa, 2017; I. R. Mackenzie & Neumann, 2017; Young et al., 2018).

1.4 FTD and FTLD Presentation Variations

FTLD pathology is typically observed in the frontal and temporal lobes, insular cortex and orbitofrontal cortices (Erkkinen et al., 2018; Heyburn & Moussa, 2017; Hofmann et al., 2019; J. R. Mann et al., 2019). The severity of FTLD progression and subsequent cognitive impairment can vary from mild to a fast-progressive degeneration, which can manifest prior to the onset of canonical ALS motor symptoms (Lomen-Hoerth et al., 2003; Strong et al., 2003). FTLD can be identified histopathologically in post-mortem tissue based on the signature of aggregated proteins (Heyburn & Moussa, 2017; Hofmann et al., 2019; D. M. A. Mann & Snowden, 2017). Typical presentations of FTLD manifest as one of three distinct molecular derivatives based on aggregated proteins, such as FTLD-FUS, FTLD-Tau and FTLD-TDP, all of which can be identified neuropathologically to show accumulation of the specific protein (FUS, Tau and TDP-43, respectively; Gao et al., 2018; Hofmann et al., 2019; Sleegers et al., 2010). The first FTLD derivative to be identified was Tau (Hofmann et al., 2019; Sleegers et al., 2010), a microtubule-binding protein involved in many neurodegenerative diseases. FTLD-Tau disrupts microtubule stability, and axonal transport (Sleegers et al., 2010). FTLD-Tau is frequently observed in patients with Pick's disease (a FTD variant with Tau accumulation), although familial FTD patients with mutations on the MAPT gene can also exhibit tau pathology representing approximately 35 – 45% of FTLD cases. FTLD-FUS represents roughly 5 – 10% of FTLD cases. FUS is a RNA-binding protein regulating RNA complexes in the nucleus among other functions

(Heyburn & Moussa, 2017; Hofmann et al., 2019; Sleegers et al., 2010). Perturbed FUS trafficking can produce a loss of function or gain of toxicity, though it is not known which specific mechanism ultimately leads to the loss of cell viability. Furthermore, FTLD-FUS does not exhibit the same pattern of pathology observed in FTLD-TDP despite belonging to the same RNA-binding protein family. This suggests perhaps that there is a different mechanism and or pathway that produces degeneration in these cases (Sleegers et al., 2010). The majority of FTLD cases are of the TDP variant, with approximately 45 – 60% of post-mortem analyses showing immunoreactivity to ubiquitin with TDP-43 being the primary constituent of the inclusions (Hofmann et al., 2019; Sleegers et al., 2010)

FTD can be categorized based on symptoms and typically presents in one of three variants. Namely, behavioural variant FTD (variant of interest herein), and two language variants, semantic dementia and primary non-fluent aphasia. Presentations of behavioural variant FTD are 1.5 – 3 times more common than the semantic dementia and primary non-fluent aphasia variants (Erkkinen et al., 2018; Heyburn & Moussa, 2017; Hofmann et al., 2019). Characteristically, semantic dementia is rarely familial, though reliably linked to TDP-43 pathology and presents with bilateral atrophy (often asymmetrically biased) of the temporal lobes diminishing the ability to comprehend language (Heyburn & Moussa, 2017; D. M. A. Mann & Snowden, 2017). Primary non-fluent aphasia is characterized by asymmetric degeneration of the left cortical hemisphere inducing speech production deficits and is linked to TDP-43 pathology (Heyburn & Moussa, 2017; D. M. A. Mann & Snowden, 2017). Behavioural variant FTD presentations are most frequently familial, strongly associated with TDP-43 pathology and demonstrate frontal and anterior temporal lobe atrophy (Heyburn & Moussa, 2017; D. M. A. Mann & Snowden, 2017). Behavioural variant FTD is diagnosed based on the degree of alterations to compulsivity and or perseveration, empathy, social behaviour and altered dietary patterns (Erkkinen et al., 2018; Heyburn & Moussa, 2017; Young et al., 2018). Importantly, these behavioural variant FTD features are not characteristic of typical AD, and parsing out these clinical phenotypes in patients facilitates the differentiation between AD and FTD ensuring timely diagnoses (Erkkinen et al., 2018; Heyburn & Moussa, 2017; Young et al., 2018). There are also atypical FTD variants that present with Parkinson's disease (PD)/ Parkinsonian-related disorders, motor neuron disease, and or limb apraxia (Hogan et al., 2016; Onyike & Diehl-Schmid, 2013). Nevertheless, the

identification of FTD variants is confirmed through post-mortem analyses of FTLTD pathological protein signatures (Heyburn & Moussa, 2017; Young et al., 2018).

1.5 FTD Clinical Identification

Briefly mentioned previously, FTD variants can be identified with some success through clinical approaches. However, evidence of, behavioural and or cognitive deterioration must be observed by a clinician or reliable caretaker before an evaluation for possible FTD is permitted. Possible FTD can then be diagnosed should at least three of the following criteria as defined by the International Behavioural Variant FTD Criteria Consortium be met: (a) early behavioural disinhibition (e.g., impulsivity and deterioration of social etiquette/behaviour); (b) early loss of sympathy and or empathy; (c) early apathy; (d) early perseverative and or compulsive like behaviour; (e) hyperorality and alterations to diet; (f) demonstrated deficits of executive function with largely unaltered visuospatial faculties and episodic memory (Rascovsky et al., 2011; Young et al., 2018). Collectively, these behaviour and cognitive characteristics are often referred to as behavioural and psychological symptoms of dementia (BPSD; Erkinen et al., 2018; Tible et al., 2017; Young et al., 2018). Probable FTD cases would satisfy the possible FTD conditions and would fall into the probable category if verified by neuroimaging (e.g., magnetic resonance imaging, computerized tomography & positron emission tomography), and showing some evidence of FTLTD pathology (Young et al., 2018). Definitive FTD can be diagnosed after meeting the possible FTD criteria, but additionally must demonstrate either evidence of FTLTD pathology (via brain biopsy or autopsy), or a verified pathogenic mutation (Erkinen et al., 2018; Rascovsky et al., 2011; Young et al., 2018).

Due to the heterogenous nature of FTD and its mostly psychopathological manifestations, misdiagnosing FTD as a psychiatric or other neurodegenerative disorder is possible; especially in the early stages of disease progression (Erkinen et al., 2018; Young et al., 2018). Bipolar disorder, schizophrenia, depression and obsessive compulsive disorder are just a selection of possible misdiagnoses which can occur in up to 50% of cases (Erkinen et al., 2018). Furthermore, AD can also complicate FTD diagnoses; however a combination of clinical phenotypes and imaging techniques can increase the accuracy of an FTD diagnosis (Erkinen et

al., 2018; Hansson et al., 2019). Mentioned previously, FTD is diagnosed based on a collection of cognitive alterations, namely, a dysexecutive neuropsychological profile and relatively intact memory and visuospatial performance, features that are not typical of AD (Erkkinen et al., 2018; Heyburn & Moussa, 2017; Young et al., 2018). AD patients do, however, frequently exhibit mesial temporal and posterior atrophy, which is not characteristic of FTD, and can be revealed by structural magnetic resonance imaging. Differentiation is also possible using positron emission tomography with amyloid binding tracer techniques (Erkkinen et al., 2018). Moreover, a non-imaging technique that is not reliant on phenotypical FTD cognitive alterations is cerebrospinal fluid (CSF) collection. CSF assessment can reveal the ratio of amyloid beta_{42/40} which is used as a biomarker for AD to distinguish AD from mild cognitive impairment and other dementias (Erkkinen et al., 2018; Hansson et al., 2019).

1.6 FTD/ALS Exist on a Single Spectrum

The relatively frequent co-occurrence of FTD and ALS has led to the neurodegenerative diseases being recognized to exist on a single clinicopathological spectrum, with etiological, pathological and genetic commonalities (Erkkinen et al., 2018; Gao et al., 2018; Hofmann et al., 2019; Ringholz et al., 2005; Sleegers et al., 2010; Van Langenhove et al., 2012). Cognitive dysfunction has also been substantiated as a critical component of ALS. This is supported by neuroimaging investigations illustrating that up to 50% of ALS patients lacking overt dementia demonstrate mild atrophy of the frontal lobe, comparable to anatomical and morphological alterations present in FTD (Lomen-Hoerth et al., 2003; Massman et al., 1996; Talbot et al., 1995). Ultimately, up to 70% of ALS cases are complicated by FTD (Ling et al., 2013; Strong et al., 2003; Woolley & Strong, 2015). Confounding of FTD cases by ALS has also been highlighted, with ~15% of FTD cases exhibiting ALS motor deficits (Ling et al., 2013). Additional evidence of an FTD/ALS link stems from spinal cord post-mortem analysis of FTD patients (infrequently examined) revealing cytoplasmic inclusions exhibiting immunoreactivity to ubiquitin in ~25% of cases (I. R. A. Mackenzie, 2007; I. R. A. Mackenzie & H. Feldman, 2005). Ubiquitinated inclusions are a hallmark of TDP-43 proteinopathy in ALS, and the colocalization of TDP-43 and ubiquitin is rare in other neurodegenerative diseases (Gao et al., 2018; I. R. A. Mackenzie, 2007; Young et al., 2018). Based on the collective discourse surrounding FTD/ALS reviewed thus far, the

putative understanding of FTD/ALS changed to acknowledge their existence on a single clinicopathological spectrum, with the two diseases presenting etiological, pathological, genetic and clinical convergences (Gao et al., 2018; Heyburn & Moussa, 2017; Ling et al., 2013). Nevertheless, a more comprehensive understanding of the precise pathomechanisms by which TDP-43 proteinopathy, FTD/ALS related mutations and cognitive dysfunction contribute to motor- and neuro-degeneration is desperately needed.

1.7 FTD/ALS Genetic Mutations

Characteristically, FTD and ALS are heterogenous diseases which can arise sporadically, or from various gene mutations that have been identified as causative or increase the risk of developing FTD/ALS (Chen et al., 2013; Hofmann et al., 2019). There are many FTD/ALS related mutations (in excess of 50), with a few commonly researched ones such as, chromosome 9 open reading frame 72 (*C9ORF72*), fused in sarcoma (*FUS*), ubiquilin-2 (*UBQLN2*), superoxide dismutase 1 (*SOD1*) and TDP-43 (*TARDBP*; Gao et al., 2018; J. R. Mann et al., 2019). A multitude of distinct pathological alterations can be produced by these mutations, such as neuroinflammation, RNA instability, protein aggregation and misfolding, oxidative stress, irregular axonal transport and excitotoxicity (Gao et al., 2018; Picher-Martel et al., 2019; Renton et al., 2014).

SOD1 is a cytoplasmic protein involved in the mitigation of oxidative stress, through the detoxification of superoxide radicals (Chen et al., 2013). *SOD1* was also the first causative ALS gene to be discovered, though those afflicted by this mutation present with peculiarities when contrasted with classical ALS symptomatology (Chen et al., 2013; Heyburn & Moussa, 2017; Renton et al., 2014). The most notable contrasts observed in *SOD1* patients are an extended disease time course, the rarity of cognitive dysfunction and the rarity of detection in sALS cases (Picher-Martel et al., 2019; Renton et al., 2014). The specific processes enabling *SOD1* mutations to produce ALS pathology are currently unknown (Chen et al., 2013). Additionally, the *SOD1* mutation represents only a small proportion of ALS patients, and does not exhibit the *FUS* or TDP-43 pathology observed in most ALS cases. Consequently, questions have been

raised regarding the role of SOD1 in ALS, and whether it is unique among other ALS variants (Chen et al., 2013; Heyburn & Moussa, 2017; Picher-Martel et al., 2019; Renton et al., 2014).

The FTD/ALS-linked protein FUS (sometimes referred to as translocated in liposarcoma; TLS) is a member of the heterogeneous ribonucleoprotein particle family of which TDP-43 also belongs (Chen et al., 2013; Harrison & Shorter, 2017). Similarly to TDP-43, the putative function of FUS is RNA metabolism; it also possesses an intrinsically disordered low-complexity domain rendering it prone to aggregation, and further, is capable of undergoing liquid-liquid phase separation (Chen et al., 2013; Harrison & Shorter, 2017; Hofmann et al., 2019). More specifically, FUS is involved in the nucleocytoplasmic trafficking of RNA, processing of microRNA and long-intronic sequence and -noncoding RNA stabilization (Harrison & Shorter, 2017). On a broad level FUS mutations lead to deficits in RNA metabolism and dysregulation of the mitochondrial manganese SOD gene (SOD2) transcription (Dhar et al., 2014). Despite some overlaps between FUS and TDP-43, the majority of cases with FUS-immunoreactive cytoplasmic inclusions are ubiquitin- and TDP-43-negative. A possible explanation for this would be a shared FUS/TDP-43 pathway with FUS acting downstream of TDP-43 (Kabashi et al., 2011; Renton et al., 2014). Nonetheless, the pathomechanisms of FUS have yet to be thoroughly characterized.

UBQLN2 is an FTD/ALS-linked protein involved in the ubiquitin proteasome system (protein degradation), and is also a constituent of TDP-43 inclusions. The presence of UBQLN2 in TDP-43 aggregates occurs whether the disease manifests as sALS or fALS (Picher-Martel et al., 2019). UBQLN2 and ubiquitin proteasome system dysfunction has been highly characterized in the pathogenesis of ALS, with FTD concomitantly presenting in UBQLN2-ALS (Picher-Martel et al., 2019; Renton et al., 2014). Specifically, UBQLN2 mutations result in dysregulated protein degradation, which consequently, can cause aggregated proteins and neurodegeneration (Chen et al., 2013). Moreover, UBQLN2 has been shown to directly interact with TDP-43. While the significance of this is not clear, it is thought to enhance TDP-43 induced toxicity (Cassel & Reitz, 2013; Picher-Martel et al., 2019).

C9ORF72 is the most commonly mutated protein in fALS representing approximately 40% of familial cases whereby a hexanucleotide repeat expansion mutation (HREM; GGGGCC) within the gene produces degeneration (Gao et al., 2018; Heyburn & Moussa, 2017; Mathis et al., 2019). An excess of 70+ HREMs is commonplace in mutated C9ORF72, whereas, neurologically healthy subjects have ≤ 30 G4C2 HREMs (Gao et al., 2018; Heyburn & Moussa, 2017; Mathis et al., 2019). Notably, a C9ORF72 and TDP-43 link has been identified and investigated, highlighting a correlation between HREM and perturbed trafficking, mislocalization and accumulation of TDP-43 in the cerebellum of ALS patients (Heyburn & Moussa, 2017).

The discovery of ubiquitinated TDP-43 (TARDBP) in both FTD and ALS provided the first ground-breaking link between the two diseases (Gao et al., 2018; Renton et al., 2014). Mutated TDP-43 represents approximately 4% of fALS cases and 2% of sALS cases, although TDP-43 proteinopathy is detected in 95-97% of ALS cases (Chen et al., 2013; Gao et al., 2018; Ling et al., 2013; Renton et al., 2014). TDP-43 mutations are almost always located in the C-terminal region (a prion-like low-complexity domain), and the location of these mutations has been suggested to increase TDP-43 aggregation and self-assembly (Banks et al., 2008; Ling et al., 2013; J. R. Mann et al., 2019). Given that TDP-43 is the primary focus of this investigation, the following sections will discuss TDP-43 in greater detail.

1.8 TDP-43 Proteinopathy

TDP-43 is a 414 amino acid protein member of the heterogeneous ribonucleoprotein particle family and is comprised of four functional domains. There is a nuclear localization sequence, two RNA-recognition motifs and a prion-like low-complexity domain at the C-terminal, which is rich in glycine (Banks et al., 2008; Boeynaems et al., 2018; Gasset-Rosa et al., 2019; Hansson et al., 2019; J. R. Mann et al., 2019). Under normal physiological conditions TDP-43 is tightly auto-regulated by controlling its own mRNA levels (via a negative feedback loop), and is a predominantly nuclear protein (~70%), though it shuttles between the nucleus and cytoplasm (Gao et al., 2018; Heyburn & Moussa, 2017; Hofmann et al., 2019; Sreedharan et al., 2008). TDP-43 is involved in a multitude of functions such as transcription, translational regulation,

RNA splicing, mRNA stability and RNA stress granule (SG) response (Gao et al., 2018; Heyburn & Moussa, 2017; Hofmann et al., 2019). TDP-43 is capable of exerting its regulatory effects via DNA/RNA binding, splicing and protein-protein interactions (Gao et al., 2018; Heyburn & Moussa, 2017; Hofmann et al., 2019). The most frequent targets are RNA binding sites, directing the regulation of mRNA splicing, translation, transportation and degradation (Gao et al., 2018; Heyburn & Moussa, 2017; Sreedharan et al., 2008).

Under certain pathological conditions TDP-43 function can be disrupted leading it to become neurotoxic. Furthermore, TDP-43 proteinopathy can manifest with or without the presence of related genetic mutations. Several mechanisms have been proposed for these changes in TDP-43 activity. It remains unclear, however, what specific biological alteration(s) produce the ALS pattern of neurodegeneration that causes TDP-43 dysregulation (Hofmann et al., 2019). An aspect related to its dysregulation is the perturbation of TDP-43 trafficking between the nucleus and cytoplasm, which is rooted in a number of effects related to its nuclear depletion and accumulation in the cytoplasm (Gao et al., 2018). For example, loss of nuclear pore components in natural aging can alter the distribution and concentration of TDP-43, inducing TDP-43 proteinopathy (D'Angelo et al., 2009; Gasset-Rosa et al., 2019). This might explain how TDP-43 proteinopathy can induce cognitive dysfunction and memory deficits in elderly individuals lacking pathological diagnoses of FTD/ALS (Nag et al., 2017; Wilson et al., 2013). Of particular importance, nuclear depletion of TDP-43 is not a requisite for the occurrence of neuronal toxicity (Austin et al., 2014). However, the presence of mutant TDP-43 within the cytosol is sufficient to produce neurodegeneration (Arnold et al., 2013a; Austin et al., 2014; Gao et al., 2018).

A critical component of ALS pathology is protein misfolding. Protein misfolding describes the process of proteins transitioning from a normative conformation (normally folded), frequently soluble conformations, into altered or non-functional detergent-resistant conformations (misfolded; Gasset-Rosa et al., 2019; J. R. Mann et al., 2019). Notably, misfolded TDP-43 may propagate in a prion-like fashion recruiting normally folded TDP43, increasing the propensity of its normal counterpart to misfold and aggregate as well (Gao et al., 2018; Ling et al., 2013). In the context of FTD/ALS, misfolded TDP-43 is critical for the generation of proteinaceous inclusions comprised of full-length and or fragmented, misfolded and aggregated protein.

However, protein misfolding and aggregation is also characteristic of other major neurodegenerative diseases such as AD, PD and Huntington's disease (Gasset-Rosa et al., 2019; J. R. Mann et al., 2019).

Characteristically, TDP-43 proteinopathy within an ALS-specific pattern of neurodegeneration presents predominantly within the frontal and temporal lobes, orbitofrontal cortices, insular cortex and spinal cord (Arai et al., 2006; Erkinen et al., 2018; Heyburn & Moussa, 2017; Hofmann et al., 2019). Neurodegeneration resulting from TDP-43 proteinopathy is observed in 95-97% of ALS cases, 50% of FTD cases and intriguingly over 50% of confirmed AD cases (Gao et al., 2018; Ling et al., 2013). Moreover, TDP-43 proteinopathy is a documented secondary pathological feature of other neurodegenerative diseases such as Huntington's disease, PD and AD (Banks et al., 2008; Gao et al., 2018; Heyburn & Moussa, 2017; Ling et al., 2013). Nevertheless, a clear outline of the essential mechanism(s) underlying TDP-43 proteinopathy, and the manner in which it contributes to neurotoxic and cognitive deficits, has not been elucidated.

1.9 TDP-43 Propagation, Aggregation and Phase Transitions

The exact mechanisms that underlie TDP-43 proteinopathy and in what capacity it contributes to neurotoxic functions has not been clearly defined. Specifically, it is unclear whether TDP-43 proteinopathy occurs due to a loss of function (via TDP-43 nuclear depletion), or a gain of toxicity (via cytosolic misfolding and aggregation of TDP-43), which results in decreased cell viability and neuronal loss. The prion-like low-complexity domain of TDP-43 has led to some recent advancements in potentially establishing a more comprehensive understanding of the pathomechanisms of TDP-43 proteinopathy. All identified TDP-43 mutations are situated in the glycine-rich low-complexity domain, with the exception of a few discovered in RNA-recognition motifs (Banks et al., 2008; Ling et al., 2013; J. R. Mann et al., 2019). Due to the majority of mutations being located within low-complexity domains, and because low-complexity domains are common in RNA-binding proteins, they are quickly becoming a primary focus of research into tauopathies and synucleinopathies (Boeynaems et al., 2018; Gasset-Rosa et al., 2019; Ling et al., 2013; J. R. Mann et al., 2019). Low-complexity domains are also

considered to be intrinsically disordered regions due to their composition consisting of only a few amino acids that are repetitive in sequence (Boeynaems et al., 2018; Gasset-Rosa et al., 2019; Ling et al., 2013). The composition of low-complexity domains makes them vulnerable to rapid conformational alterations from their native state and self-assembly (Boeynaems et al., 2018; Gasset-Rosa et al., 2019; J. R. Mann et al., 2019). The TDP-43 low-complexity domain is also predominantly an intrinsically disordered region, which causes it to promote its own aggregation (Gasset-Rosa et al., 2019; J. R. Mann et al., 2019).

Pathological TDP-43 which is mislocalized, misfolded and aggregated within cytoplasm can be recruited or colocalized with SGs (Gao et al., 2018; Ling et al., 2013; Wolozin, 2019). SGs are membraneless organelles, which under conditions of oxidative or cellular stress prevent non-essential protein translation by rapidly facilitating expression of protective proteins during a stress response. SGs achieve this by sequestering, nucleating and compartmentalizing non-essential proteins and utilizing stalled mRNA pre-initiation complexes that have been stored (Bozzo et al., 2017; Gao et al., 2018; Gomes & Shorter, 2019; J. R. Mann et al., 2019). ALS disease pathology has been demonstrated to present with reduced nuclear import (stress; compounded by reduced nuclear pore viability in natural aging), and mitochondrial dysfunction which has been implicated in/with neuronal oxidative stress (Bozzo et al., 2017; D'Angelo et al., 2009; Gao et al., 2019; Gasset-Rosa et al., 2019; Wang et al., 2017). Problematically, the prolonged presence of these stress-inducing mechanisms may inadvertently cause SG seeding behaviour and the enhancement of protein self-interactions. More specifically, SGs coalescing with pathological TDP-43 and sequestering non-pathological correctly folded TDP-43 into aggregates (Bozzo et al., 2017; Gao et al., 2019). Conformationally unaltered TDP-43 interactions with pathological TDP-43 may then induce the fibrilization of normally folded TDP-43 via its intrinsically disordered prion-like low-complexity domains, likely leading to a loss of function (Bozzo et al., 2017; J. R. Mann et al., 2019; Parker et al., 2012). Supporting this notion, neurotoxic SG seeding behaviour has been ameliorated in a TDP-43 rodent model utilizing anti-sense oligonucleotide-mediated depletion of SG components providing evidence for potential SG seeding behaviour in TDP-43 proteinopathy (J. R. Mann et al., 2019). Intriguingly, however, immunohistochemistry and immunofluorescence reveals that neurotoxic SG formation and TDP-

43 seeding behaviour is almost non-existent in tissue samples of ALS patients (Gasset-Rosa et al., 2019).

Recently, it has been proposed that pathological TDP-43 granules are independent of SGs, with SGs possibly serving as intermediaries for pathological TDP-43 to transition through (Gasset-Rosa et al., 2019; J. R. Mann et al., 2019; Wolozin, 2019). The interactions between proteins and RNA is mediated by low-complexity domains through a cellular mechanism known as liquid-liquid phase separation (Boeynaems et al., 2018; Gasset-Rosa et al., 2019; Gomes & Shorter, 2019; J. R. Mann et al., 2019; Wolozin, 2019). Liquid-liquid phase separation is the process by which molecules separate through condensation into liquid-like (not a liquid by classical definition; associative polymers with physical crosslinks) compartments, producing distinct coexisting dense and dilute phases (Boeynaems et al., 2018; Gasset-Rosa et al., 2019; J. R. Mann et al., 2019). This process is promoted by weak and transient exchanges between low-complexity domains and multivalent protein or nucleic acid interaction domains (Boeynaems et al., 2018; Gasset-Rosa et al., 2019; J. R. Mann et al., 2019). This is contingent on specific types of the cellular interactions (e.g, protein-protein, RNA-RNA, & protein-RNA), making intracellular compartmentalization akin to that of membraneless organelles like SGs possible (Boeynaems et al., 2018; Gasset-Rosa et al., 2019; J. R. Mann et al., 2019). The intrinsically disordered regions determine the nature of phase transitions, including the density and organization of protein modules contained in droplets through specific and non-specific protein and nucleic acid interactions (Boeynaems et al., 2018; J. R. Mann et al., 2019). Critically, mutations residing in the TDP-43 low-complexity domain modify liquid-liquid phase separation behaviour, increasing the propensity for TDP-43 aggregation within droplets, and enhancing the rate of maturation and fibrilization of originally reversible protein assemblies, resulting in droplet solidification (Boeynaems et al., 2018). Indeed, this suggests that aberrant phase transitions may be implicated in the formation of pathological TDP-43. This is supported by a recent optogenetic investigation using a Cry2olig-TDP-43-mCherry expression construct (optoTDP43), which is able to trigger light-induced TDP-43 proteinopathy and phase separation in cultured human (HEK293; ReNcell VM) cells, and potentially seed endogenous TDP-43 aggregation (J. R. Mann et al., 2019). This is also consistent with findings from a separate investigation of other RNA-binding proteins (e.g., FUS), in which granule formation using arabidopsis cryptochrome-2 (Cry2) was optically

induced (Shin et al., 2017). Additionally, support is provided by an in vivo optogenetic investigation in zebrafish using light-stimulation of a *mnr2b*-hs BAC promoter driven Cry2oligo-tagged huTDP-43^{A315T} expression construct (opTDP-43h^{A315T}). Blue light stimulation of the opTDP-43h^{A315T} construct triggered pathological cytoplasmic aggregation of opTDP-43h^{A315T}, which induced seeding of non-optogenetic *mnr2b*-hs driven EGFP-tagged zebrafish TDP-43 (Asakawa et al., 2020).

The specific pathomechanism(s) causing aberrant phase transitions of TDP-43 have not been delineated (Boeynaems et al., 2018; Gasset-Rosa et al., 2019; J. R. Mann et al., 2019). It has been suggested, however, that this pathological process may be rooted in reduced nuclear import, a component of natural aging, which may be exacerbated in ALS pathology (Boeynaems et al., 2018; Gasset-Rosa et al., 2019). It is possible that reduced nuclear import then increases cytosolic TDP-43 and dysregulates TDP-43 auto-regulation, increasing its synthesis and accumulation. This cascade of events, including TDP-43 nuclear depletion, is likely sufficient to induce cytoplasmic TDP-43 liquid-liquid phase separation causing cell death (Gao et al., 2018; Gasset-Rosa et al., 2019; Heyburn & Moussa, 2017; Hofmann et al., 2019; J. R. Mann et al., 2019; Wolozin, 2019)

1.10 Mutant TDP-43 Mouse Models

There is an urgent need for the development of new therapeutic strategies for patients afflicted by FTD/ALS. Cognitive testing in mouse models of FTD/ALS can potentially expedite the process of drug discovery by focusing on the cognitive aspects (executive dysfunction) primarily affected in FTD/ALS (Kasper et al., 2015; Watermeyer et al., 2015). Given the predominant role of TDP-43 in FTD/ALS pathology, in recent years many transgenic TDP-43 mouse models have been developed to express human wild-type (WT) or FTD/ALS familial mutations of TDP-43. These mutant mouse models are invaluable assets in the investigation of TDP-43 proteinopathy given that they can recapitulate important features of both sALS and fALS pathology observed in humans (Igaz et al., 2011; Swarup et al., 2011; Wegorzewska et al., 2009; Xu et al., 2011). Furthermore, overexpression of wild-type and mutant forms of TDP-43 was shown to be associated with protein aggregation and motor and cognitive deficits in TDP-43 mouse models

(Arnold et al., 2013b; Swarup et al., 2011; Swarup & Julien, 2011). However, transgenic lines do not perfectly recapitulate ALS pathology. Some mouse lines overexpressing mutant TDP-43 either display extremely aggressive disease progression reaching terminal end points too quickly (4-8 weeks), lack ALS phenotypes and pathology, or are highly variable whereas others have only mild phenotypes. Additionally, alternative TDP-43 transgenic mouse lines such as the TDP-43^{flox/flox}-VAcHT-Cre knockout mice, although demonstrating ALS phenotypes, may not be as representative of ALS disease pathology because of the knockout (Iguchi et al., 2013; Stallings et al., 2010; Wils et al., 2010; Xu et al., 2010, 2011).

Accordingly, in the present work extra consideration was given to the appropriate selection of mouse line(s) with phenotypes of low variability, reliable disease pathology and defined genetic backgrounds. Furthermore, ensuring the diversification of mutations, promoters and levels of expression of the selected mouse models may potentially facilitate a broader exploratory analysis of FTD/ALS cognitive phenotypes, which might help delineate common cognitive phenotypes despite different mutations. Based on available information and factors addressed above, we opted to evaluate two unique transgenic mouse lines incorporating human FTD/ALS-linked mutants of TDP-43 (TDP-43^{Q331Klow} and TDP-43^{G348C}). These models recapitulate some central features characteristic to FTD/ALS pathology in humans, and are viable for 12-month long investigations, allowing for studies of progressive changes in cognition. This is an encouraging development, given that knowledge regarding the capacity of TDP-43 proteinopathy to elicit cognitive alterations in mouse models is limited (although an intriguing ALS knock-in [KI] mouse model became available, only after I started this work; White et al., 2018).

1.11 The TDP-43^{Q331Klow} Mouse Model of FTD/ALS

The TDP-43^{Q331Klow} transgenic mouse model was originally generated and characterized by Don Cleveland's group at the University of California (Arnold et al., 2013a). The mice were generated to express the ALS-linked mutation huTDP-43*Q331K (lysine in position 331 instead of glutamine) by injecting a vector containing N-terminal myc-tagged full length mutant TDP-43^{Q331Klow} driven by murine prion promoter. Generation of the mouse model was achieved through random integration of complimentary DNA into the genome of a fertilized C57BL/6 X

C3H hybrid. The TDP-43^{Q331Klow} mouse model exhibits a very moderate 0.5-fold increase of TDP-43 expression of normal endogenous mouse TDP-43 levels (this contrasts with a similar model, TDP-43^{Q331K}, which exhibits a 2.5-3-fold increase). Mutant TDP-43^{Q331Klow} expression driven by the prion promoter is predominantly expressed in the central nervous system, specifically in brain and spinal cord neurons and astrocytes. Mutant TDP-43^{Q331Klow} toxicity induces the down-regulation of endogenous TDP-43 predominantly via TDP-43 auto-regulation. (Arnold et al., 2013a; *Jax Lab Prnp-TARDBP*Q331K*, 2020).

The mutant TDP-43^{Q331Klow} mouse line does not present with some pathological hallmarks of TDP-43 proteinopathy such as TDP-43 nuclear depletion and mislocalization, cytoplasmic inclusions, aggregation or truncated c-terminal fragments. However, the TDP-43^{Q331Klow} mutant mice still present with a progressive motor phenotype exhibiting minimal variation, where L5 ventral root motor axons and a neurons remain intact (Arnold et al., 2013a). At 3 months of age there are identifiable differences in the development of tremors when comparing TDP-43^{Q331Klow} mutants to their non-transgenic (ntg) control and WT-huTDP-43 (overexpression without mutation) counterparts. Due to the age-dependent nature of these deficits, motor function progressively deteriorates. By 10 months of age there is a significant difference in the grip strength of TDP-43^{Q331Klow} mutants (Arnold et al., 2013a, 2013b). Evaluation of the TDP-43^{Q331Klow} mutants after 17 months of age revealed significantly stunted, if not stalled, motor degeneration with minimal worsening post 10-months.

Postsynaptic neuromuscular junction quantification via gastrocnemius muscle α -bungarotoxin staining revealed no reduction in neuromuscular junction endplates. Furthermore, morphological evaluation of gastrocnemius muscle sections from 10-month-old TDP-43^{Q331Klow} mutants revealed no morphological abnormalities in the muscle fibres. Minor degeneration is present in the spinal cord, specifically degeneration of descending corticospinal tracts of lateral and dorsal columns. Generally, the TDP-43^{Q331Klow} mutants exhibit functional deficits (decreased rotarod performance) without significant alterations to the structural features of lower motor neuron synapses, similar to ntg controls and WT-huTDP43. Cognitive alterations were not evaluated in these mice (Arnold et al., 2013a).

1.12 The G348C Mouse Model of FTD/ALS

The TDP-43^{G348C} mutant mouse line was created by Jean-Pierre Julien's group at Laval University. The ALS-linked huTDP-43^{G348C} mutation (cystine in position 348 instead of glycine) was integrated into the mouse genome of a C57BL/6 X C3H fertilized hybrid using a bacterial artificial chromosome clone and the endogenous promoter. The TDP-43^{G348C} mutant mouse line exhibits a 3-fold increase of TDP-43 expression compared with normal endogenous mouse TDP-43 levels. In human ALS cases quantitative real-time analysis of spinal cord has shown a 2.5-fold increase of TDP-43 mRNA, highlighting the similarity of the TDP-43^{G348C} mutant mouse model. The huTDP-43^{G348C} transgene is also ubiquitously expressed in all tissues in which normal endogenous mouse TDP-43 is expressed. Furthermore, endogenous murine TDP-43 is down-regulated in the TDP-43^{G348C} mutant mouse model (Swarup et al., 2011).

The TDP-43^{G348C} mutant mouse line presents with nuclear depletion, mislocalization, and cytosolic accumulation and aggregation of TDP-43, features closely recapitulating human TDP-43 proteinopathy (Swarup et al., 2011). Critically, the TDP-43^{G348C} mutant mouse model is viable, whereas other overexpressing mutant TDP-43 lines have extremely rapid and aggressive pathology rendering them unfit for investigations beyond a few weeks or months. Additionally, the TDP-43^{G348C} mutants present with age-dependent motor deficits, as indicated by accelerating rotarod analysis. TDP-43^{G348C} mutant mice exhibited significant differences in comparison to ntg- and WT-huTDP-43 control mice as early as 8 months of age, with performance continuing to deteriorate in an age-dependent manner. Furthermore, at 10-months-old L5 ventral root motor axons of TDP-43^{G348C} mutant mice remain intact (Swarup et al., 2011). Neuromuscular junctions were also assessed in 10-months-old TDP-43^{G348C} mutant mice with gastrocnemius muscle α -bungarotoxin staining, revealing that up to 15% of neuromuscular junctions were denervated and over 20% were partially denervated compared to ntg control mice (Swarup et al., 2011). At 3-months-old the TDP-43^{G348C} mutant mice revealed no morphological motor axon abnormalities. However, 10-month-old TDP-43^{G348C} mutant mice present with significant alterations to motor axon morphology. Double immunofluorescence with NeuN and cleaved caspase-3 antibodies indicated neuronal damage in the spinal cords of these mice (Swarup et al., 2011).

Select cognitive aspects have been evaluated in the TDP-43^{G348C} mutant mouse line, specifically, spatial learning using the Barnes maze task and contextual fear responding/learning (Pavlovian fear conditioning) with a step-through passive avoidance light-dark box. These tasks revealed TDP-43^{G348C} mutant mice demonstrate age dependent contextual and spatial memory deficits between 7-10 months. Nonetheless, executive dysfunction has not yet been evaluated in the TDP-43^{G348C} mutant mouse line (Swarup et al., 2011).

1.13 Automated Touchscreens and Translation

Neurological diseases are extremely complex and the initial changes are often subtle and difficult to consistently and accurately assess; thus the use of sensitive/selective tests is particularly important in this area (Gaskin et al., 2017; Van den Broeck et al., 2020). Conventional cognitive testing methodologies often have large variations across laboratories, and despite efforts to control for such variances in conventional testing, different experiments may still produce differing results. Generally, the evidence suggests a propensity for non-automated and non-standardized conventional cognitive testing methodologies to be unintentionally variable (e.g., animal handling variances, effect of experimenter sex and smell & testing methodology variance; Beraldo et al., 2019; Crabbe et al., 1999). For this reason, the automated touchscreen system developed by Tim Bussey and Lisa Saksida (principal investigators of our lab) and their collaborators has been adopted for use in this investigation. Globally there are about 300 laboratories, about 25% percent of them represented by pharmaceutical companies, using touchscreen technology for cognitive testing in rodents (Beraldo et al., 2019; Dumont et al., 2020). Automated touchscreens have been adopted largely due to their utility and consistency across laboratories in detecting cognitive alterations and differences in common mouse lines and neurodegenerative diseases (Beraldo et al., 2019; Bussey et al., 2008; Dumont et al., 2020; Horner et al., 2013). These touchscreen systems are consistent across laboratories in terms of tests, protocols, and parameters, and are identical to human cognitive evaluations in certain situations, facilitating translation (Bussey et al., 2008; Graybeal et al., 2014; Heath et al., 2019; Horner et al., 2013; Nithianantharajah et al., 2015; Romberg et al., 2013). Automated touchscreens provide a multitude of benefits including, but not limited to, computer controlled standardized protocols (inter-trial interval, delay periods, stimulus presentations, etc.),

heightened cognitive impairment sensitivity, high throughput capability, inter-laboratory replicability and critically, significantly diminished experimenter and environmental influence (Beraldo et al., 2019; Dumont et al., 2020). Furthermore, automated touchscreen tasks/protocols are not reliant on intact motor abilities, allowing mice with motor dysfunction to be evaluated without major impacts on the results (Morton et al., 2006).

1.14 Touchscreen Evaluation of Cognition in Mice

A steadily growing selection of touchscreen tasks for evaluating different aspects of cognition in rodents is now available. Here, we looked to evaluate distinct mouse models of TDP-43 proteinopathy (TDP-43^{Q331Klow} & TDP-43^{G348C}) to test for robust cognitive phenotypes across these mouse models, which could then be used in the identification of therapeutic targets and drug development. For this purpose, features of executive function dysregulated in FTD/ALS were assessed in these mice with specific tasks: attention (5-choice serial reaction time task [5-CSRTT]), cognitive flexibility (pairwise visual discrimination [PVD] and reversal), long-term learning and memory (paired associates learning [PAL]), and motivation/apathy (progressive and fixed ratio [PRFR]). As discussed previously, these features of executive function are reported to be dysregulated prior to the onset of classical motor symptoms in human ALS (Lomen-Hoerth et al., 2003; Strong et al., 2003). The sensitivity to impairments afforded by automated touchscreens may enable detection of similar cognitive impairments in TDP-43 mutant mouse models prior to motor dysfunction. This manner of testing aligns with similar computerized tasks used to investigate the same features of executive function in other human neurodegenerative diseases, including ALS (Barson et al., 2000; Heath et al., 2019; Stojkovic et al., 2016). All tasks used herein have already been established and validated by our lab, former lab members and collaborators.

1.15.1 Pairwise Visual Discrimination (PVD) Task and Reversal

The PVD and reversal task evaluates learning ability and cognitive flexibility, which is the ability to alter behaviour, based on a shift in rules, patterns or contingencies. Cognitive flexibility is assessed through the presentation of two visual stimuli simultaneously, which are initially preferred equally by the rodent. The rodent is required to learn that a response (nose-poke) to

only one of these visual stimuli is rewarded (S+), whereas the other visual stimulus (S-) is not rewarded. Once the animal has acquired the task, the reward which was contingent on selection of the S+ is reversed. Following this reversal, the previous S+ is unrewarded (new S-) and the previous S- is rewarded (new S+). During acquisition, the animal must visually discriminate between equally preferred stimuli and acquire the stimulus-reward relationship. Subsequent to the reversal of this relationship, the animal must be able to inhibit its prepotent responses to the previously rewarded stimulus and simultaneously acquire the new stimulus-reward relationship. The ability to be cognitively flexible is disrupted in FTD/ALS patients (Gao et al., 2018; Machts et al., 2014; Zakzanis, 1998). Furthermore, the reversal component of the PVD task is dependent on the orbitofrontal cortex and striatum, areas known to degenerate in FTD/ALS pathology (Erkkinen et al., 2018).

1.15.2 Different Paired Associates Learning Task (dPAL)

The dPAL task evaluates visuospatial memory and adopts the important components of the Cambridge Neuropsychological Test Automated Battery PAL, a highly sensitive task which is used to discriminate between sufferers of early-stage AD and individuals afflicted by cognitive impairment stemming from different neurological conditions such as FTD/ALS (Lee et al., 2020). Visuospatial memory performance is evaluated by presenting rodents with unique visual stimuli in two of three possible spatial locations, which they are required to nose-poke. A single compound (shape-location) stimulus is always positively associated with reward (S+), and one is always associated with a punishment (S-) in the form of a tone and time-out delay. Although visuospatial performance has been reported to be relatively spared in FTD/ALS pathology, because of the success of PAL in mouse and human studies of neurodegenerative disease, TDP-43^{Q331Klow} & TDP-43^{G348C} were evaluated with this task (Erkkinen et al., 2018).

1.15.3 5 Choice Serial Reaction Time Task (5-CSRTT)

The 5-CSRTT evaluates sustained attention, one of the principle cognitive abilities affected by FTD/ALS, even early in disease progression (Igaz et al., 2011; Mantovan et al., 2003; Zakzanis, 1998). The 5-CSRTT requires the animal to respond to a momentary and spatially randomized light stimulus in one of five possible locations arranged in a horizontal line. Responses are

recorded by nose-pokes to the light stimulus. There is a substantial number of metrics evaluated in this task, the primary ones being accuracy (response to correct location), premature responses (response before stimulus presentation), omissions (failure to respond), perseverative responses (continued responding following previously correct stimulus response), as well a number of latency metrics (correct response latency, incorrect response latency & reward collection latency). Initial training conditions for the 5-CSRTT are relatively lenient, using 4 second and 2 second stimulus illumination durations. Once an animal has reached criterion (80% accuracy, fewer than 20% omissions) probe trials can be initiated. The animals are then evaluated with four novel stimulus illuminations duration for two consecutive days each (1.5s, 1.0s, 0.8s, and 0.6s). The shorter the stimulus illumination duration, the greater the demand on attention to successfully perform the task.

1.15.4 Progressive Ratio Fixed Ratio Task (PRFR)

The PRFR task evaluates motivation and apathy in rodents. Apathy is also a condition observed in human FTD/ALS (Radakovic et al., 2016; Zamboni et al., 2008), and a variant of this task is a part of the EMOTICOM battery used previously by our lab (Heath et al., 2019). The PRFR task has been previously described by our lab (Heath et al., 2016). Motivation/apathy is evaluated by requiring the subject to respond (via nose-poke) to a visual light stimulus (illuminated white square; which always appears in the same location), which appears centrally on a screen to receive a reward. The animal is required to elicit a predetermined number of responses, based on the ratio selected, to obtain reward. There is a substantial number of metrics evaluated in this task, the primary ones being target touches (correct response), breakpoint (highest number of responses within last trial), blank touches (response to non-illuminated window) and trials completed.

1.15 Investigation Objective

There is substantial heterogeneity in the clinical presentation, disease progression and disease outcomes of FTD/ALS (Banks et al., 2008; Chen et al., 2013; Chiò et al., 2018; Hardiman, 2010). Furthermore, the heterogenous nature of FTD/ALS creates significant difficulty in the

identification of a key common neuropathological mechanism inherent to all FTD/ALS patients, and in fact such a mechanism may not exist. However, FTD/ALS share overlapping clinical and genetic features, and TDP-43 proteinopathy is present in 95-97% of all ALS cases, and 45-50% of all FTD cases (Gao et al., 2018; Ling et al., 2013; I. R. Mackenzie & Neumann, 2017). Thus, TDP-43 proteinopathy cuts across the FTD and ALS continuum. In light of the importance of TDP-43, and combined with the importance of (premorbid) cognitive deficits in both FTD and ALS discussed above, in the present study we focused on the question of how TDP-43 mutations in TDP-43^{Q331Klow} and TDP-43^{G348C} mice affect cognition. While TDP-43^{Q331Klow} and TDP-43^{G348C} mice have not been comprehensively evaluated for their cognitive abilities. I hypothesized that TDP-43 mutations impair cognition in mouse models of FTD/ALS, appearing earlier than motor dysfunction using automated touchscreen technology and validated tasks. If the automated touchscreens can reveal an early cognitive phenotype across the two FTD/ALS mutant mouse models (TDP-43^{Q331Klow} and TDP-43^{G348C}), there might be potential to accelerate the identification of therapeutic targets and the development of treatment options capable of acting on the neuropathological mechanism(s) afflicting 95% of ALS and nearly 50% of FTD patients.

2. Materials and Methods

2.1 Q331KLow Mice

The TDP-43^{Q331Klow} mice [Tg(Prnp-TARDBP*Q331K)109Dwc/line 109/ Stock number 017930] and littermate control mice (C57BL/6NJ; Stock number 005304) used in this study were generated at Western University and bred from commercially available mouse lines obtained from Jackson Laboratories (Bar Harbor, Maine). The TDP-43^{Q331Klow} mice were heterozygous for the ALS-linked Q331K mutation (huTDP-43*Q331K) and driven by the murine prion promoter.

The mice utilized in this study, twenty-seven TDP-43^{Q331Klow} males and eighteen C57BL/6NJ wild-type littermate controls were between three and four months of age during the start of

behavioural testing. At this age TDP-43^{Q331Klow} mice present no deficits in motor performance (Arnold et al., 2013a).

2.2 G348C Mice

The TDP-43^{G348C} mice used in the study were graciously provided by Dr. Jean-Pierre Julien (Centre de Recherche du Centre Hospitalier Universitaire de Québec; Laval University) and subsequently bred at the University of Western. Cohorts of littermate control mice generated at Western University were bred from a commercially available control line (C57BL/6J; Stock number 000664) obtained from Jackson Laboratories (Bar Harbor, Maine). The TDP-43^{G348C} mice were heterozygous for the ALS-linked G348C mutation (huTDP-43*G348C) and were generated through amplification of TARDBP (NM_007375) by polymerase chain reaction from a human bacterial artificial chromosome clone (clone ROCI-11, number 829B14) and the endogenous promoter (Swarup et al., 2011). The TDP-43^{G348C} model expresses a 3-fold increase in TDP-43 compared with normal endogenous mouse TDP-43 levels (Swarup et al., 2011).

The twenty-two TDP-43^{G348C} male mice and fifteen C57BL/6J wild-type littermate controls ranged between three and four months at the commencement of behavioural testing. The TDP-43^{G348C} present no deficits in motor performance at this age (Swarup et al., 2011).

2.3 Ethics

Animals used throughout this study were all monitored, handled and maintained by myself, or otherwise University of Western Animal Care and Veterinarian Services. Animal use protocols (2016-103; 2016-104) and procedures were in compliance with approved animal use protocols at the University of Western, and in line with the Canadian Council of Animal Care stipulations.

2.4 Housing, Food Restriction

Animals were housed in an enclosed colony room specifically designed for the maintenance of mice. The housing room is regulated by a standard automated 12-hour light/dark cycle (lights on

at 7:00 A.M.). Colony room air humidity and temperature was also regulated by an automated system and was held between 40%-60% and 22-25°C respectively. All mice were housed individually in clear polyethylene containers (19.56cm x 30.91cm x 13.34cm). The containers were shelved using Maxi-Miser positive individually ventilated systems, commercially available at Thoren Caging Systems Inc (Hazelton, Pennsylvania). Animal enrichment was not provided.

All animals underwent food restriction one week prior to behavioural testing and were maintained at 85% of their free feeding weight until sacrificed. Food provided to animals ranged between 1-3 grams (3.35kcal/gram) of precut pellets with a macronutrient breakdown of 21.3% protein, 3.8% fat, 54% carbohydrates, and 20.9% micronutrients/other. Precut dustless food pellets are commercially available at Bio-Serv (Flemington, New Jersey). Water was available *ad libitum* unless specifically noted otherwise. Food treats were not provided.

2.5 Locomotion Apparatus

Animal locomotor behaviour was assessed using open field locomotor activity boxes produced by Omnitech Electronics (Columbus, Ohio). The locomotion boxes were paired with Fusion software allowing 32 animals to be assessed simultaneously and the complete experimental data of each animal to be individually recorded. The locomotor boxes used for behavioural testing were specifically designed for mice. The locomotor boxes were constructed of clear polyethylene with ventilation holes integrated into the lid. A set of 16 infrared beam arrays are also integrated into the locomotor boxes along the horizontal X and Y axes. The hardware uses these beams for the detection of the animal within space and its behavioural orientation. The software can produce a number of analyses from detected rodent behaviours.

2.6 Grip Force Apparatus

Animal neuromuscular function performance was evaluated using a grip force apparatus obtained through Columbus Instruments (Columbus, Ohio). The grip force apparatus specifically evaluates peak force exerted by the animal when grasping the pull bar assembly. The pull bar assembly used for neuromuscular function performance was specifically designed for mice.

Motor performance readouts were displayed on the digital screen built into the apparatus and manually recorded.

2.7 Wire Hang Apparatus

The sustained neuromuscular function performance of animals was also assessed using a wire hang apparatus. The animals were suspended upside down from a metal grate elevated 60 cm from its base. The amount of time that elapsed between the animal being mounted and dismounting into a soft bedding-filled pit was then manually scored and recorded.

2.8 Touchscreen Apparatus

Behavioural investigations were conducted using the automated Bussey-Saksida touchscreen testing system (model 80614; Lafayette Instruments, Lafayette, Indiana) designed for mice. The touchscreen apparatus is constructed in a trapezoidal shape and is situated within a chamber that blocks external light and attenuates sound. Heat from the touchscreens is managed by fans built into each chamber keeping the temperature between 22-24°C. These fans also diminish any potential noise pollution from neighbouring chambers. The space accessible to the animal, and where behavioural testing occurs is 46mm wide at the reward magazine tray, 238mm wide at touchscreen and 170mm Deep (241.4 Sq. cm). The floor of the touchscreen apparatus is a perforated grate floor with circular cut-outs. The touchscreen chambers all feature built in speakers, and a light built into the top of the enclosing chamber where cameras are also mounted. The reward magazine tray is built into the narrow end of the apparatus opposite of the touchscreen and administers liquid reward. The liquid reward is pumped through replaceable tubing into a metal opening within the reward magazine tray. Infrared beams are also integrated into the reward magazine tray to detect animal entry and exit of the reward magazine tray. Additionally, responses to the touchscreens (12.1 in.; resolution 800 x 600) are detected with infrared beams to enhance the accuracy of animal touch response detection. Unintentional responses by animals (e.g., responses elicited by tails) is prevented through the use of black perspex masks that have task-specific cut-outs. The touchscreen testing system is mated to ABET II software (Lafayette Instruments) produced by Lafayette Instruments which controls the touchscreens in each individual chamber and records behavioural responses.

2.9 Rodent Shaping

The touchscreen testing system necessitates instrumental responses, and animal shaping procedures utilize appetitive conditioning to promote such behaviours through training. Mice are trained through a series of phases that progressively shapes appropriate touchscreen responding. Food restriction is also implemented to enhance the effectiveness of food reward as an appetitive motivator. Although a sizable variety of tasks exist for touchscreen testing, largely the training consists of a few stages which are highly similar, followed by task-specific training. The shaping procedure is a 7-step process for the tasks used herein (5-CSRTT, PRFR, PVD & PAL), and are nearly identical throughout with slight variations to omissions, correction trials and inter-trial intervals (ITI; 5 – 20s). To provide further clarification, the animals which complete the initial shaping procedures and subsequent task-specific training do not undergo shaping again (except where necessary) if they are immediately transitioned to another touchscreen task (e.g., 5-CSRTT progressing to PRFR task). Additionally, mice were permitted only one session (training/probe trial) per day.

Neilson brand strawberry milkshake was utilized as liquid food reinforcer (task-dependent volumes; 7 μ l, 21 μ l & 150 μ l) to maintain animal motivation during the course of touchscreen testing. Neilson branded milkshake is commercially available through Saputo (Montreal, Quebec).

2.10 5-CSRTT Shaping

2.10.1 Stage 1: The first phase (Habituation-1), allowed the animal to briefly acclimate themselves with the testing chamber environment for a period of 10 minutes. All features of the touchscreen system and chamber were switched off during this time (no stimuli or reward) with the exception of the camera (house light off) and ventilation fan.

2.10.2 Stage 2: Across the following two days the mice underwent Habituation-2a. During habituation-2a the mice were allotted 20-minutes of exposure to the testing chamber environment with all features of the touchscreen testing system enabled, including liquid strawberry

milkshake reward. Habituation-2a allowed for unlimited trials during the 20-minute period. The first trial was initiated with the reward magazine tray light turned on; a tone (3Khz; 1000ms) was subsequently played, while strawberry milkshake was simultaneously dispensed (150 μ l) into the reward magazine tray. The ABET II program then waited for the mouse to enter the magazine tray (detected by IR beams); once the mouse withdrew from the magazine tray the light turned off. After 10 seconds elapsed the magazine tray light turned back on. However, during this trial, and all trials that followed the milkshake reward was reduced to 7 μ l with the tone duration unchanged. If the mouse had pre-emptively entered the magazine tray an extra second would be added to the delay period. This process was repeated until the 20-minutes expired, at which point the animal was immediately removed from the testing chamber.

2.10.3 Stage 3: The final habituation phase was Habituation-2b. Here the animals remained in the testing chambers for 40-minutes. The animals also underwent the same reward administration protocol as described in stage 2.

2.10.4 Stage 4: This is the first phase which encouraged the mouse to interact with the touchscreen and is referred to as initial touch. The mouse was placed into the testing chamber with the house lights off. A maximum of 30 trials were permitted and time was capped to 60 minutes. A stimulus was also presented in this phase; an illuminated white square (4 x 4cm) appearing in 1 of 5 possible locations within the 5-CSRTT specific perspex mask cut-out. The stimulus was only presented in one location at a time; all other window locations were blank. The stimulus was also presented in a pseudo-random fashion, preventing a position from being repeated in succession more than 3 times. The stimulus presentation lasted 30 seconds, following this the image was automatically removed and milkshake was administered into an illuminated reward magazine tray (7 μ l) paired with a tone (3Khz; 1000ms). IR beam detection of the mouse entering the reward magazine tray turned off the light and initiated an ITI (5 seconds). Once the ITI ended another stimulus was presented. A response to the screen in the location in which the stimulus was presented removed the stimulus presentation and immediately administered 3 times the milkshake reward (21 μ l). Following reward collection by the mouse, the ITI was reinitiated, and the next stimulus was then presented.

2.10.5 Stage 5: The next phase of the shaping procedure is called must touch. The mice were given a maximum of 30 trials to be completed within a 60-minute period. Tone and ITI parameters were identical to stage 4. Must touch required the mouse to respond to the stimulus presented in 1 of 5 possible locations. However, the mouse was required to touch the stimulus to trigger the tone and milkshake reward administration. Blank window touches and elapsed time produced no response from the testing system; the mouse was required to touch the correct stimulus. Successful responses, reward collection and withdrawal from the reward magazine tray started the ITI, followed by another stimulus presentation. 30 trials completed within 60-minutes was required for progression to stage 6.

2.10.6 Stage 6: This phase is referred to as must initiate. The trial, time, tone and ITI parameters for must initiate were identical to stages 4 and 5. Once the must initiate schedule began the reward magazine tray was illuminated and a free 7 μ l of milkshake was dispensed. The mouse was required to enter and withdraw from the reward magazine tray before the first trial could commence. Every subsequent trial was required to be initiated in the same manner. The reward magazine tray was illuminated (no free reward), and the mouse was required to nose poke into the reward magazine tray and then withdraw. The stimulus was then presented in 1 of 5 possible locations. A successful response, reward collection and withdrawal from the reward magazine tray initiated the ITI, followed by the reward magazine tray being illuminated again. 30 trials completed within 60-minutes was required for progression to stage 7.

2.10.7 Stage 7: This phase continues “must initiate” training and following an ITI, added in the requirement for mice to abstain from touching incorrect locations. This phase is referred to as punish incorrect and as in stages 4 – 6 the trial, time, tone and ITI parameters were identical. Punish incorrect mimicked stage 6 with a key alteration: incorrect responses to a non-illuminated window (e.g., not the stimulus) resulted in a timeout with a bright house light being turned on for 5 seconds and no reward provided. Once the 5 seconds had elapsed the ITI (5 seconds) began and the mouse was required to complete a correction trial (stimulus location from previous trial repeated). Correction trials were repeated until the mouse correctly responded subsequently eliciting administration of the tone and reward.

Touchscreen Shaping Schedule

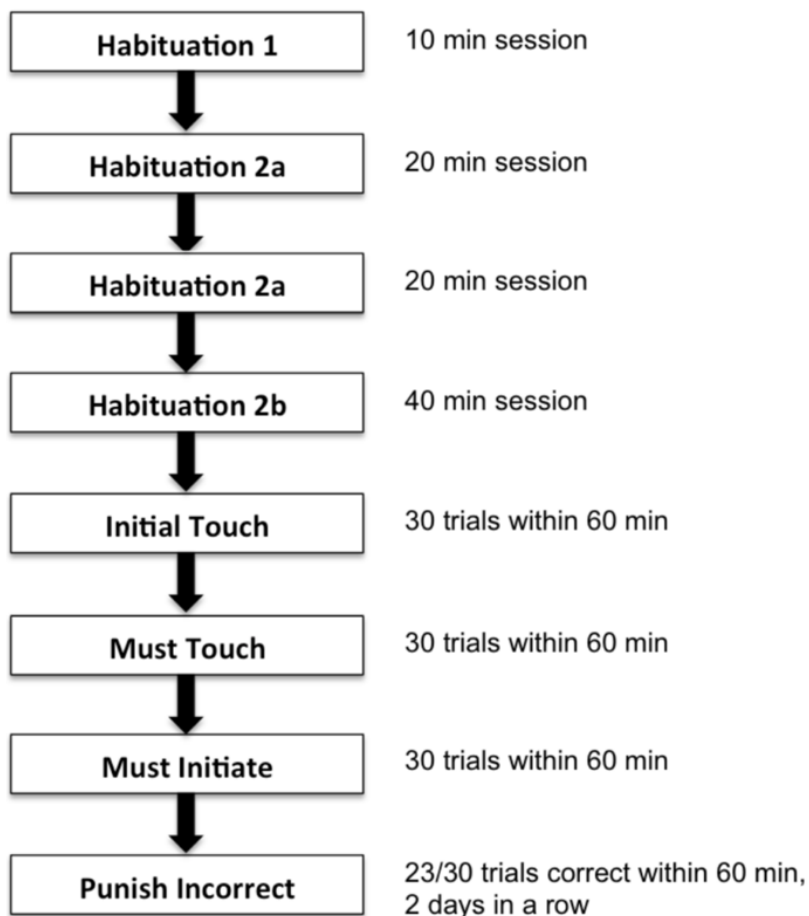


Figure 1. Flow chart of general shaping schedule prior to task specific training.

2.11 5-CSRTT Training

2.11.1 Stage 8: 5-CSRTT training to baseline-4s stimulus was the first training phase. The 5-CSRTT training was used to establish a baseline in performance. The parameters for max schedule time, tone, ITI, reward volume and incorrect response ITI were unchanged from stages 4 – 7. The maximum number of trials during training was constant at 50. The training session commenced with the reward magazine tray being illuminated and primed with 7 μ l of free milkshake reward. Withdrawal from the reward magazine tray initiated the first trial with a 5 second delay interval. Following the delay, the stimulus was presented in 1 of 5 possible locations pseudo-randomly. Stimulus responses were required to be initiated within a set

timeframe. A mouse could respond to the stimulus (white square) during the 4 second illumination period in the location it was presented. If the mouse failed to respond, there was a limited hold period lasting 5 seconds. During this window of time, a response at the location in which the stimulus was presented was considered to be correct, and subsequently triggered the reward magazine tray to illuminate and dispense milkshake reward (7 μ l) paired with a tone (3Khz; 1000ms). Withdrawal from the reward magazine tray then initiated the ITI, after which the reward magazine tray was re-illuminated allowing the mouse to progress to the next trial by entering and withdrawing from the reward magazine tray. Incorrect responses, premature responses (response during 5s delay), and omissions (failure to respond within limited hold period) resulted in a 5 second timeout paired with the house light turned on. Once the timeout had expired the house light turned off and the ITI-incorrect began, lasting 5 seconds. The 4 second stimulus training was continued until the mice were able to reach criterion ($\geq 80\%$ accuracy [total correct trials / total number of trials with response] & $\leq 20\%$ omissions [total trials missed / total trials presented]) for three consecutive days.

2.11.2 Stage 9: 5-CSRTT training to baseline-2s stimulus was the second training phase. Within this stage the stimulus duration was reduced from 4 seconds to 2 seconds, all other training conditions and parameters were identical to stage 8, including criterion thresholds. Where necessary, animals that met criterion before their counterparts were placed on maintenance and repeated stage 9 once per week.

2.12 5-CSRTT Probe Trials

Following completion of stage 9 the mice were evaluated with four novel stimulus durations (1.5s, 1.0s, 0.8s, & 0.6s). By reducing the duration of stimulus presentations, the demand on attention is increased making the task more challenging. Each stimulus duration was completed for two consecutive days followed by two consecutive days of a baseline 2 second stimulus duration before transitioning to the next probe. Performance was evaluated using the criterion outlined in stages 8 and 9, however, there was no requirement to meet the criterion thresholds to progress through probe trials.

2.13 Investigation Time Points

The mice were evaluated longitudinally as they aged with the first probe trials being completed while the mice were 4 – 5 months old. The mice were then placed on a maintenance schedule with a 2 second stimulus duration until they reach the desired age. Maintenance was performed once per week on the same day (e.g., Friday), also ensuring to keep the time of testing consistent. This process was necessary to ensure the animals would not require retraining. The second time point was completed when the mice were 8 – 9 months old.

2.14 PRFR Shaping

Shaping for the PRFR task was completed prior to 5-CSRTT Training. Refer to rodent shaping and 5-CSRTT training (sections 2.11 & 2.12 respectively).

2.15 PRFR Training

2.15.1 Stage 9a: This stage was comprised of a variety of fixed ratio (FR) training schedules starting with FR1. The FR1 schedule required the mice to complete 30 trials within 60-minutes. Within a trial a single operant response elicited a single food reinforcer. Each trial presented the stimulus indefinitely within the central window (5-SCRTT Perspex mask; section 2.11, stage 4). The stimulus was removed once the mouse had successfully responded. For this single correct response, a tone was played (3Khz; 1000ms) and strawberry milkshake reward (7 μ l) was delivered simultaneously into the illuminated reward magazine tray. Following withdrawal, the magazine tray light turned off and an ITI (4.5s) began before the next stimulus presentation. Once the mice reached criterion (30 trials within 60-minutes; single session) they immediately progressed to FR2.

2.15.2 Stage 9b: The FR2 schedule was identical to that of the FR1 schedule with the exception of two key alterations. Here, the reinforcer requirement was increased to two operant responses for administration of a single food reinforcer. Additionally, continual responding to the stimulus was promoted by its brief removal (500ms), following a successful response indicated by a

single rapid audible chirp (3Khz; 10ms). Once the mice reached criterion (30 trials within 60-minutes; single session) they immediately progressed to FR3.

2.15.3 Stage 9c: The FR3 schedule was identical to that of FR2, with exception of three operant responses being required for administration a single milkshake reinforcement. Once criterion was met (30 trials within 60-minutes; single session) the mice immediately progressed to FR5.

2.15.4 Stage 9d: The FR5 schedule was identical to that of FR2/3, with exception of five operant responses being necessary for delivery of a single milkshake reinforcement. Once criterion was met (30 trials within 60-minutes; two consecutive sessions) the mice immediately progressed to PR testing.

2.15.5 Stage 10: This stage was comprised of a variety of PR testing schedules. PR4 was the first of these schedules requiring mice to complete as many trials as possible within a 60-minute session. All PR schedules started in the same manner, requiring a single operant response to obtain a single food reinforcer (7 μ l) from the illuminated reward magazine tray, which coincided with a tone (3Khz; 1000ms). Following reward collection and withdrawal from the reward magazine tray, an ITI (4.5s) was initiated before the next stimulus presentation. All subsequent trials increased on a linear ramp (e.g., PR4 ramp; 1, 5, 9, 13...responses per trial) where repeated touches were promoted by a brief removal of the stimulus (500ms), following a successful response signaled by a single rapid audible chirp (3Khz; 10ms). Sessions could be completed by reaching the maximum time limit, or terminated if no response to the screen, or reward magazine tray entry was detected within a 5-minute period. This process was repeated three times consecutively.

2.15.6 Stage 11: Following PR4 the mice were returned to FR5 for two days (section 2.16, stage 9d) to mitigate potential performance deterioration due to repeated subjection to the PR schedule.

2.15.7 Stage 12: Following stage 11 the testing from stage 10 was repeated for another three consecutive days (section 2.16, stage 10).

2.15.8 Stage 13: During this stage the mice went through a three-day high-demand PR block, with the linear ramp being increased each day starting with PR4 (n +4), then PR8 (n +8) and concluded with PR12 (n +12). The testing protocol is as described in stage 10 (section 2.16), however each schedule was completed only once.

2.15.9 Stage 14: Following the high-demand PR block the mice were returned to FR5 two days (section 2.16, stage 9d) to prevent any potential performance deterioration due to repeated exposure to the PR schedule.

2.15.10 Stage 15: Here, the mice went through a final high-demand PR block as described previously (section 2.16, stage 13) before testing was completed.

2.16 PVD Shaping

As stated previously, the training schedule is largely unchanged across tasks. However, the PVD task does have some slight modifications noted where applicable.

2.16.1 Stage 1: Habituation 1; refer to 5-CSRTT training (section 2.11).

2.16.2 Stage 2: Habituation 2a; refer to 5-CSRTT training (section 2.11).

2.16.3 Stage 3: Habituation 2b; refer to 5-CSRTT training (section 2.11).

2.16.4 Stage 4: Initial Touch; refer to 5-CSRTT training (section 2.11).

Modifications: ITI 20s; Selected shape stimulus (1 of 40 chosen randomly) not designated for testing (acquisition/reversal) presented in 1 of 2 possible window locations (location without stimulus is blank) within the PVD specific perspex mask cut-out.

2.16.5 Stage 5: Must Touch; refer to 5-CSRTT training (section 2.11).

Modifications: Refer to stage 4.

2.16.6 Stage 6: Must Initiate; refer to 5-CSRTT training (section 2.11).

Modifications: Refer to stage 4.

2.16.7 Stage 7: Punish Incorrect; refer to 5-CSRTT training (section 2.11).

Modifications: No correction trials, no omissions (stimulus duration infinite); Refer to stage 4.

2.17 PVD Training

Stage 8: This is an acquisition phase, where the mouse was required to utilize the visual features of two different stimuli presented simultaneously to learn a stimulus-reward relationship. During the PVD acquisition phase the maximum number of trials was capped at 30 and the schedule timer was limited to 60 minutes. Additionally, timeouts paired to the house light were set to 5 seconds, ITI was 20 seconds, tone was 3Khz lasting 1000ms and paired with the milkshake reward (7 μ l). To initiate the session, 7 μ l of free milkshake reward was primed in the reward magazine tray, once the mouse withdrew the first trial began (detected by IR beams). A simultaneous presentation of S+ and S- stimuli in the two windows then followed. The stimuli were presented pseudo-randomly, such that image location repetitions did not exceed three consecutive left or right presentations. Correct responses to the S+ then simultaneously elicited a tone and reward administration into the illuminated reward magazine tray. Withdrawal from the reward magazine tray triggered the ITI. Once the ITI had ended, the reward magazine tray illuminated and the mouse was required to enter and withdraw to initiate the next trial. Incorrect responses (touching the S-) resulted in a 5 second timeout paired with the house light turning on. Once the timeout had expired the house light turned off and the ITI-incorrect began, lasting 20 seconds. Following the ITI the reward magazine tray was illuminated and the mouse was required to enter and withdraw to complete a correction trial. Correction trials presented the S+ and S- from the previous trial in their prior spatial locations. This was repeated for each subsequent trial until the mouse correctly responded to the S+. Correction trial responses did not contribute toward completion criterion for the session. Once the mice have reached criterion (24/30 correct for two consecutive days) they were transitioned to the next stage.

2.17.1 Stage 9: Immediately following stage 8 the performance of the mice was baselined for two consecutive days. The protocol was identical to stage 8, however, there was no correct response threshold requirement to progress to the next stage.

2.17.2 Stage 10: This stage is referred to as reversal. All conditions, penalties and parameters were identical to that of stages 8 and 9, with one exception. The stimulus-milkshake reward pairing was reversed. Here, the previous S+ is unrewarded (new S-) and the previous S- is rewarded (new S+). Correction trial results did not contribute toward completion criterion for the session.

2.18 dPAL Shaping

Shaping for mice being investigated with the dPAL task was completed prior to PVD Training. Refer to rodent shaping and PVD training (sections 2.11 & 2.18 respectively).

2.19 dPAL Training

2.19.1 Stage 8: This is an acquisition phase, where the mouse was required to utilize the combined visual and spatial features of two distinct stimuli presented simultaneously to acquire correct image and location pairings. The dPAL task utilized a triple window perspex mask layout. During dPAL acquisition the maximum number of trials was 36, with the schedule timer terminating sessions after 60-minutes. Additionally, the ITI was locked to 20 seconds, tone was 3Khz lasting 1000ms and paired to the milkshake reward, which had its distribution volume set to 7 μ l. To start the session 7 μ l of free milkshake was primed in the reward magazine tray, once the mouse withdrew from the reward magazine tray the first trial began (detected by IR beams). A simultaneous presentation of a S+ image/location coupling and a S- image/location coupling was then presented in 2 of 3 windows, the third window was blank. Correctly responding to the S+ image/location elicited a tone concomitant with the administration of milkshake reinforcement into the illuminated reward magazine tray. Once the mouse withdrew from the reward magazine tray the ITI started. Following the ITI the mouse was then required to enter and withdraw from the reward magazine to progress to the next trial. Importantly, incorrect responses did not elicit a delay time out period, further an omission feature was not present. Mice could not

progress to subsequent trials without a correct response being made. Progression criterion was set to 36 trials completed within a single 60-minute session.

2.19.2 Stage 9: The dPAL evaluation stage immediately followed stage 8, and consisted of 45 sessions (5 sessions [1 bin] per week) . Parameters for number of trials, schedule timer, ITI, tone, and milkshake reinforcer administration were all identical to stage 8. The demands of the task during the dPAL evaluation phase differed only with the introduction of a time out delay period (5s) and correction trials. The timeout delay was triggered by an incorrect response selection (S- image/location coupling) and was paired to the house light turning on. Once the timeout delay had elapsed the ITI was initiated, which was then followed by the reward magazine tray being illuminated. At this point mice were required to enter and withdraw from the reward magazine tray to start a correction trial. A response was required, as omissions were not a feature of this task. Correction trials re-presented the S+ and S- image/location couplings presented in the previous trial. This was repeated for each subsequent trial until the mouse correctly responded to the S+ image/location coupling. Correction trial results did not contribute toward completion criterion for the session. Completion criterion was defined as 36 trials completed within a single 60-minute session, for 45 days.

2.20 Primary Touchscreen Parameters

The ABET II touchscreen software automatically organizes and compiles rodent behavioural responses into various metrics for subsequent performance evaluations and post-processing quality control. The central metrics used to analyze behaviour are as follows:

Sessions/Trials to Criterion (Acquisition; PVD, 5-CSRTT): number of sessions/trials required by an animal to reach the desired performance baselines (e.g., 80%) during training.

Accuracy (% Correct; PVD, dPAL, 5-CSRTT): the number of successful operant responses to the S+ represented as a percentage.

Correction Trials (PVD, dPAL): the number of trial re-presentations required by the animal before a correct response to the S+ is emitted.

Breakpoint (PR): the peak number of responses elicited by an animal for a single food reinforcer within the last trial successfully completed.

Omissions (5-CSRTT): the failure of an animal to elicit an operant response to the touchscreen during the stimulus presentation and 5-second limited hold.

Perseverative Response (5-CSRTT, PRFR): the total number of operant responses elicited following stimulus removal.

Correct Touch Latency (PVD, dPAL, 5-CSRTT, PRFR): the amount of elapsed time following a stimulus presentation and a successful operant response to the S+.

Incorrect Touch Latency (PVD, dPAL, 5-CSRTT, PRFR): the amount of elapsed time following a stimulus presentation and an incorrect operant response to the S-.

Reward Collection Latency (PVD, dPAL, 5-CSRTT, PRFR): the amount of elapsed time following a successful operant response to the S+ and IR-beam detection of entry into the reward magazine tray.

2.21 Cohorts and Behavioural Testing Schedule

Data has been obtained from two separate cohorts of the TDP-43^{Q331Klow} mutant mouse line and their littermate controls. Additionally, data has also been obtained from two separate cohort of the TDP-43^{G348C} mouse line and their littermate controls.

	AGE (MONTHS)	AGE (MONTHS)	AGE (MONTHS)	AGE (MONTHS)	AGE (MONTHS)				
	AGING MICE + FOOD RESTRICTION AT 3 MONTHS	4	5	6	7	8	9	10	11
COHORT 1 Q331Klow wt n=9, het n=12	BATTERY OF MOTOR TESTS, 3 DAYS BEFORE TOUCHSCREEN TESTING; 3 SEPARATE DAYS	PAIRWISE VISUAL DISCRIMINATION (PVD) IMAGES: MARBLE/FAN			MAINTENANCE + BATTERY OF MOTOR TESTS, 3 DAYS BEFORE TOUCHSCREEN TESTING; 3 SEPARATE DAYS	DIFFERENT PAIRED ASSOCIATES LEARNING TASK (dPAL) IMAGES: FLOWER/PLANE/SPIDER			
COHORT 2 Q331Klow wt n=9, het n=15		5-CHOICE SERIAL REACTION TIME TASK (5-CSRTT) IMAGES: BLANK WHITE SQUARE				5-CHOICE SERIAL REACTION TIME TASK (5-CSRTT) IMAGES: BLANK WHITE SQUARE			PROGRESSIVE RATIO/FIXED RATIO (PRFR) IMAGES: BLANK WHITE SQUARE
COHORT 1 G348C wt n=11, het n=14		PAIRWISE VISUAL DISCRIMINATION (PVD) IMAGES: MARBLE/FAN				DIFFERENT PAIRED ASSOCIATES LEARNING TASK (dPAL) IMAGES: FLOWER/PLANE/SPIDER			
COHORT 2 G348C wt n=4, het n=8		5-CHOICE SERIAL REACTION TIME TASK (5-CSRTT) IMAGES: BLANK WHITE SQUARE				5-CHOICE SERIAL REACTION TIME TASK (5-CSRTT) IMAGES: BLANK WHITE SQUARE			PROGRESSIVE RATIO/FIXED RATIO (PRFR) IMAGES: BLANK WHITE SQUARE

Figure 2. Experimental design outlining the sequence of behavioural testing in TDP-43^{Q331Klow} and TDP-43^{G348C} mutant mice.

2.22 Statistical Analyses

JASP stats version 0.13.1 (<https://jasp-stats.org>) and GraphPad PRISM version 8.4.3 (GraphPad Software, Inc., San Diego, California) were used to conduct all statistical analyses. PVD, PAL, 5-CSRTT, PRFR and motor tests were analysed based on mean performance over sessions (10, 45, 2, 2; respectively). Between-group differences were evaluated with t-test or Welch's t-test, contingent on distribution of data. Repeated-measures data were analysed using two-way repeated measures- (RM) analysis of variance (ANOVA) with significance set to $p < 0.05$. Violations of sphericity indicated by Mauchly's test of sphericity were corrected with the Greenhouse-Geisser correction. Homogeneity of variance was tested using Levene's test. All post-hoc tests carried out utilized either the Bonferroni correction or simple main effect analyses. Data presented as mean \pm standard error of measurement (SEM). Significance set to $p < 0.05$. All data were analyzed separately at 4-months, 8-months and 11-months of age.

3. Results

3.1 Motor Performance Battery: TDP-43^{Q331Klow} Mice

Rodent motor performance was evaluated prior to cognitive testing and during maintenance periods to identify any potential ALS-like motor deficits, and the possibility of such deficits affecting performance during touchscreen tasks.

Initially, we determined grip force in 4-month-old and 8-month old TDP-43^{Q331Klow} mutant mice. We found no difference in grip strength in 4 month-old TDP-43^{Q331Klow} mutants compared with littermate controls (**Figure 3A**; Welch's t-test, $t_{(18.82)} = 0.654$, $p = 0.520$). In contrast, in 8-month-old TDP-43^{Q331Klow} mutants we observed a significantly reduced peak grip force strength when compared to littermate controls. (**Figure 3B**; Welch's t-test, $t_{(40.36)} = 3.385$, $p = 0.001$).

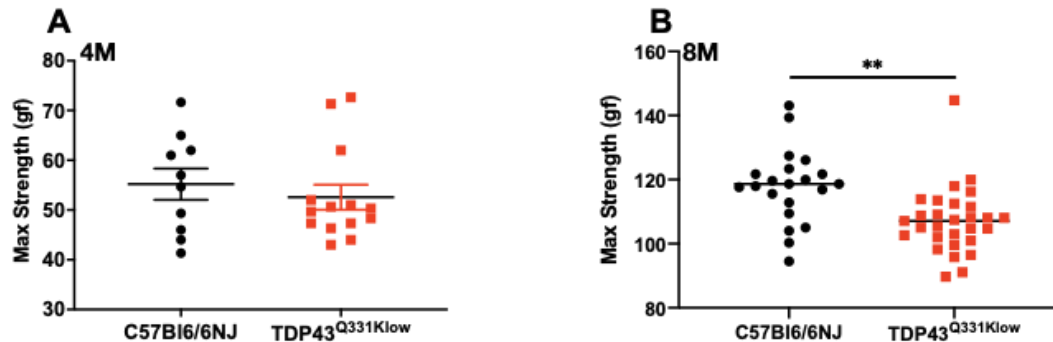


Figure 3. TDP-43^{Q331Klow} mutant mice 4-month and 8-month peak grip force performance. At 4-months no significant differences in peak grip force were observed. At 8-months TDP-43^{Q331Klow} mutants had lower peak grip force strength compared to controls (het n=27, wt n=18, **p<0.01).

Sustained motor performance was evaluated with wire hang tests in 4-month-old and 8-month-old TDP-43^{Q331Klow} mutant mice. We could not detect any difference in performance in these two ages for the TDP-43 mutant mice compared to controls (**Figure 4A**; *trial 1*: $t_{(6.82)} = 0.260$, $p = 0.801$; *trial 2*: no statistical difference; identical values: *trial 3*: $t_{(8)} = 1.000$, $p = 0.346$, **Figure 4B**; *trial 1*: $t_{(8)} = 1.000$, $p = 0.346$; *trial 2*: $t_{(8)} = 1.000$, $p = 0.346$; *trial 3*: $t_{(6.82)} = 0.260$, $p = 0.801$).

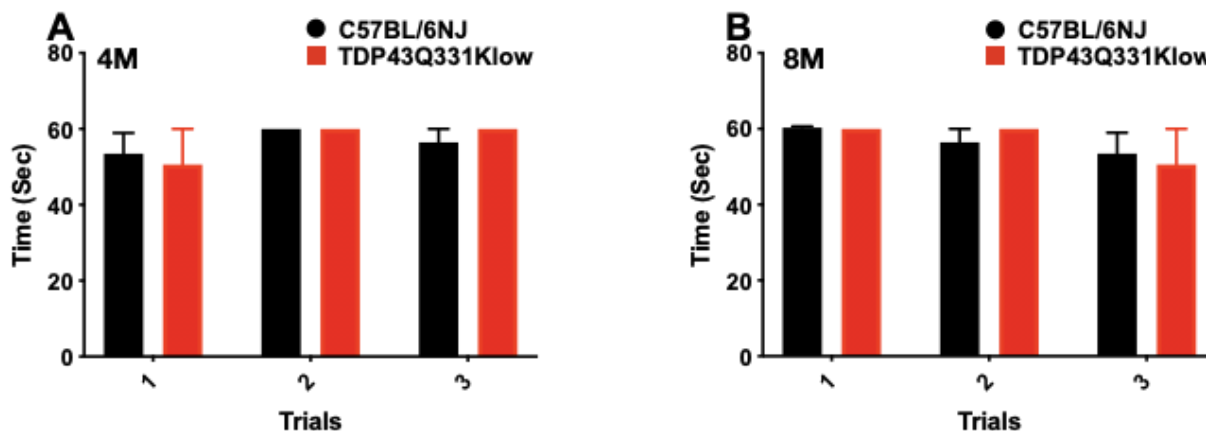


Figure 4. TDP-43^{Q331Klow} mutant mice 4-month and 8-month wire hang performance. No significant differences were observed at 4- or 8-months (het n=27, wt n=18).

To investigate overall movement, we used automated locomotor boxes (Janickova, Prado, et al., 2017; Janickova, Rosborough, et al., 2017). No significant differences were detected in locomotor activity in 4-month-old TDP-43^{Q331Klow} mutant mice when compared to littermate controls (**Figure 5A**; no main effect of genotype, $F_{(1,22)} = 0.029$, $p = 0.865$; main effect of time, $F_{(4.18,92.03)} = 18.832$, $p = 0.001$; and no significant genotype and time interaction, $F_{(4.18,92.03)} = 0.410$, $p = 0.809$). Similar results were obtained at 8 months of age (**Figure 5B**; no genotype effect $F_{(1,12)} = 4.210$, $p = 0.063$; no effect of time, $F_{(11,132)} = 0.780$, $p = 0.660$; and no significant interaction between genotype and time $F_{(11,132)} = 1.033$, $p = 0.421$). Interestingly, as observed previously, mice under food restriction at 8 months of age did not habituate to the locomotor boxes (Mels, 2018).

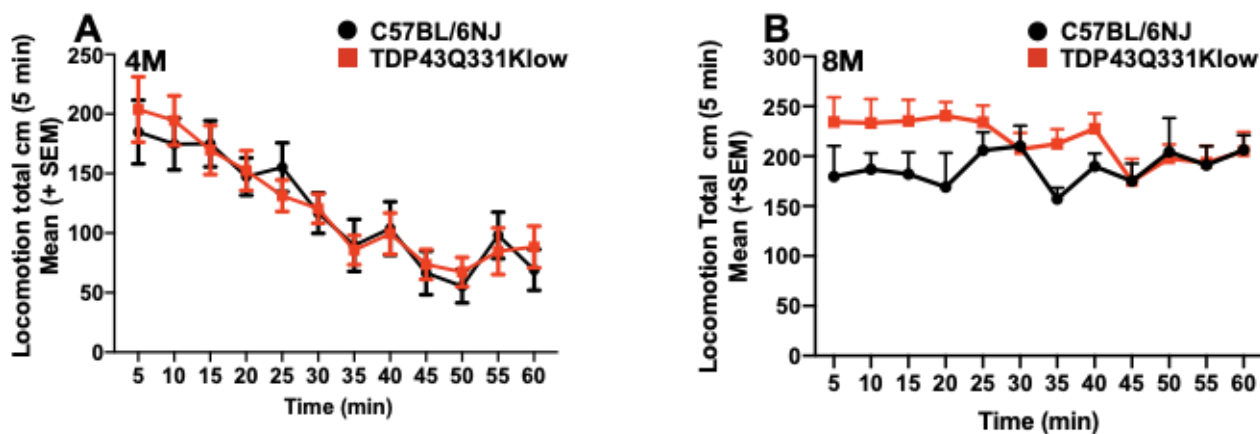


Figure 5. TDP-43^{Q331Klow} mutant mice 4-month and 8-month locomotor behaviour.

No significant differences were observed at 4- or 8-months. Mean locomotion in 5-minute intervals over a sustained 60-minute testing period (het n=27, wt n=18).

3.2 Motor Performance Battery: TDP-43^{G348C} Mice

We also determined grip force in 4-month-old and 8-month old TDP-43^{G348C} mutant mice. We observed no difference in grip strength in 4 month-old TDP-43^{G348C} mutants compared with littermate controls (**Figure 6A**; Welch's t-test, $t_{(24.85)} = 1.078$, $p = 0.291$). Interestingly, similar to results obtained in TDP-43^{Q331Klow} mutant mice, 8-month-old TDP-43^{G348C} mutants presented reduced peak grip force strength when compared to littermate controls. (**Figure 6B**; Welch's t-test, $t_{(22.57)} = 2.625$, $p = 0.015$).

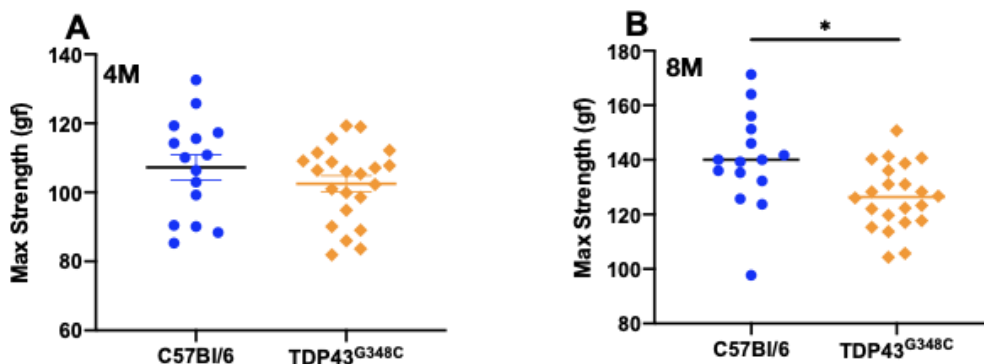


Figure 6. TDP-43^{G348C} mutant mice 4-month and 8-month peak grip force performance. At 4-months no significant differences in peak grip force were observed. At 8-months TDP-43^{G348C} mutants had lower peak grip force strength compared to controls (het n=22, wt n=15, data are mean \pm SEM, * $p < 0.05$).

We also looked to evaluate sustained motor performance in the TDP-43^{G348C} mice at 4- and 8-months-old. Motor performance appeared unaltered at these two ages for TDP-43^{G348C} mutant mice when compared to controls, similar to the results obtained with TDP-43^{Q331Klow} (**Figure 7A**; trial 1: $t_{(39.77)} = 0.334$, $p = 0.739$; trial 2: $t_{(21)} = 1.801$, $p = 0.086$; trial 3: $t_{(44.65)} = 0.350$, $p = 0.727$, **Figure 7B**; trial 1: $t_{(34.69)} = 0.354$, $p = 0.725$; trial 2: $t_{(14)} = 1.467$, $p = 0.164$; trial 3: $t_{(21)} = 1.000$, $p = 0.328$).

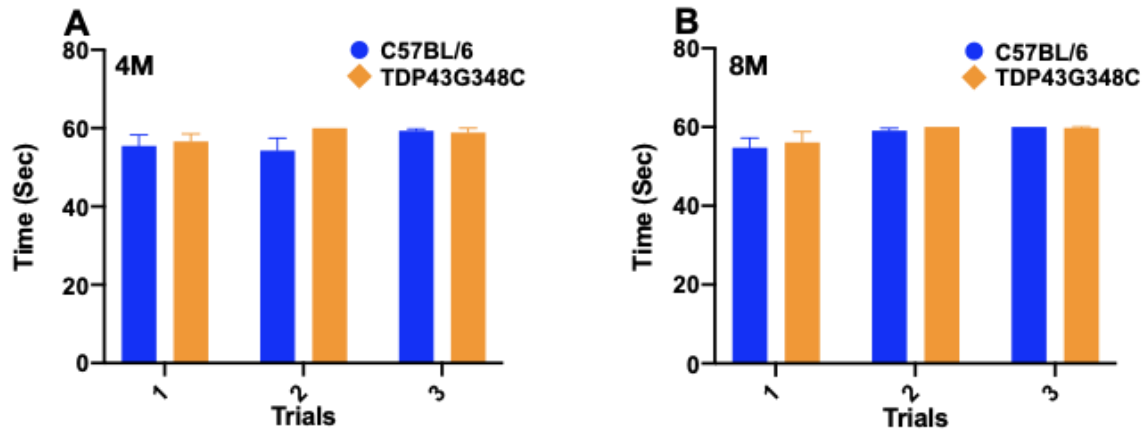


Figure 7. TDP-43^{G348C} mutant mice 4-month and 8-month wire hang performance. No significant differences were observed at 4- or 8-months (het n=22, wt n=15).

No significant differences were detected in locomotor activity in 4-month-old TDP-43^{Q331Klow} mutant mice when compared to littermate controls (**Figure 8A**; no main effect of genotype, $F_{(1,42)} = 0.059$, $p = 0.810$; main effect of time, $F_{(5.05,212.47)} = 3.387$, $p = 0.006$; and no significant genotype and time interaction, $F_{(5.05,212.47)} = 0.511$, $p = 0.770$). Similar results were obtained at 8 months of age (**Figure 8B**; no genotype effect $F_{(1,10)} = 0.426$, $p = 0.529$; no effect of time, $F_{(11,110)} = 0.945$, $p = 0.501$; and no significant interaction between genotype and time $F_{(11,110)} = 0.611$, $p = 0.816$). Again, mice under food restriction at 8 months of age did not habituate to the locomotor boxes (Mels, 2018). Overall, motor performance in the two TDP-43 mouse lines showed essentially similar results, with a decrease in grip strength in 8-month-old mice, without any other gross change.

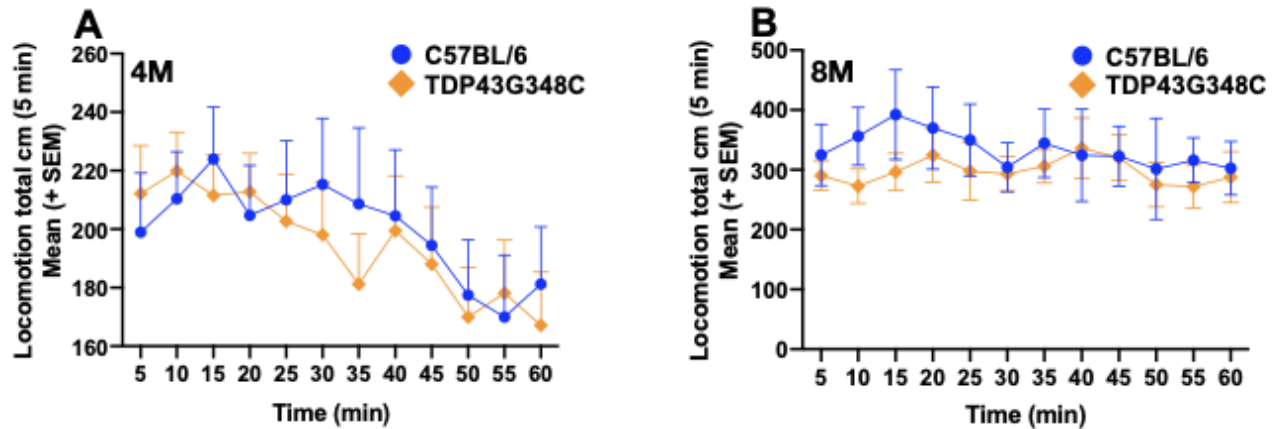


Figure 8. TDP-43^{G348C} mutant mice 4-month and 8-month locomotor behaviour. No significant differences were observed at 4- or 8-months. Mean locomotion in 5-minute intervals over a sustained 60-minute testing period (het n=22, wt n=15).

3.3 PVD Task Learning and Cognitive Flexibility in 4-month-old TDP-43^{Q331Klow}

Learning and cognitive flexibility were assessed in TDP-43^{Q331Klow} mutants for potential FTD/ALS-related cognitive deficits using the PVD and reversal touchscreen test.

TDP-43^{Q331Klow} mutants required more sessions to reach performance criterion in comparison to their littermate controls (**Figure 9A**; Welch's t-test, $t_{(20,12)} = 2.447$, $p = 0.023$).

Once mice reached a stable performance, the contingency on the PVD task was reversed (Fig. 9B). TDP-43^{Q331Klow} mutant mice made significantly more errors during reversal learning at 4-months-old in comparison to littermate controls (**Figure 9B**; Main effect of genotype, $F_{(1,14)} = 8.456$, $p = 0.011$; main effect of session, $F_{(4,14,58,04)} = 47.668$, $p < 0.001$; no interaction effect between genotype and session $F_{(4,14,58,04)} = 1.970$, $p = 0.109$). Consistent with these results, TDP-43^{Q331Klow} mutants required significantly more correction trials in comparison to littermate controls (**Figure 9C**; significant main effect of genotype $F_{(1,15)} = 7.735$, $p = 0.014$; significant main effect of session, $F_{(3,92,58,83)} = 24.092$, $p < 0.001$; no interaction effect between genotype and session, $F_{(3,92,58,83)} = 0.847$, $p = 0.499$).

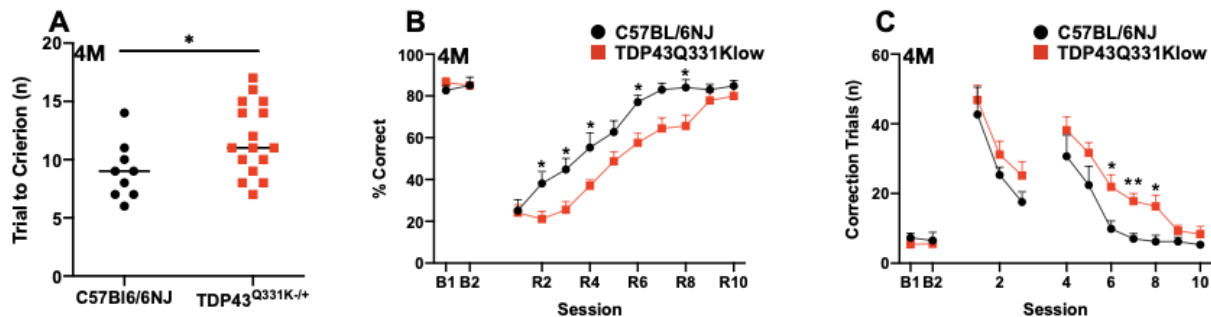


Figure 9. TDP-43^{Q331Klow} mutant mice 4-months, PVD task acquisition (A; learning), reversal learning performance (B), and correction trials (C). TDP-43^{Q331Klow} mutants required significantly more sessions to acquire the task, had significantly lower accuracy during reversal learning, and required significantly more correction trials (het n=12, wt n=9, data are mean \pm SEM, * p <0.05, ** p <0.01).

We also analysed various latency measures in 4-month-old TDP-43^{Q331Klow} mutants undergoing PVD testing to gain insight into their motivation to perform the task. TDP-43^{Q331Klow} mutants needed marginally more time to collect reward following correct responses in comparison to littermate controls (**Figure 10A**; significant main effect of genotype, $F_{(1,18)} = 6.042$, $p = 0.024$; significant main effect of session, $F_{(2.44,43.92)} = 3.368$, $p = 0.035$; no interaction between genotype and session, $F_{(2.44,43.92)} = 0.994$, $p = 0.392$). When making correct responses TDP-43^{Q331Klow} mutant mice required significantly more time in contrast to littermate controls (**Figure 10B**; significant main effect of genotype, $F_{(1,18)} = 6.977$, $p = 0.017$, indicating on average TDP-43^{Q331Klow} mutant mice required more time for correct responses per session; significant main effect of session, $F_{(2.53,45.58)} = 12.088$, $p = <0.001$; There was no interaction effect between genotype and session $F_{(2.53,45.58)} = 2.649$, $p = 0.069$). We also assessed incorrect touch latencies in TDP-43^{Q331Klow} mutant mice and similar to the results of correct touch latency, TDP-43^{Q331Klow} mutant mice required significantly more time prior to emitting an incorrect response in comparison to littermate controls in the first reversal tests, lowering their performance to that of controls in the later stages of testing (**Figure 10C**; significant main effect of genotype, $F_{(1,15)} = 10.23$, $p = 0.006$, indicating on average TDP-43^{Q331Klow} mutant mice needed additional time to emit an incorrect response per session; significant effect of session, $F_{(5.44,81.73)} = 5.777$, $p = <0.001$; no interaction effect between genotype and session $F_{(5.44,81.73)} = 1.820$, $p = 0.112$).

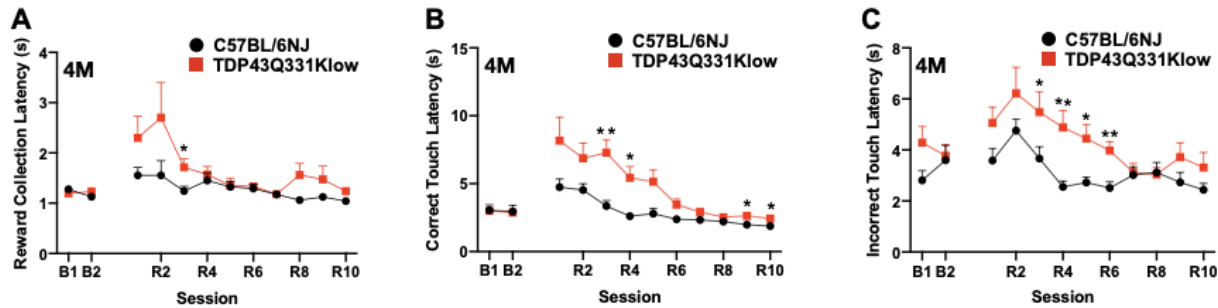


Figure 10. 4-month-old TDP-43^{Q331Klow} mutant mice latency data. Reward collection latency (A), correct touch latency (B) and incorrect touch latency (C). TDP-43^{Q331Klow} mutants required marginally more time to collect reward, significantly more time to initiate correct responses and significantly more time to emit incorrect responses (het n=12, wt n=9, data are mean \pm SEM, * $p < 0.05$, ** $p < 0.01$).

3.4. 4-month-old TDP-43^{G348C} Learning and Cognitive Flexibility in the PVD Task

We performed similar PVD assays in TDP-43^{G348C} mutants to determine whether there are common PVD deficits that overlap between mouse models.

Similar to TDP-43^{Q331Klow} mutant mice, TDP-43^{G348C} mutants require more sessions to reach performance criterion in comparison to their littermate controls (**Figure 11A**; Welch's t-test, $t_{(22.09)} = 2.077$, $p = 0.049$).

We then tested for FTD/ALS-like impairments in cognitive flexibility in these mice. We reversed the stimulus-reward contingency and found that TDP-43^{G348C} mutant mice made significantly more errors during reversal learning at 4-months-old in comparison to littermate controls (**Figure 11B**; significant main effect of genotype, $F_{(1,18)} = 6.235$, $p = 0.022$; significant main effect of session, $F_{(3.79,68.28)} = 39.11$, $p < 0.001$; no interaction effect between genotype and session $F_{(3.79,68.28)} = 1.023$, $p = 0.399$). Throughout the reversal, particularly in later stages, 4-month-old TDP-43^{G348C} mutant mice did not significantly differ from littermate controls in the number of required correction trials (**Figure 11C**; no genotype effect, $F_{(1,18)} = 2.280$, $p = 0.148$; significant main effect of session, $F_{(3.74,67.39)} = 18.341$, $p < 0.001^a$; no significant interaction detected between genotype and session, $F_{(3.74,67.39)} = 0.983$, $p = 0.419$).

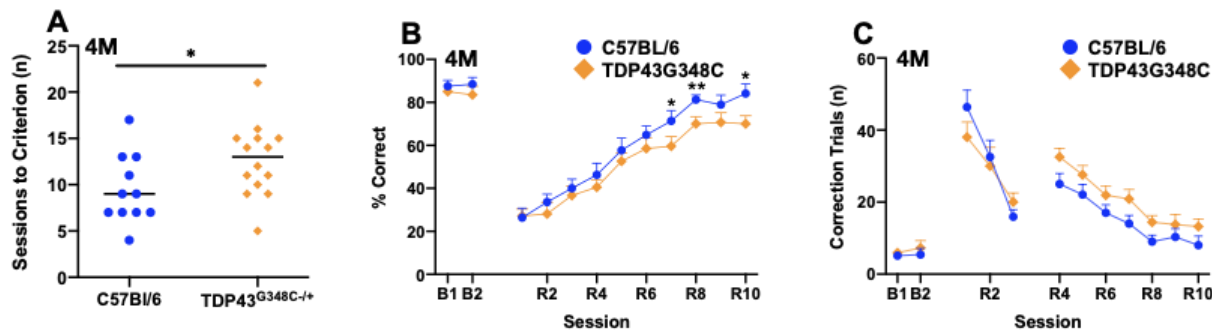


Figure 11. TDP-43^{G348C} mutant mice 4-month, PVD task acquisition (A; learning) and reversal learning performance (B) and correction trials (C). It was found that TDP-43^{G348C} mutants required significantly more sessions to acquire the task, had significantly lower accuracy during reversal learning and exhibited a highly similar number of required correction trials (het n=14, wt n=11, data are mean \pm SEM, * p <0.05, ** p <0.01).

We also sought to evaluate motivation of 4-month-old TDP-43^{G348C} mice in the PVD task through observed latencies as done similarly in the TDP-43^{Q331K^{low}} mice. It was revealed that 4-month-old TDP-43^{G348C} mutant mice reward collection latencies did not significantly differ compared to littermate controls (**Figure 12A**; no genotype effect, $F_{(1,22)} = 0.168$, $p = 0.686$; no effect of session $F_{(2.47,54.44)} = 2.678$, $p = 0.066$; no. interaction effect between genotype and session, $F_{(2.47,54.44)} = 0.495$, $p = 0.652$). We continued latency evaluations with correct touch latencies. It was revealed that TDP-43^{G348C} mutant mice required significantly less time before eliciting a correct response in contrast to littermate controls (**Figure 12B**; no effect of genotype, $F_{(1,23)} = 0.011$, $p = 0.917$; significant main effect of session, $F_{(4.51,103.80)} = 10.528$, $p = <0.001^a$; significant interaction effect between genotype and session $F_{(4.51,103.80)} = 2.385$, $p = 0.049$). This interaction was explored with simple main effects revealing a significantly lower correct touch latency at R10 during the reversal phase, $p = 0.029$. Incorrect touch latencies were also evaluated in 4-month-old TDP-43^{G348C} mutant mice. It was revealed that mutant mice did not significantly differ from littermate controls (**Figure 12C**; no effect of genotype, $F_{(1,20)} = 0.687$, $p = 0.417$; no effect of session, $F_{(6.03,120.63)} = 1.618$, $p = 0.147$; no interaction effect between genotype and session $F_{(6.03,120.63)} = 1.796$, $p = 0.105$).

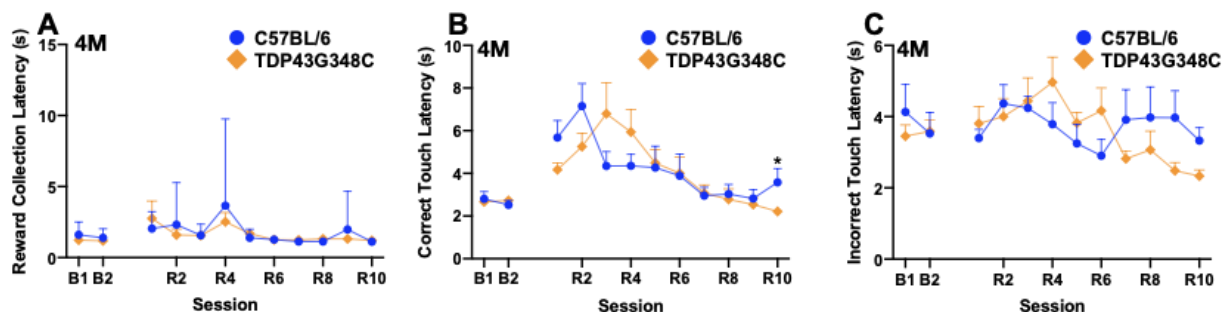


Figure 12. TDP-43^{G348C} mutant mice 4-month PVD task reward collection latency (A), correct touch latency (B) and incorrect touch latency (C). No significant differences were observed in reward collection latencies, correct touch latencies and incorrect touch latencies (het n=14, wt n=11, data are mean \pm SEM, * $p < 0.05$).

To clearly visualize and compare the major similarities in performance from the PVD task in the two TDP-43 mutant mouse lines we assembled a graph with the main findings (**Figure 13**; significant main effect of genotype, $F_{(3,32)} = 5.590$, $p = 0.003$; significant main effect of session, $F_{(4.89,156.57)} = 96.827$, $p < 0.001$; no interaction effect between genotype and session $F_{(4.89,156.57)} = 1.241$, $p = 0.399$). These findings highlight that both TDP-43^{Q331Klow} and TDP-43^{G348C} mutant mouse lines exhibit highly similar deficits during acquisition, and their performance during reversal learning also demonstrates very strong similarities.

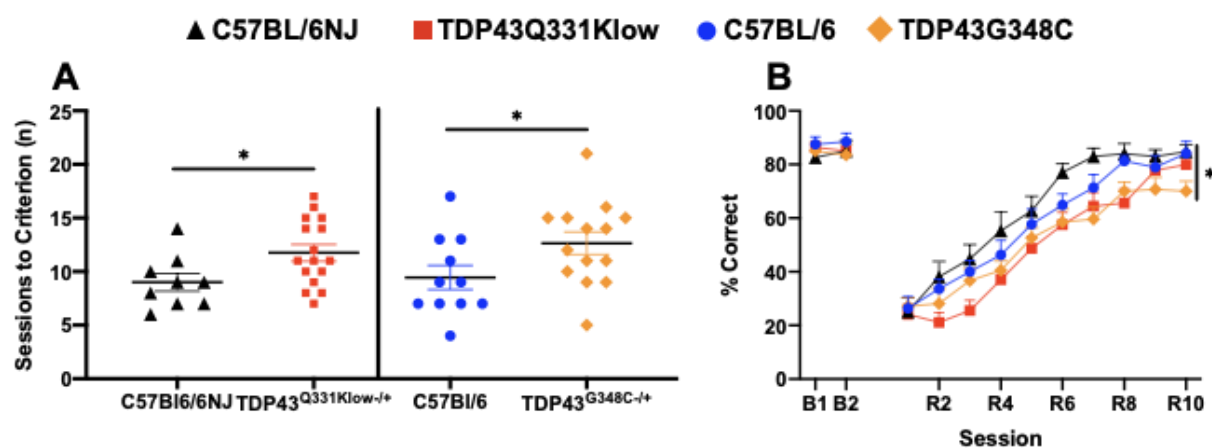


Figure 13. Combined PVD task data from TDP-43^{Q331Klow} and TDP-43^{G348C} mutant mice (Figures 9A-B; 14A-B). TDP-43^{Q331Klow} and TDP-43^{G348C} mutants display a similar pattern of deficits during task acquisition and during the reversal learning phase.

3.5 dPAL Visuospatial Memory Performance of 8-month-old TDP-43^{Q331Klow}

Visuospatial memory performance was assessed in TDP-43^{Q331Klow} mutants to determine potential FTD/ALS-related cognitive deficits using the dPAL task.

Given the deficits in visual discrimination and reversal observed in both TDP-43 mice we further tested for learning and memory impairments using the PAL task. Both mouse lines were tested in PAL after their PVD testing. No significant differences in accuracy were observed in 8-month old TDP-43^{Q331Klow} mutant mice compared to littermate controls (**Figure 14A**; no effect of genotype, $F_{(1,25)} = 0.759$, $p = 0.392$; significant main effect of week, $F_{(4.92,123.01)} = 93.396$, $p < 0.001$; No significant interaction effect between genotype and session $F_{(4.92,123.01)} = 1.38$, $p = 0.235$). Similar to PVD we evaluated latency data as a proxy for motivation in TDP-43^{Q331Klow} mice. Reward collection latencies were evaluated in 8-month-old TDP-43^{Q331Klow} mutant mice revealing no significant differences from littermate controls (**Figure 14B**; significant main effect of genotype, $F_{(1,25)} = 6.201$, $p = 0.020$; significant main effect of week, $F_{(3.42,85.71)} = 2.851$, $p = 0.036$; no interaction effect between genotype and week, $F_{(3.42,85.71)} = 1.287$, $p = 0.283$). Likewise, in the PAL test we found no significant differences when mutants were compared to littermate controls for correct touch latency (**Figure 14C**; no effect of genotype, $F_{(1,25)} = 4.070$, $p = 0.054$; significant main effect of week, $F_{(2.00,50.06)} = 8.704$, $p < 0.001$; no significant interaction effect between genotype and session $F_{(2.00,50.06)} = 1.745$, $p = 0.185$). Similarly, TDP-43^{Q331Klow} mutant mice revealed no significant differences from littermate controls in incorrect touch latencies (**Figure 14D**; significant main effect of genotype, $F_{(1,125)} = 4.262$, $p = 0.049$; no effect of week, $F_{(1.81,45.30)} = 2.237$, $p = 0.123$; no significant interaction effect between genotype and session $F_{(1.81,45.30)} = 1.129$, $p = 0.328$).

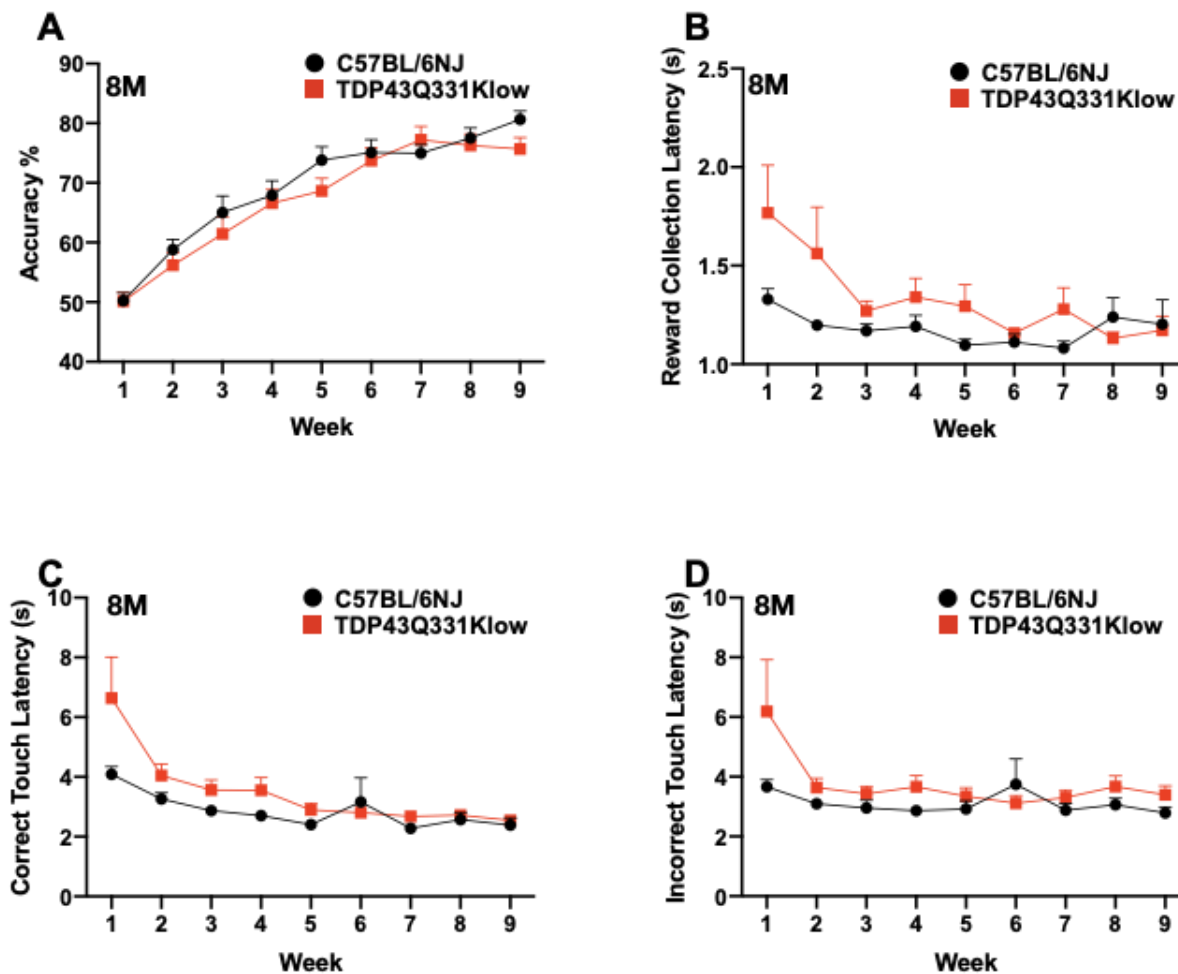


Figure 14. TDP-43^{Q331Klow} mutant mice 8-month PAL task accuracy (A), reward collection latency (B), correct touch latency (C) and incorrect touch latency (D). No significant differences were observed in any of the dPAL measures (het n=12, wt n=9).

3.6 dPAL Visuospatial Memory Performance of 8-month-old TDP-43^{G348C}

In similar fashion to TDP-43^{Q331Klow} mice, PVD assessments were subsequently followed up with visuospatial memory evaluations in TDP-43^{G348C} mice using the dPAL task.

Accuracy was evaluated in 8-month old TDP-43^{G348C} mutant mice during the dPAL task revealing no significant differences from littermate controls (**Figure 15A**; no effect of genotype, $F_{(1,23)} = 0.852$, $p = 0.366$; significant main effect of week, $F_{(4,16,95.76)} = 77.50$, $p < 0.001$; no interaction effect between genotype and session $F_{(4,16,95.76)} = 0.388$, $p = 0.824$). Reward collection latencies were also evaluated in 8-month-old TDP-43^{G348C} mutant mice. No significant differences were detected from comparisons to littermate controls (**Figure 15B**; no effect of

genotype, $F_{(1,23)} = 2.877$, $p = 0.103$; no effect of week, $F_{(1,26,29)} = 2.598$, $p = 0.111$; No interaction effect between genotype and week, $F_{(1,26,29)} = 2.512$, $p = 0.117$). Similarly, correct touch latencies were assessed in 8-month old TDP-43^{G348C} mutant mice and no significant differences were revealed when mutants were contrasted to littermate controls (**Figure 15C**; no effect of genotype, $F_{(1,23)} = 0.665$, $p = 0.423$; significant main effect of week, $F_{(1,75,40,25)} = 16.893$, $p < 0.001$; no significant interaction effect between genotype and session $F_{(1,75,40,25)} = 1.508$, $p = 234$). The last latency measure assessed in 8-month-old TDP-43^{G348C} mutant mice was incorrect touch latencies. No significant differences were detected from comparisons to littermate controls (**Figure 18D**; no effect of genotype, $F_{(1,23)} = 0.492$, $p = 0.490$; significant main effect of week, $F_{(1,95,44,95)} = 8.947$, $p = 0.001$; No interaction effect between genotype and session $F_{(1,95,44,95)} = 1.585$, $p = 0.217$).

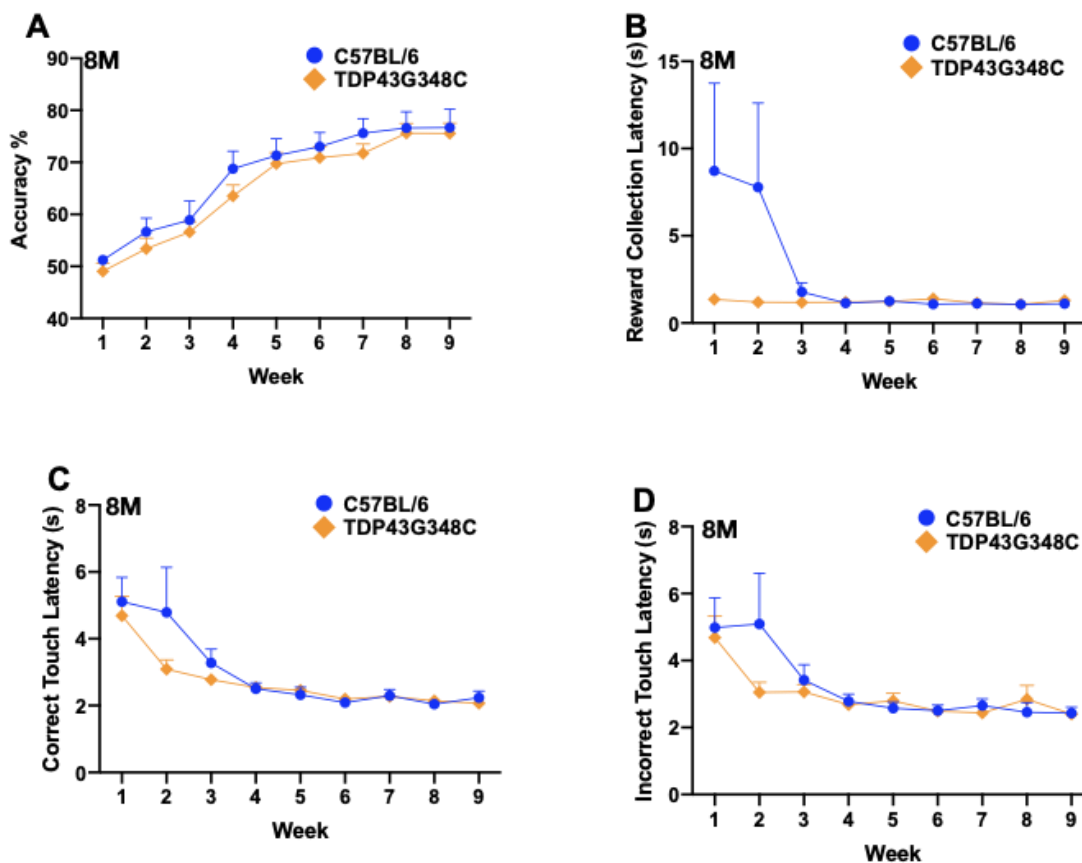


Figure 15. TDP-43^{G348C} mutant mice 8-month PAL task accuracy (A), reward collection latency (B), correct touch latency (C) and incorrect touch latency (D). No significant differences were observed among dPAL measures (het n=14, wt n=11).

3.7 5-CSRTT Probe of Attention Performance in 4-month-old TDP-43^{Q331Klow}

To further investigate executive function, we tested the TDP-43 mouse lines in a test of attention, 5-CSRTT.

TDP-43^{Q331Klow} mutant mice performed as well as control mice during 5-CSRTT training at 4 and 2 s (**Figure 16A**; Welch's t-test, $t_{(23.72)} = 0.1743$, $p = 0.863$, **Figure 16B**; Welch's t-test, $t_{(14.86)} = 0.2279$, $p = 0.822$).

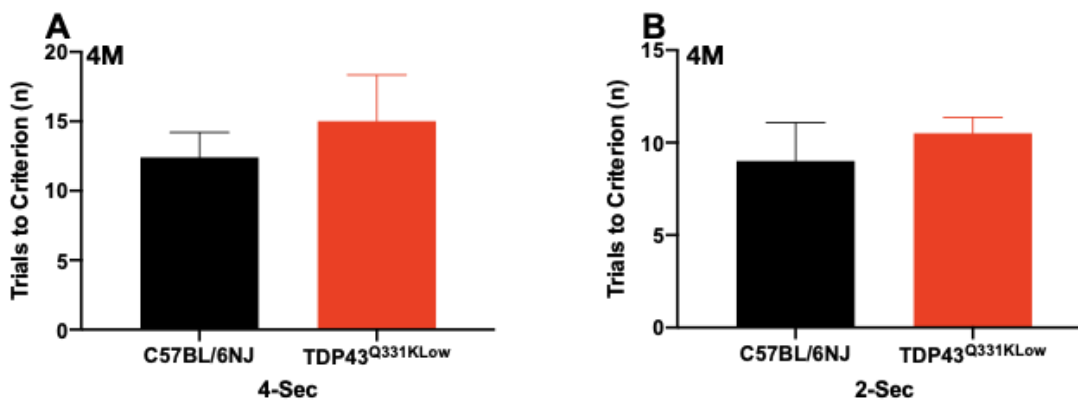


Figure 16. TDP-43^{Q331Klow} mutant mice 4-month 5-CSRTT trials to acquisition 4- and 2-seconds. No significant differences were observed (het n=15, wt n=9).

To investigate attentional demand 4-month-old mice were tested in probe trials (1.5, 1.0, 0.8 and 0.6s). Surprisingly, mutants differ significantly from littermate controls displaying *higher* accuracy (**Figure 17A**; main effect of genotype was significant, $F_{(1,21)} = 5.449$, $p = 0.030$; a significant main effect of stimulus duration, $F_{(3,63)} = 24.074$, $p < 0.001$, indicating significantly higher accuracy at longer stimulus durations; no interaction effect between genotype and stimulus duration $F_{(3,63)} = 0.422$, $p = 0.738$). Omissions were also recorded and we found a small but significant effect of increased omissions at 0.6s (**Figure 17B**; no effect of genotype, $F_{(1,21)} = 1.319$, $p = 0.264$; significant main effect of stimulus duration, $F_{(3,63)} = 43.222$, $p < 0.001$, indicating significantly higher omissions at longer stimulus durations; significant interaction effect between genotype and stimulus duration, $F_{(3,63)} = 3.299$, $p = 0.026$, This interaction was

explored with simple main effects which revealed significantly higher omissions during the 0.6-second stimulus duration, $p = 0.019$).

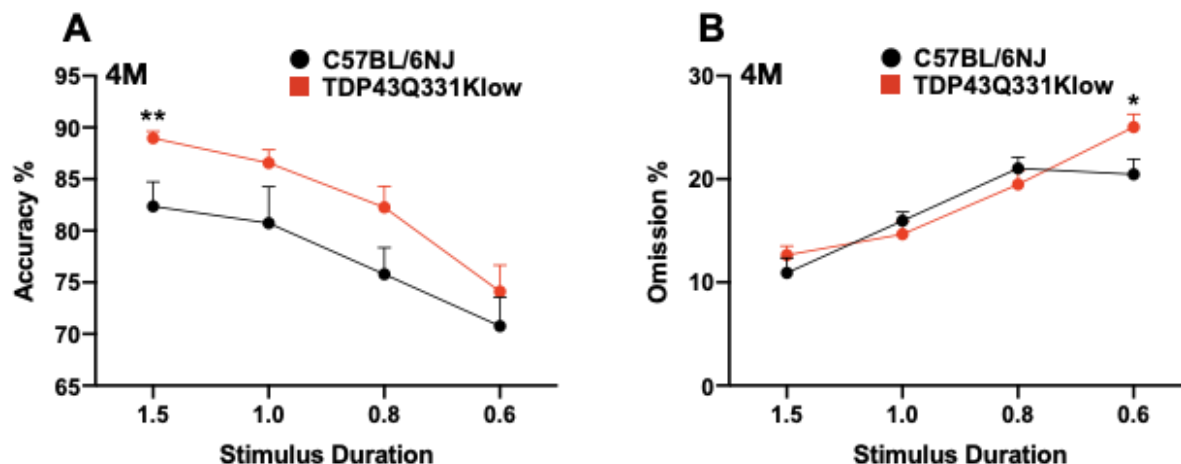


Figure 17. TDP-43^{Q331Klow} mutant mice 4-month 5-CSRTT accuracy (A) and omission (B). It was found that TDP-43^{Q331Klow} mutants exhibited significantly higher accuracy and omissions in comparison to controls (het n=15, wt n=9, data are mean \pm SEM, * $<p=0.05$, ** $<p=0.01$).

In line with other touchscreen tasks, various latency metrics were evaluated for insight into TDP-43^{Q331Klow} motivation. Reward collection latencies were investigated in 4-month-old TDP-43^{Q331Klow} mutant mice. It was found that mutants did not differ significantly from littermate controls (**Figure 18A**; no effect of genotype, $F_{(1,21)} = 2.367$, $p = 0.139$; no effect of stimulus duration, $F_{(2.03,42.80)} = 1.496$, $p = 0.235$; no significant interaction effect between genotype and stimulus duration, $F_{(2.03,42.80)} = 2.433$, $p = 0.099$). Similarly, correct touch latencies were evaluated in 4-month-old TDP-43^{Q331Klow} mutant mice. It was revealed that mutant mice did not significantly differ from littermate controls (**Figure 18B**; no effect of genotype, $F_{(1,21)} = 0.509$, $p = 0.483$; significant main effect of stimulus duration, $F_{(1.95,41.00)} = 32.789$, $p = <0.001$; No interaction effect between genotype and stimulus duration, $F_{(1.95,41.00)} = 0.489$, $p = 0.612$). The final 5-CSRTT latency metric assessed was incorrect touch latencies in 4-month-old TDP-43^{Q331Klow} mutant mice. It was found that mutant mice did not significantly differ from littermate controls (**Figure 18C**; No genotype effect, $F_{(1,21)} = 0.215$, $p = 0.648$; no stimulus duration effect, $F_{(3,63)} = 0.693$, $p = 0.560$; no interaction effect, $F_{(3,63)} = 0.904$, $p = 0.444$).

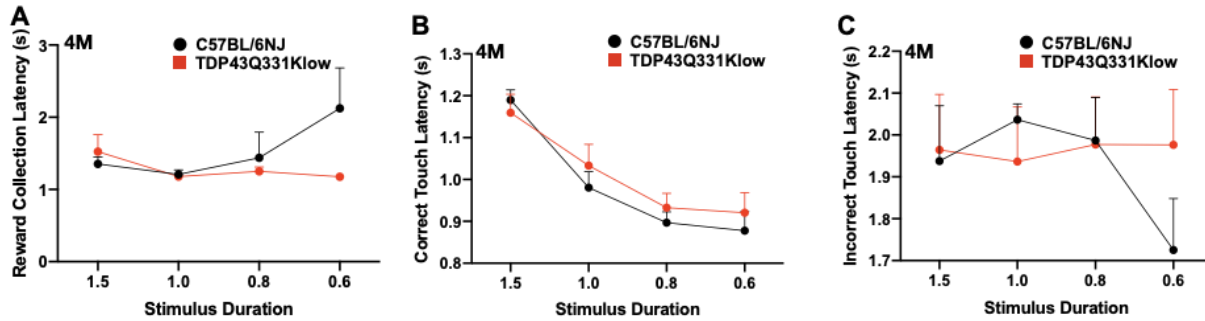


Figure 18. TDP-43^{Q331Klow} mutant mice 4-month 5-CSRTT reward collection latency (A) correct touch latency (B) and incorrect touch latency (C) No significant differences were observed (het n=15, wt n=9).

A behavioural component of interest during 5-CSRTT touchscreen testing is the actions surrounding the performance of responses to the touchscreens. Accordingly, we looked to evaluate premature and perseverative responses. It was found that 4-month-old TDP-43^{Q331Klow} mutant mice did not significantly differ from littermate controls in the number of premature responses emitted (**Figure 19A**; no effect of genotype, $F_{(1,19)} = 0.298$, $p = 0.591$; significant main effect of stimulus duration, $F_{(3,57)} = 3.177$, $p = 0.031$; no interaction effect between genotype and stimulus duration, $F_{(3,57)} = 0.942$, $p = 0.426$). Perseverative post-correct responses were also evaluated in 4-month-old TDP-43^{Q331Klow} mutant mice. It was found that mutants exhibited significantly higher perseverative responses when compared to littermate controls (**Figure 19B**; no effect of genotype, $F_{(1,20)} = 1.205$, $p = 0.285$; no effect of stimulus duration, $F_{(3,60)} = 0.531$, $p = 0.663$; significant interaction effect between genotype and stimulus duration, $F_{(3,60)} = 4.442$, $p = 0.007$). This interaction was explored with simple main effects revealing significantly higher TDP-43^{Q331Klow} mutant perseverative post-correct responses during the 1.0-second stimulus duration, $p = 0.017$. Similarly, perseverative post-incorrect responses were also evaluated in 4-month-old TDP-43^{Q331Klow} mutant mice. It was revealed that mutants did not differ from littermate controls with respect to perseverative responses (**Figure 19C**; No genotype effects, $F_{(1,5)} = 0.235$, $p = 0.649$; no effect of stimulus duration, $F_{(1.03,5.15)} = 0.454$, $p = 0.535$; No interaction effect between genotype and stimulus duration, $F_{(1.03,5.15)} = 0.536$, $p = 0.501$).

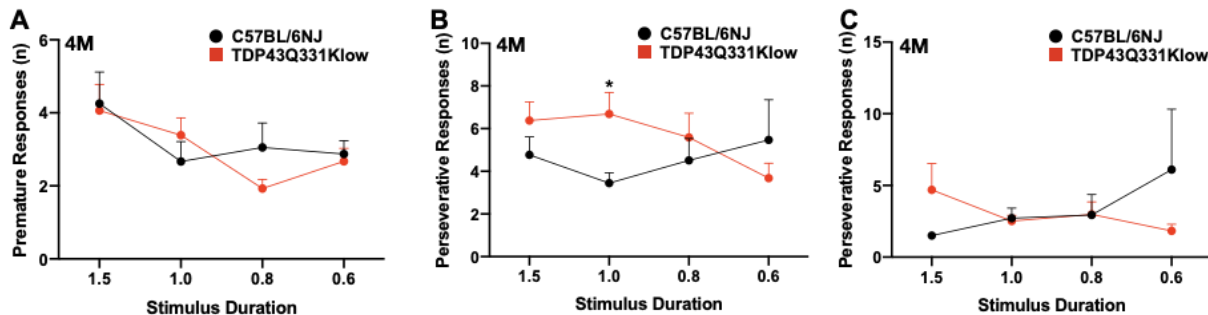


Figure 19. TDP-43^{Q331Klow} mutant mice 4-month 5-CSRTT premature responses (A), perseverative post-correct responses (B) and perseverative post-incorrect responses (C) No significant differences were observed among measures (het n=15, wt n=9, data are mean \pm SEM, * $p < 0.05$).

3.8 5-CSRTT Probe of Attention Performance in 8-month-old TDP-43^{Q331Klow}

To test for age-dependent effects of attention, we tested the TDP-43 mouse lines at a second time point in the 5-CSRTT.

TDP-43^{Q331Klow} mutant mice show progressive pathological changes (Arnold et al., 2013a). Accordingly, we wanted to explore whether older TDP-43 mice would have attentional performance at least consistent with 4-month-old TDP-43^{Q331K} mutant mice, or alternatively worse performance. To evaluate accuracy 8-month-old TDP-43^{Q331Klow} mutant mice were investigated. It was found that mutant mice significantly differ from littermate controls displaying higher accuracy (**Figure 20A**; no effect of genotype, $F_{(1,22)} = 2.628$, $p = 0.119$; significant main effect of stimulus duration, $F_{(3,66)} = 32.76$, $p < 0.001$, indicating significantly higher accuracy at longer stimulus durations; no significant interaction effect $F_{(3,66)} = 1.031$, $p = 0.385$). We also looked to reevaluate omissions in 8-month-old TDP-43^{Q331Klow} mutant mice. It was found that mutants significantly differed from littermate controls with higher omission behaviour (**Figure 20B**; no effect of genotype, $F_{(1,22)} = 0.059$, $p = 0.811$; significant main effect of stimulus duration, $F_{(3,66)} = 49.88$, $p < 0.001$, indicating significantly higher omissions at longer stimulus durations; significant interaction effect between genotype and stimulus duration, $F_{(3,66)} = 4.414$, $p = 0.009$). This interaction was explored with simple main effects which revealed significantly higher omissions during the 0.6-second stimulus duration, $p = 0.019$.

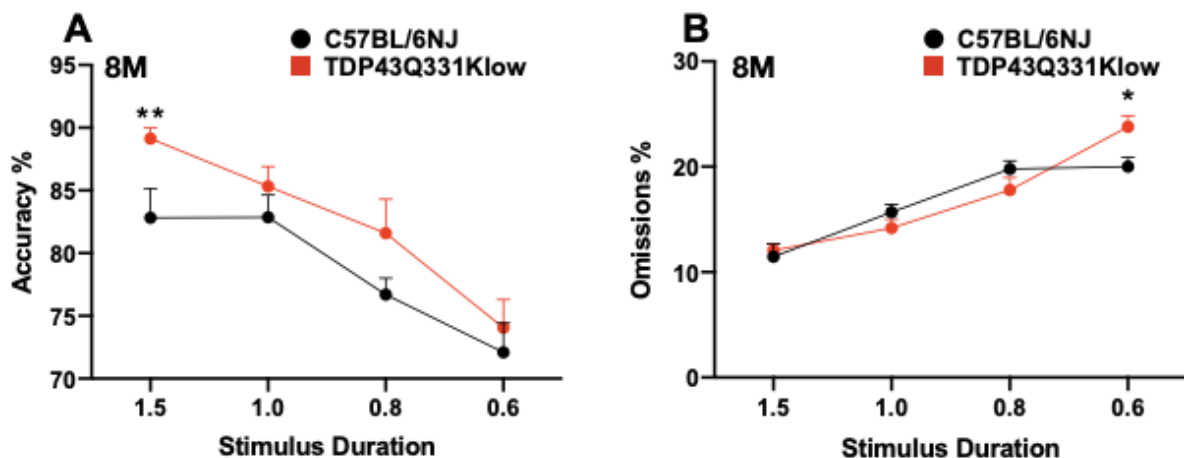


Figure 20. TDP-43^{Q331Klow} mutant mice 8-month 5-CSRTT accuracy (A) and omissions (B). It was found that TDP-43^{Q331Klow} mutants exhibited significantly higher accuracy in comparison to controls. Additionally, significantly higher omissions when compared to controls (het n=15, wt n=9, data are mean \pm SEM, * p =0.05, ** p =0.01).

Here we looked to re-evaluate latency measures in 8-month-old TDP-43^{Q331Klow} mice to observe any potential changes due to age-dependent TDP-43 mutant disease progression. Reward collection latencies were evaluated in 8-month-old TDP-43^{Q331Klow} mutant mice. It was found that mutant reward collection latencies did not significantly differ from littermate controls (**Figure 21A**; no effect of genotype, $F_{(1,22)} = 0.038$, $p = 0.847$; no effect of stimulus duration, $F_{(1.32,24.91)} = 0.843$, $p = 0.381$; no significant interaction effect, $F_{(1.32,24.91)} = 0.219$, $p = 0.674$). Similarly, correct touch latencies were also evaluated in 8-month-old TDP-43^{Q331Klow} mutant mice. It was revealed that mutants did not exhibit any significant differences from littermate controls (**Figure 21B**; no effect of genotype, $F_{(1,21)} = 0.874$, $p = 0.361$; significant effect of stimulus duration, $F_{(3,63)} = 22.86$, $p = <0.001$; No interaction effect, $F_{(3,63)} = 2.138$, $p = 0.104$). Lastly incorrect touch latencies were evaluated in 8-month-old TDP-43^{Q331Klow} mutant mice. It was revealed that mutant incorrect touch latencies did not significantly differ from littermate controls (**Figure 21C**; No genotype effect, $F_{(1,22)} = 0.947$, $p = 0.341$; no stimulus duration effect, $F_{(3,66)} = 0.485$, $p = 0.694$; No interaction effect, $F_{(3,66)} = 0.943$, $p = 0.425$).

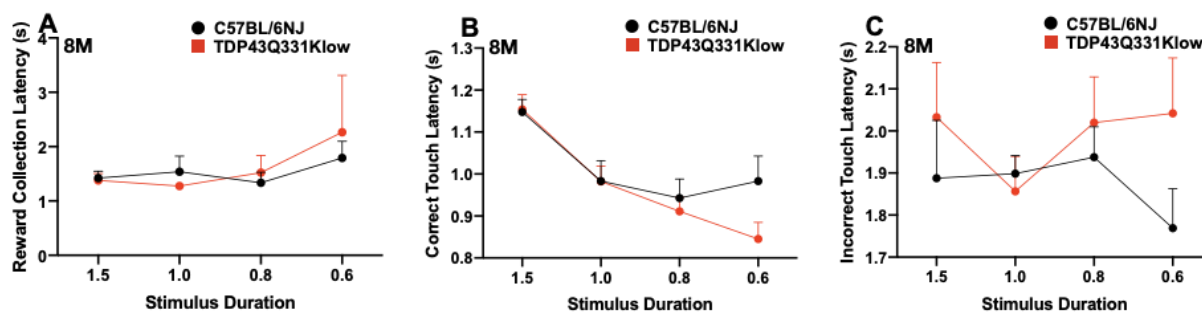


Figure 21. TDP-43^{Q331Klow} mutant mice 8-month 5-CSRTT reward collection latency. No significant differences were observed (het n=15, wt n=9).

All behavioural response aspects surrounding the performance of responses to the touchscreens were re-evaluated again to observe any age-dependent effects. Premature responses of 8-month-old TDP-43^{Q331Klow} mutant mice were investigated. It was revealed that mutants' premature responses did not differ significantly from littermate controls (**Figure 22A**; no genotype effect, $F_{(1,22)} = 2.188$, $p = 0.153$; no stimulus duration effect, $F_{(2,04,44,92)} = 2.253$, $p = 0.116$; no significant interaction effect duration, $F_{(3,24)} = 0.111$, $p = 0.899$). Similarly, perseverative post-correct responses in 8-month-old TDP-43^{Q331Klow} mutant mice were investigated. It was revealed that mutant perseverative responses did not differ significantly from littermate controls (**Figure 22B**; no effect of genotype, $F_{(1,22)} = 6.142$, $p = 0.980$; no effect of stimulus duration, $F_{(3,66)} = 1.719$, $p = 0.172$; no interaction effect, $F_{(3,66)} = 1.801$, $p = 0.156$). To assess perseverative post-incorrect responses 8-month-old TDP-43^{Q331Klow} mutant mice were investigated. It was revealed that mutant mice did not differ from littermate controls with respect to perseverative responses (**Figure 22C**; no genotype effect, $F_{(1,22)} = 2.498$, $p = 0.128$; no effect of stimulus duration, $F_{(1.59,35.16)} = 0.751$, $p = 0.452$; no interaction effect, $F_{(1.59,35.16)} = 1.074$, $p = 0.339$).

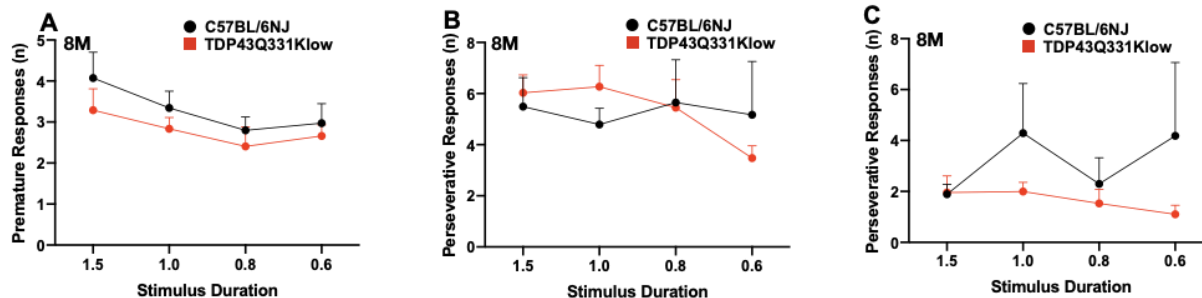


Figure 22. TDP-43^{Q331Klow} mutant mice 8-month 5-CSRTT premature responses (A), perseverative post-correct responses (B) and perseverative post-incorrect (C). No significant differences were observed (het n=15, wt n=9).

3.9 5-CSRTT Probe of Attention Performance in 4-month-old TDP-43^{G348C}

In line with using the same tasks to explore cognitive aspects in each mutant TDP-43 mouse line, we looked to re-evaluate TDP-43^{G348C} mice with the 5-CSRTT test of attention to determine potential changes resulting in age-dependent progression of TDP-43 pathology (Swarup et al., 2011).

Similarly, acquisition was also evaluated in 4-month-old TDP-43^{G348C} mutant mice. It was found that mutants did not differ significantly from littermate controls with respect to sessions required to reach performance criterion with 4-second (Figure 23A; Welch's t-test, $t_{(4.43)} = 0.0928$, $p = 0.930$), or 2-second stimulus durations (Figure 23B; Welch's t-test, $t_{(4.12)} = 0.5573$, $p = 0.606$).

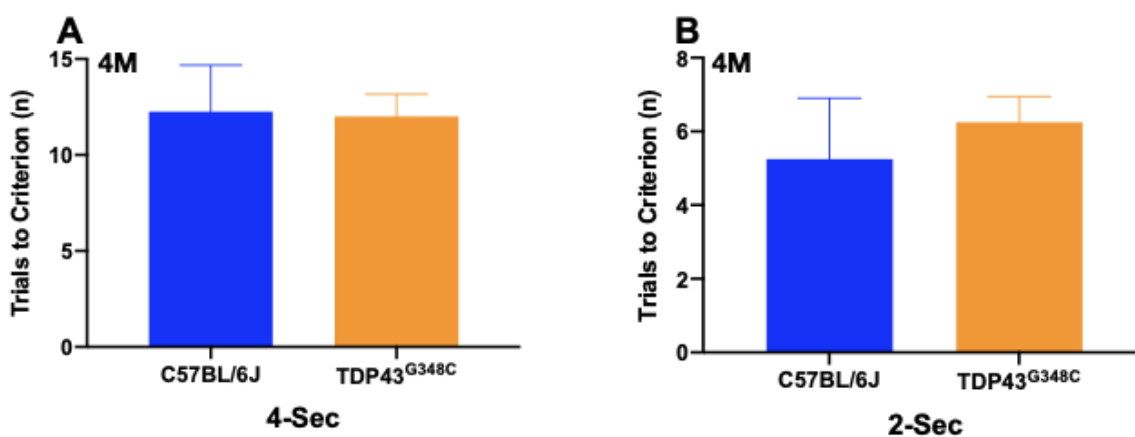


Figure 23. TDP-43^{G348C} mutant mice 4-month 5-CSRTT trials to acquisition 4- and 2-seconds. No significant differences were observed (het n=8, wt n=4).

Again, with the 5-CSRTT we looked to evaluate attentional demands in the TDP-43^{G348C} mutant mice, and in the same manner as the TDP-43^{Q331Klow} mice. To assess accuracy 4-month-old TDP-43^{G348C} mutant mice were investigated. It was revealed that mutants did not significantly differ from littermate controls in task accuracy (**Figure 24A**; no effect of genotype, $F_{(1,10)} = 3.050$, $p = 0.111$; main effect of stimulus duration, $F_{(3,30)} = 15.699$, $p < 0.001$; no interaction effect, $F_{(3,30)} = 0.585$, $p = 0.629$). Omissions were also evaluated in 4-month-old TDP-43^{G348C} mutant mice. It was found that mutants did not differ significantly from littermate controls in omission behaviour (**Figure 24B**; no genotype effect, $F_{(1,10)} = 3.099$, $p = 0.109$; significant main effect of stimulus duration, $F_{(3,30)} = 23.151$, $p < 0.001$; no interaction effect, $F_{(3,30)} = 0.933$, $p = 0.437$).

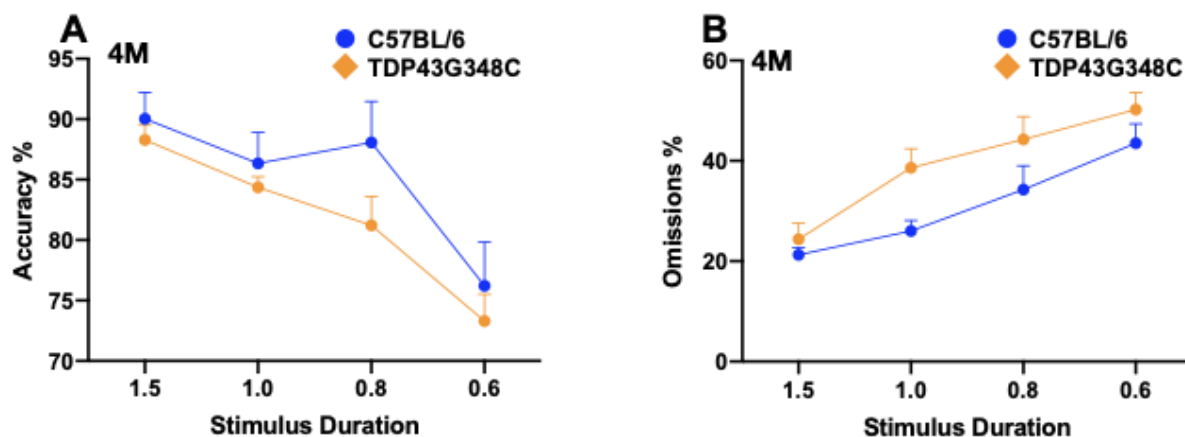


Figure 24. TDP-43G348C mutant mice 4-month 5-CSRTT accuracy (A) and omissions (B). No significant differences were observed (het n=8, wt n=4).

As a way to assess motivation in TDP-43^{G348C} mutant mice as with the TDP-43^{Q331Klow} mutants we looked to evaluate various latency measures in the 5-CSRTT. Reward collection latencies with 4-month-old TDP-43^{G348C} mutant mice were assessed. It was found that mutant reward collection latencies did not significantly differ from littermate controls (**Figure 25A**; no effect of genotype, $F_{(1,10)} = 2.663$, $p = 0.134$; no effect of stimulus duration, $F_{(1,19,11.98)} = 1.501$, $p = 0.251$; no significant interaction effect, $F_{(1,19,11.98)} = 1.788$, $p = 0.209$). The resulting correct touch latencies of 4-month-old TDP-43^{G348C} mutant mice were similarly evaluated. It was revealed that mutants did not significantly differ from littermate controls (**Figure 25B**; no effect genotype, $F_{(1,10)} = 1.049$, $p = 0.330$; significant effect of stimulus duration, $F_{(1,95,19.56)} = 5.672$, $p = 0.012$; no

interaction effect, $F_{(1.95,19.56)} = 0.129$, $p = 0.876$). Incorrect touch latencies of 4-month-old TDP-43^{G348C} mutant mice were also investigated. It was found that mutant incorrect touch latencies did not significantly differ from littermate controls (**Figure 25C**; no genotype effects, $F_{(1,10)} = 0.744$, $p = .0409$; no stimulus duration effect, $F_{(3,30)} = 1.192$, $p = 0.329$; no interaction effect, $F_{(3,30)} = 1.069$, $p = 0.377$).

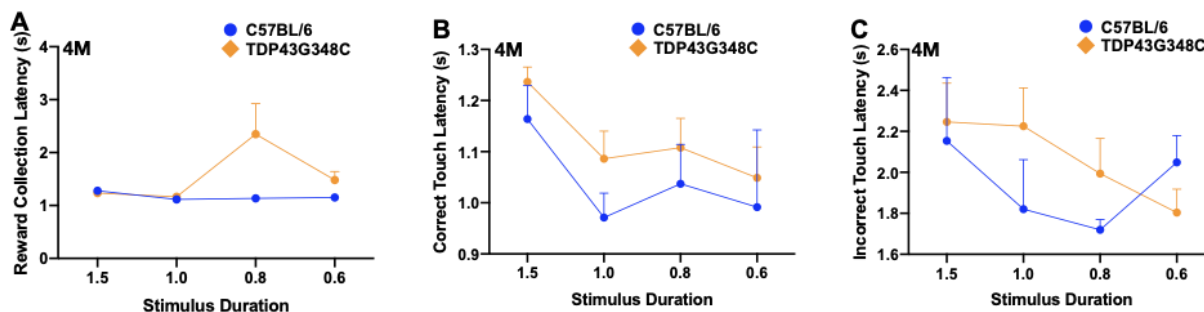


Figure 25. TDP-43^{G348C} mutant mice 4-month 5-CSRTT reward collection latency (A), correct touch latency (B) and incorrect touch latency (C). No significant differences were observed (het n=8, wt n=4).

Maintaining consistency, TDP-43^{G348C} mutant mice were also evaluated for possible abnormal behavioural responses surrounding the performance of responses to the touchscreen. Premature responses were evaluated in 4-month-old TDP-43^{G348C} mutant mice. It was found that mutant premature responses did not differ significantly from littermate controls (**Figure 26A**; no genotype effect, $F_{(1,8)} = 0.164$, $p = 0.696$; no stimulus duration effect, $F_{(3,24)} = 0.029$, $p = 0.993$; no significant interaction effect, $F_{(3,24)} = 2.093$, $p = 0.128$). Similarly, perseverative post-correct responses were assessed in 4-month-old TDP-43^{G348C} mutant mice. It was found that mutant perseverative responses did not differ significantly from littermate controls (**Figure 26B**; no effect of genotype, $F_{(1,10)} = 0.251$, $p = 0.627$; no effect of stimulus duration, $F_{(3,30)} = 1.769$, $p = 0.174$; no interaction effect, $F_{(3,30)} = 6.273$, $p = 0.835$). The last among response data was perseverative post-incorrect responses. 4-month-old TDP-43^{G348C} mutant mice did not differ significantly from littermate controls with respect to perseverative responses (**Figure 26C**; no genotype effect, $F_{(1,10)} = 1.232$, $p = 0.293$; significant effect of stimulus duration, $F_{(3,30)} = 4.700$, $p = 0.008$; no interaction effect, $F_{(3,30)} = 0.976$, $p = 0.417$).

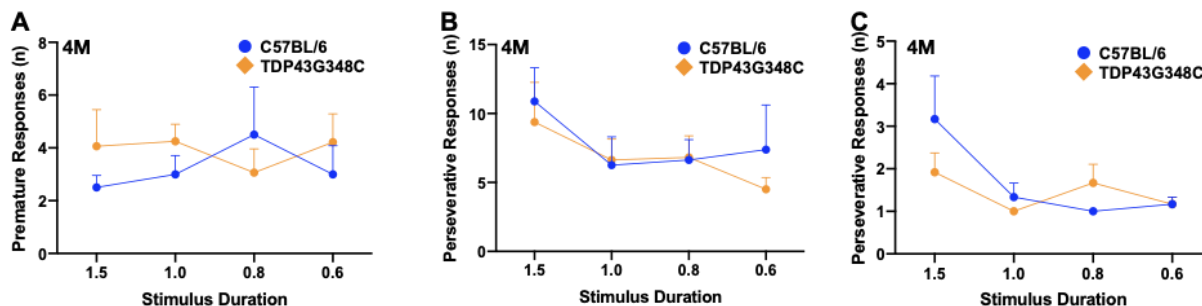


Figure 26. TDP-43G348C mutant mice 4-month 5-CSRTT premature responses (A), perseverative post-correct responses (B) and perseverative post-incorrect responses (C). No significant differences were observed (het n=8, wt n=4).

3.10 5-CSRTT Probe of Attention Performance in 8-month-old TDP-43^{G348C}

The TDP-43^{G348C} mutant mice were re-evaluated in similar fashion to the TDP-43Q331K^{low} mice to assess progress age-dependent effects of TDP-43 altering cognitive performance observed in 4-month-old mice.

The accuracy of 8-month-old TDP-43^{G348C} mutant mice were the first to be re-investigated. It was found that mutants did not significantly differ from littermate controls in task accuracy (**Figure 27A**; no effect of genotype, $F_{(1,6)} = 1.665$, $p = 0.224$; significant main effect of stimulus duration, $F_{(3,18)} = 10.129$, $p < 0.001$; no interaction effect $F_{(3,18)} = 1.436$, $p = 0.265$). Similarly, omission behaviour was also re-investigated in 8-month-old TDP-43^{G348C} mutant mice. It was found that omission behaviour significantly differed from littermate controls (**Figure 27B**; significant main effect of genotype, $F_{(1,6)} = 10.796$, $p = 0.017$; significant main effect of stimulus duration, $F_{(3,18)} = 5.693$, $p = 0.006$, indicating increased omissions during longer stimulus durations; no interaction effect, $F_{(3,18)} = 0.956$, $p = 0.435$).

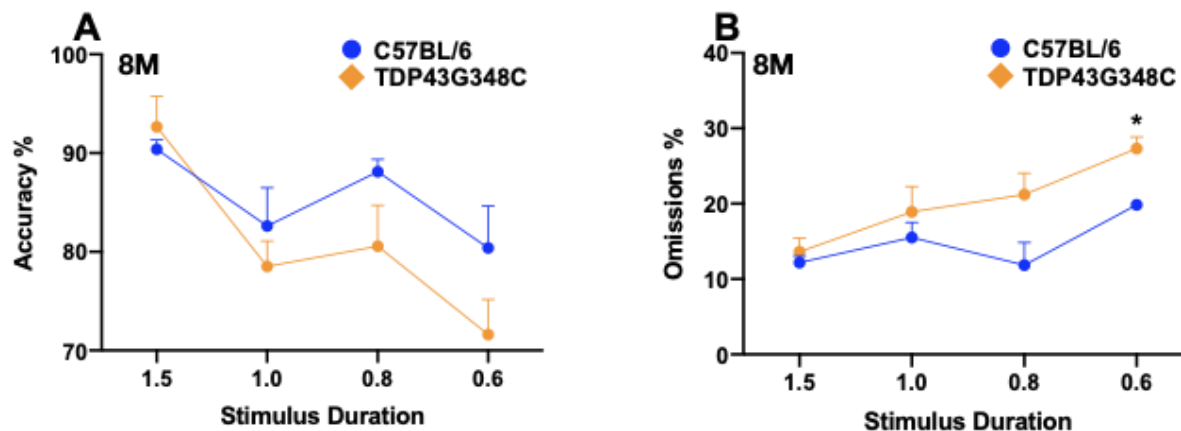


Figure 27. TDP-43G348C mutant mice 8-month 5-CSRTT accuracy. No significant differences were observed (het n=8, wt n=4, data are mean \pm SEM, * $p < 0.05$).

We also looked to re-evaluate motivation of 8-month-old TDP-43^{G348C} mutant mice by observing latencies measures as done with the TDP-43^{Q331Klow} mice. Reward collection latency behaviours were evaluated in 8-month-old TDP-43^{G348C} mutant mice. It was found that mutant reward collection latencies did not significant differ from littermate controls (**Figure 28A**; no effect of genotype, $F_{(1,6)} = 0.451$, $p = 0.527$; no effect of stimulus duration, $F_{(1,2,7.58)} = 0.190$, $p = 0.731$; no significant interaction effect, $F_{(1,26,7.58)} = 0.595$, $p = 0.502$). Correct touch latencies were also re-evaluated in 8-month-old TDP-43^{G348C} mutant mice. It was revealed that mutants significantly differed from littermate controls (**Figure 28B**; no effect genotype, $F_{(1,6)} = 3.660$, $p = 0.104$; significant effect of stimulus duration, $F_{(3,18)} = 23.499$, $p < 0.001$, indicating higher correct touch latencies during longer stimulus durations; significant interaction effect observed between genotype and stimulus duration, $F_{(3,18)} = 10.194$, $p < 0.001$). This interaction was explored with simple main effects, which revealed mutant mice exhibited significantly higher correct touch latencies during 1.5- and 1.0-second stimulus durations, $p = 0.019$ and $p = 0.020$ respectively. In similar fashion, to assess incorrect touch latencies 8-month-old TDP-43^{G348C} mutant mice were re-evaluated. It was found that mutant incorrect touch latencies differed significantly from littermate controls (**Figure 28C**; significant effect of genotype, $F_{(1,6)} = 6.503$, $p = 0.043$, indicating higher TDP-43^{G348C} mutant incorrect touch latencies on average per session; no effect of stimulus duration, $F_{(3,18)} = 2.557$, $p = 0.087$; no interaction effect, $F_{(3,18)} = 0.820$, $p = 0.500$).

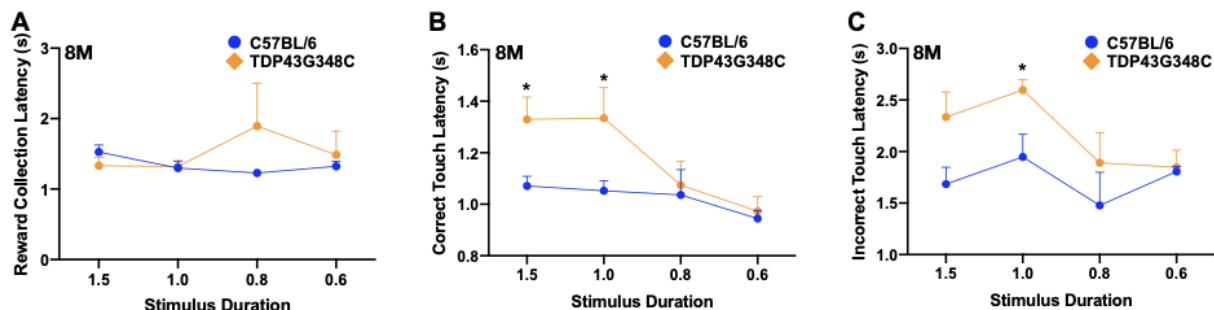


Figure 28. TDP-43G348C mutant mice 8-month 5-CSRTT reward collection latency (A) correct touch latency (B) and incorrect touch latency (C). No significant differences were observed for reward collection latency. Both correct touch- and incorrect touch latencies were significantly different from control (het n=8, wt n=4, data are mean \pm SEM, * p <0.05).

We also wanted to investigate any potential changes caused by age-dependent progression of TDP-43 in behavioural response aspects surrounding the performance of responses to touchscreens in TDP-43^{G348C} mutant mice. The first latency measure to be re-assessed was premature responses of 8-month-old TDP-43^{G348C} mutant mice. It was found that mutant premature responses did not differ significantly from littermate controls (**Figure 29A**: no genotype effect, $F_{(1,6)} = 0.559$, $p = 0.483$; no stimulus duration effect, $F_{(3,18)} = 0.027$, $p = 0.994$; no significant interaction effect, $F_{(3,18)} = 0.730$, $p = 0.547$). Similarly, perseverative post-correct responses of 8-month-old TDP-43^{G348C} mutant mice were re-evaluated. It was found that mutant perseverative responses did not differ significantly from littermate controls (**Figure 29B**; no effect of genotype, $F_{(1,6)} = 1.568$, $p = 0.257$; no effect of stimulus duration, $F_{(3,18)} = 2.830$, $p = 0.068$; no interaction effect, $F_{(3,18)} = 3.133$, $p = 0.051$). Re-assessment of perseverative post-incorrect responses in 8-month-old TDP-43^{G348C} mutant mice revealed that mutants did not significantly differ from littermate controls with respect to perseverative responses (**Figure 29C**; no genotype effect, $F_{(1,6)} = 0.167$, $p = 0.697$; no stimulus duration effect, $F_{(1,14,6,87)} = 2.804$, $p = 0.138$; no interaction effect, $F_{(1,14,6,876)} = 0.606$, $p = 0.484$).

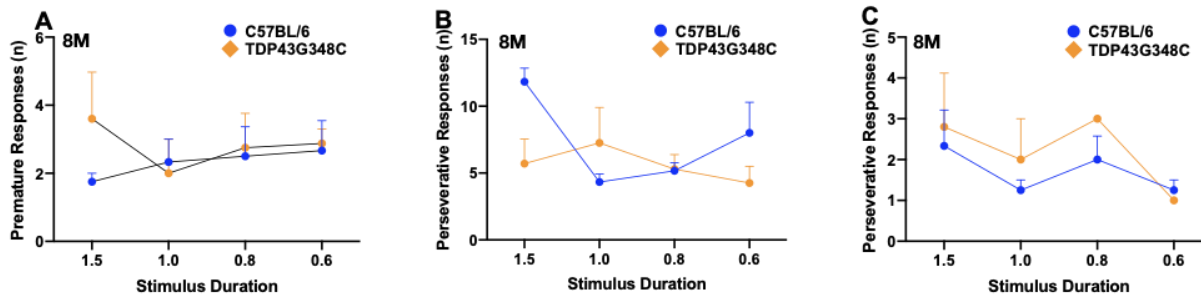


Figure 29. TDP-43G348C mutant mice 8-month 5-CSRTT premature responses (A), perseverative post-correct responses (B) and perseverative post-incorrect responses (C). No significant differences were observed (het n=8, wt n=4).

3.11 11-month-old TDP-43^{Q331Klow} Probe of Motivation Performance in PRFR

We looked to evaluate FTD/ALS-related motivation deficits in TDP-43 mutant mice as a follow up to previous experiments. The PRFR task is designed specifically to evaluate aspects of motivation. Progressive ratio and fixed ratio data were analyzed separately but are represented together graphically in some cases.

The primary metric used to assess motivation is breakpoint. Fixed-ratio breakpoints were explored in 11-month-old TDP-43^{Q331Klow} mutant mice. It was found that mutants did not differ significantly from littermate controls in breakpoints (**Figure 30A**; FR1, *ns*, identical values; FR2, *ns*, identical values; FR3, *ns*, identical values; FR5, Welch's t-test, $t_{(8)} = 1.000$, $p = 0.346$). Progressive-ratio breakpoints were also evaluated in 11-month-old TDP-43^{Q331Klow} mutant mice. It was revealed that mutants did not differ significantly from littermate controls (**Figure 30B**; no effect of genotype, $F_{(1,20)} = 0.038$, $p = 0.848$; no effect of work requirement, $F_{(2,40)} = 0.133$, $p = 0.876$; no interaction effect, $F_{(2,40)} = 0.100$, $p = 0.905$).

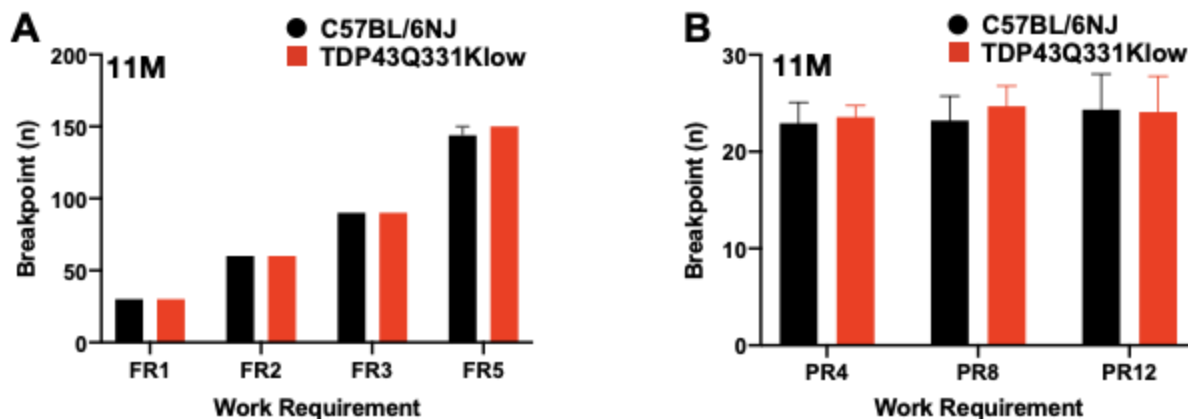


Figure 30. TDP-43Q331Klow mutant mice 11-month fixed-ratio breakpoint (A) and progressive-ratio breakpoint (B). No significant differences were observed (het n=13, wt n=9).

We also looked to evaluate target touches in TDP-43 mutant mice to observe exactly how many responses were elicited within a given PRFR schedule. Fixed ratio target touches were assessed in 11-month-old TDP-43^{Q331Klow} mutant mice. It was revealed that mutants did not differ significantly from littermate controls (**Figure 31**; FR1, *ns*, identical values; FR2, *ns*, identical values; FR3, *ns*, identical values; FR5, Welch's t-test, $t_{(8)} = 1.000$, $p = 0.346$). Similarly, progressive ratio target touches were also explored in 11-month-old TDP-43^{Q331Klow} mutant mice. It was revealed that mutants did not differ significantly from littermate controls (**Figure 31**; no genotype effect, $F_{(1,20)} = 0.002$, $p = 0.969$; significant effect of work requirement, $F_{(2,40)} = 23.094$, $p = <0.001$; no interaction effect, $F_{(2,40)} = 0.170$, $p = 0.844$).

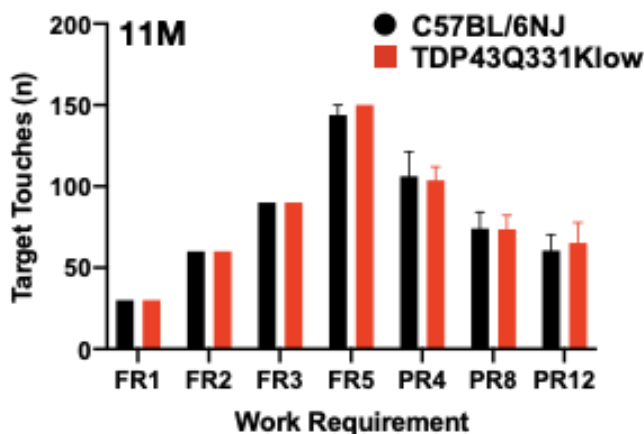


Figure 31. TDP-43Q331Klow mutant mice 11-month progressive- and fixed-ratio target touches. No significant differences were observed (het n=13, wt n=9).

We also evaluated trials completed, another measure of how much work animals are willing to expend. Evaluation of trials completed in 11-month-old TDP-43^{Q331Klow} mutant mice revealed that mutants did not significantly differ from littermate controls (**Figure 32**; FR1, *ns*, identical values; FR2, *ns*, identical values; FR3, *ns*, identical values; FR5, Welch's t-test, $t_{(8)} = 1.000$, $p = 0.346$). Similarly, we then explored progressive ratio trials completed in 11-month-old TDP-43^{Q331Klow} mutant mice. It was revealed that mutant did not differ significantly from littermate controls (**Figure 32**; no genotype effect, $F_{(1,20)} = 0.080$, $p = 0.780$; significant effect of work requirement, $F_{(2,40)} = 188.185$, $p = <0.001$; no interaction effect, $F_{(2,40)} = 1.308$, $p = 0.282$).

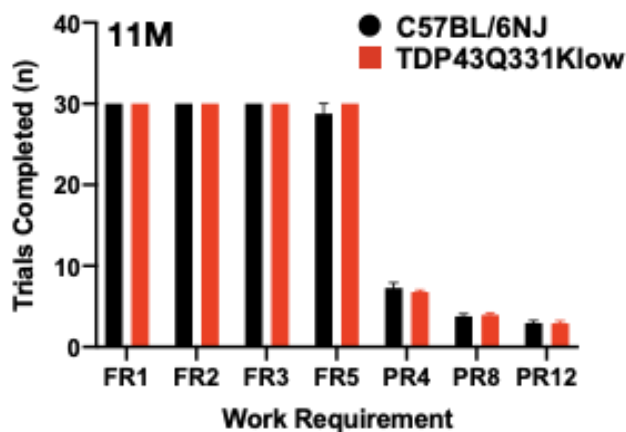


Figure 32. TDP-43^{Q331Klow} mutant mice 11-month progressive- and fixed-ratio trials completed. No significant differences were observed (het n=13, wt n=9).

We then looked to measure response latency as completed in other tasks, however this time in a task dedicated to evaluating motivation. Assessment of fixed ratio reward collection latency in 11-month-old TDP-43^{Q331Klow} mutant mice revealed that mutants differed significantly from littermate controls (**Figure 33**; FR1, Welch's t-test, $t_{(6.27)} = 2.086$, $p = 0.080$; FR2, Welch's t-test, $t_{(1.05)} = 0.324$, $p = 0.797$; FR3, Welch's t-test, $t_{(7.69)} = 2.694$, $p = 0.028$; FR5, Welch's t-test, $t_{(12.13)} = 0.379$, $p = 0.797$). Progressive ratio reward collection latencies were also evaluated in 11-month-old TDP-43^{Q331Klow} mutant mice. It was found that mutants did not differ significantly from littermate controls (**Figure 33**; no genotype effect, $F_{(1,20)} = 0.0065$, $p = 0.801$; no effect of work requirement, $F_{(2,40)} = 1.118$, $p = 0.337$; no interaction effect, $F_{(2,40)} = 0.476$, $p = 0.625$).

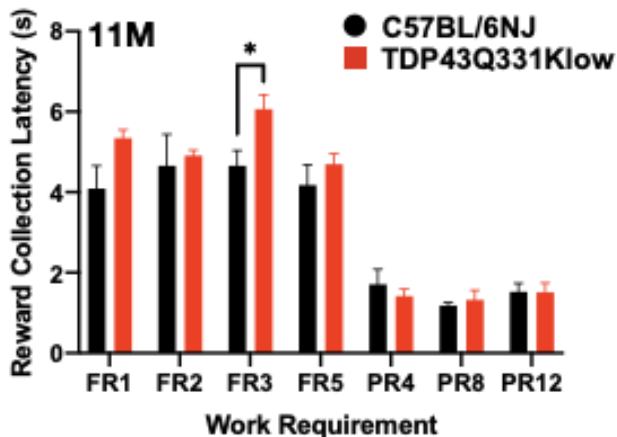


Figure 33. TDP-43Q331Klow mutant mice 11-month progressive- and fixed-ratio reward collection latency. TDP-43Q331Klow mutants exhibited significantly longer delays to reward collection during fixed ratio testing (het n=13, wt n=9, data are mean \pm SEM, * p <0.05).

To further assess aspects of motivation beyond outright breakpoints we looked to evaluate mutant TDP-43 mice with another distinct measure, post-reinforcement pause. Longer post-reinforcement pauses indicate a possible decrease in motivation. 11-month-old TDP-43^{Q331Klow} mutant mice exhibited significantly shorter pauses when compared with littermate controls (**Figure 34**; no genotype effect, $F_{(1,20)} = 1.258$, $p = 0.275$; no work requirement effect, $F_{(1.53,30.76)} = 1.202$, $p = 0.304$; significant interaction effect, $F_{(1.53,30.76)} = 4.292$, $p = 0.031$). This interaction was explored with simple main effects, which indicated mutant mice exhibited significantly shorter delays in the initiation of subsequent trials during the PR12 schedule, $p=0.031$.

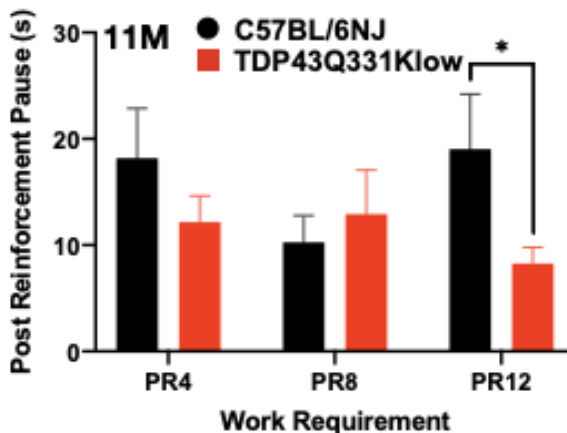


Figure 34. TDP-43Q331Klow mutant mice 11-month progressive-ratio post reinforcement pause. TDP-43Q331Klow mutants exhibited significantly shorter post reinforcement pause delays (het n=13, wt n=9, data are mean \pm SEM, * p =0.05).

3.12 11-month-old TDP-43^{G348C} Probe of Motivation Performance in PRFR

To maintain consistency and further evaluate age-dependent effects of TDP-43 pathology on aspects of motivation, TDP-43^{G348C} mutants were also evaluated with the PRFR task.

The main metric to evaluate motivation in the PRFR task was also used to evaluate TDP-43^{G348C} mutants. Assessment of fixed-ratio breakpoints in 11-month-old TDP-43^{G348C} mutant mice revealed that mutants did not differ significantly from littermate controls in measured breakpoints (**Figure 35A**; FR1, *ns*, identical values; FR2, *ns*, identical values; FR3, *ns*, identical values; FR5, *ns*, identical values). Similarly, progressive-ratio breakpoints were evaluated in 11-month-old TDP-43^{G348C} mutant mice. It was revealed that mutants did not differ significantly from littermate controls (**Figure 35B**; no effect of genotype, $F_{(1,10)} = 7.097$, $p = 0.979$; no effect of work requirement, $F_{(2,20)} = 2.219$, $p = 0.135$; no interaction effect, $F_{(2,20)} = 0.421$, $p = 0.662$).

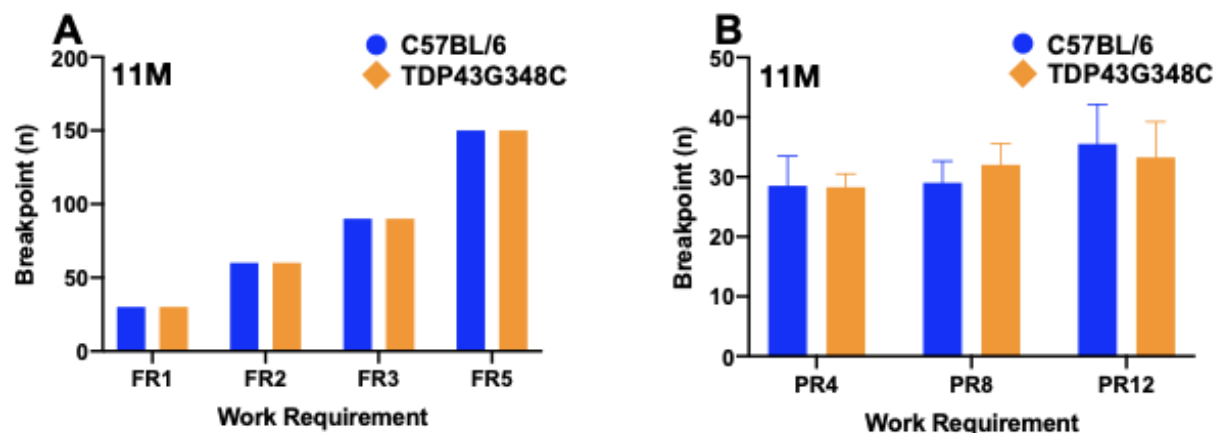


Figure 35. TDP-43G348C mutant mice 11-month progressive-ratio breakpoint. No significant differences were observed (het n=8, wt n=4).

Target touches were also investigated as an alternative measure of motivation. Assessment of fixed ratio target touches 11-month-old TDP-43^{G348C} mutant mice revealed that mutants did not differ significantly from littermate controls (**Figure 36**; FR1, *ns*, identical values; FR2, *ns*, identical values; FR3, *ns*, identical values; FR5, *ns*, identical values). Furthermore, exploration of target touches in 11-month-old TDP-43^{G348C} mutant mice did not reveal any significant differences from littermate controls (**Figure 36**; no genotype effect, $F_{(1,10)} = 3.553$, $p = 0.985$; significant effect of work requirement, $F_{(2,20)} = 7.236$, $p < 0.004$; no interaction effect, $F_{(2,20)} = 0.620$, $p = 0.548$).

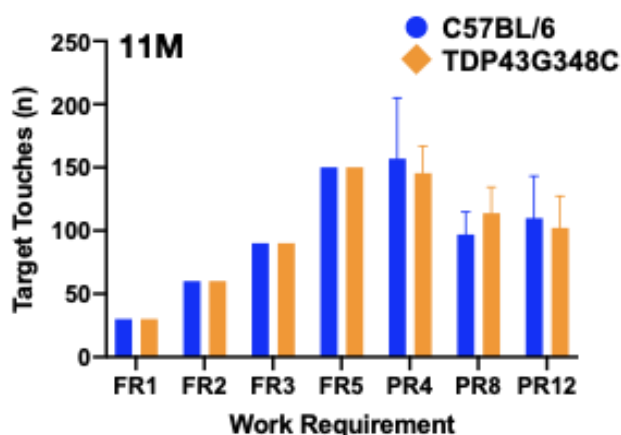


Figure 36. TDP-43G348C mutant mice 11-month progressive- and fixed-ratio target touches. No significant differences were observed (het n=8, wt n=4).

In similar fashion to 11-month-old TDP-43^{Q331Klow} mice, we explored fixed ratio trials completed in 11-month-old TDP-43^{G348C} mutant mice. It was found that mutants did not differ significantly from littermate controls (**Figure 37**; FR1, *ns*, identical values; FR2, *ns*, identical values; FR3, *ns*, identical values; FR5, *ns*, identical values). This was followed up with exploration of progressive ratio trials completed in 11-month-old TDP-43^{G348C} mutant mice. It was found that mutants do not differ significantly from littermate controls (**Figure 37**; no genotype effect, $F_{(1,10)} = 0.003$, $p = 0.961$; significant effect of work requirement, $F_{(2,20)} = 71.53$, $p < 0.001$; no interaction effect, $F_{(2,20)} = 0.343$, $p = 0.714$).

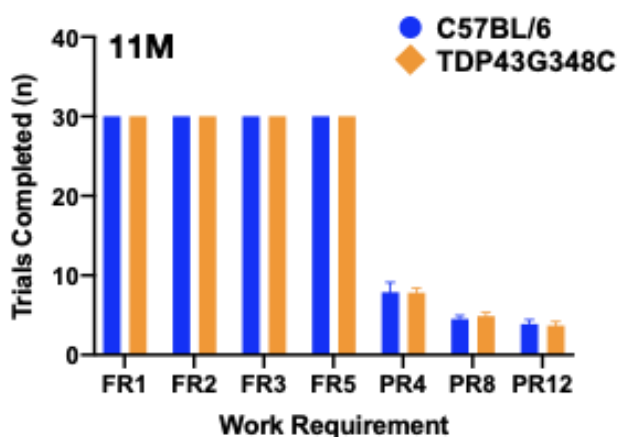


Figure 37. TDP-43G348C mutant mice 11-month progressive- and fixed-ratio trials completed. No significant differences were observed (het n=8, wt n=4).

Various latency measures were used to evaluate TDP-43^{G348C} mutant mice in the dedicated PRFR task, as was done with the TDP-43^{Q331Klow} mice. Assessment of 11-month-old TDP-43^{G348C} revealed that mutants did not differ significantly from littermate controls (**Figure 38**; FR1, Welch's t-test, $t_{(3.30)} = 1.224$, $p = 0.300$, $p = 0.080$; FR2, Welch's t-test, $t_{(2.90)} = 0.298$, $p = 0.785$; FR3, Welch's t-test, $t_{(2.04)} = 1.053$, $p = 0.400$; FR5, Welch's t-test, $t_{(7.99)} = 1.246$, $p = 0.247$). Furthermore, reward collection latencies from 11-month-old TDP-43^{G348C} mutant mice were evaluated. It was found that mutants did not significantly differ from littermate controls (**Figure 38**; no genotype effect, $F_{(1,10)} = 0.110$, $p = 0.747$; no work requirement effect, $F_{(1.32,13.27)} = 0.680$, $p = 0.465$; no interaction effect, $F_{(1.32,13.27)} = 0.331$, $p = 0.637$).

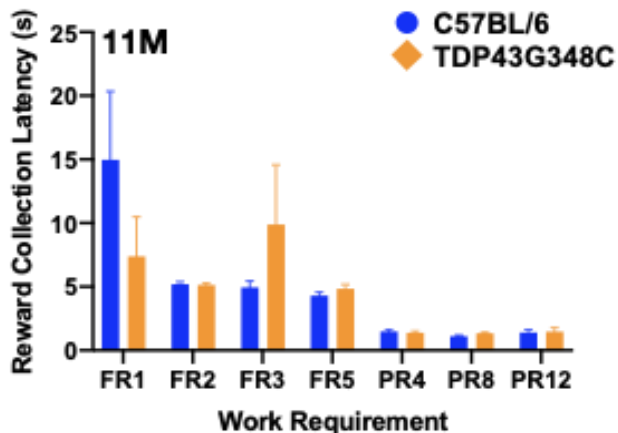


Figure 38. TDP-43G348C mutant mice 11-month progressive- and fixed-ratio reward collection latency. No significant differences were observed (het n=8, wt n=4).

The last measure evaluated was post reinforcement pause. Evaluations in 11-month-old TDP-43^{G348C} mutant mice revealed that mutants did not differ significantly when compared with littermate controls (**Figure 39**; no genotype effect, $F_{(1,10)} = 0.497$, $p = 0.497$; No work requirement effect was observed, $F_{(2,20)} = 0.253$, $p = 0.779$. no interaction effect, $F_{(2,20)} = 1.511$, $p = 0.245$).

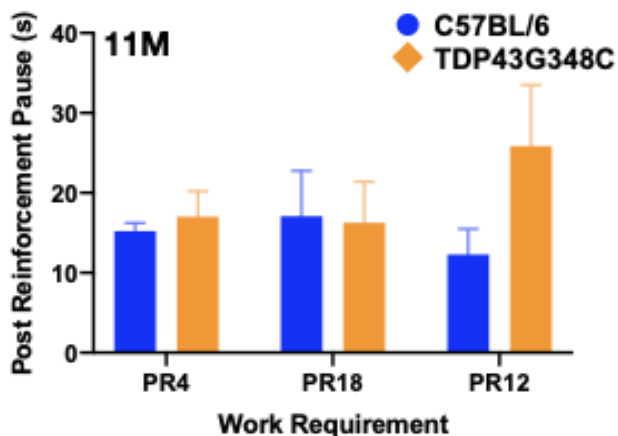


Figure 39. TDP-43G348C mutant mice 11-month progressive-ratio post reinforcement pause. No significant differences were observed from control (het n=13, wt n=9).

Q331Klow		PVD (Reversal Learning)	5-CSRTT Accuracy	5-CSRTT Omissions	5-CSRTT Perseveration	PRFR Breakpoint	PRFR Post Reinforcement Pause	PAL Accuracy	PVD (Visual Discrimination)	Motor Alterations (Battery)
4M		✗	✓	✗	✗	-	-	-	✗	✓
8M		-	✓	✗	✓	-	-	✓	-	✗
11M		-	-	-	-	✓	✗	-	-	-
G348C		PVD (Reversal Learning)	5-CSRTT Accuracy	5-CSRTT Omissions	5-CSRTT Perseveration	PRFR Breakpoint	PRFR Post Reinforcement Pause	PAL Accuracy	PVD (Visual Discrimination)	Motor Alterations (Battery)
4M		✗	✓	✓	✓	-	-	-	✗	✓
8M		-	✓	✗	✓	-	-	✓	-	✗
11M		-	-	-	-	✓	✓	-	-	-

Figure 40. Overview of TDP-43Q331Klow and TDP-43G348C mutant mouse deficits across all evaluation time points.

4. Discussion

In the present study I assessed executive function in FTD/ALS-relevant male TDP-43^{Q331Klow} and ^{-G348C} transgenic mice using automated touchscreens. Cognitive impairments were revealed in 4-month-old and 8-month-old TDP-43^{Q331Klow} and ^{-G348C} mutants. The cognitive impairments detected in 4-month-old mice manifested before FTD/ALS-related motor dysfunction. This pattern of results is very similar to observations in human FTD/ALS. Together, these findings outline the usefulness of TDP-43 mutant mouse models in combination with automated touchscreens.

4.1 Age-Dependent Motor Performance Deficits in TDP-43 Mutant Mice

In both TDP-43^{Q331Klow} and TDP-43^{G348C} mutant mice, motor performance remained largely spared, although an age-dependent deficit in peak grip force strength was revealed at 8-months of age. This finding is consistent with previous reports of age-dependent, mutation-dependent deterioration of motor performance in TDP-43^{Q331Klow} and TDP-43^{G348C} mutant mice (Arnold et al., 2013a; Swarup et al., 2011). Specifically, Arnold et al. (2013a) demonstrated that TDP-43^{Q331Klow} mutant mice have normal motor performance at 3- and 6-months of age, as indicated by accelerating rotarod analyses (Arnold et al., 2013a). Re-evaluation of TDP-43^{Q331Klow} mutant mice at 10-months of age revealed significant motor performance deficits on the accelerating rotarod (Arnold et al., 2013a). Arnold et al. (2013a) also evaluated the *TDP-43^{Q331K}* variant, which has higher transgene expression (3-fold) than the TDP-43^{Q331Klow} mice, and found that *TDP-43^{Q331K}* mice displayed progressively worsening age-dependent motor performance deficits at 3-, 6-, and 10-months of age. Further, these motor impairments were exacerbated compared to TDP-43^{Q331Klow} mutant mice (Arnold et al., 2013a). To summarize, TDP-43^{Q331Klow} exhibited moderate TDP-43 overexpression and a mild, progressive deterioration of motor performance, consistent with previous reports using other mouse models.

Swarup et al. (2011) also demonstrated that TDP-43^{G348C} mutant mice have normal motor performance at 3- and 6-months of age revealed by accelerating rotarod analyses. They then re-evaluated the TDP-43^{G348C} mutant mice and found that at 9-months of age these mice exhibit significantly reduced motor performance in an age-dependent manner (Swarup et al., 2011). This result provides additional support for our findings of age-dependent deterioration of motor

performance in both the TDP-43^{Q331Klow} and TDP-43^{G348C} mutant mice. Additionally, both the Cleveland and Julien groups reported progressive motor degeneration without extreme muscle weakness, spasticity or paralysis during characterization of both the TDP-43^{Q331Klow} and TDP-43^{G348C} mutant mice (Arnold et al., 2013a; Swarup et al., 2011). This characteristic did not differ in the TDP-43^{Q331Klow} and TDP-43^{G348C} mutant mice used for this investigation. Lastly, and perhaps most importantly, during this investigation the onset of motor performance deteriorations in TDP-43^{Q331Klow} and TDP-43^{G348C} mutant mice did not precede the detection cognitive dysfunction in these mutant mouse lines (see below).

4.2 5-CSRTT Reveals Possible BPSD-like Behaviours in TDP-43 Mutant Mice

5-CSRTT acquisition (4s & 2s) phases revealed no significant differences among TDP-43^{Q331Klow} and TDP-43^{G348C} mutant mice and their littermate controls, suggestive of a similar ability to acquire the task during these two relatively lenient training phases. Furthermore, during probe trials the TDP-43^{Q331Klow} and TDP-43^{G348C} mutant mice did not demonstrate any impairments in accuracy during any time point. In fact, it appears that the accuracy of TDP-43^{Q331Klow} mutants were improved in this task, consistent with the very significantly increased accuracy observed in these mutants during the 4- and 8-month timepoints. TDP-43^{G348C} mutant mice did not show any evidence of improvement.

4-month-old TDP-43^{Q331Klow} mutants did, however, demonstrate evidence of early increased perseverative responses. Early perseverative behaviour is one of the first and most prominent BPSD symptoms in human FTD (Erkkinen et al., 2018; Tible et al., 2017; Young et al., 2018). Recently, the Q331K mutation was humanized in mice, generating a novel TDP-43^{Q331K KI} mouse model (White et al., 2018), and reversal learning impairments driven by stimulus-bound perseverative responding have been reported in these mice (Kim et al., 2020). Between these two investigations it is evident that TDP-43^{Q331K(low/KI)} may in fact share a perseverative response phenotype. Additionally, because cognitive impairment is often reported before motor dysfunction in human FTD/ALS cases (Elamin et al., 2011; Giordana et al., 2011), the TDP-43^{Q331Klow} mutant mouse model may be ideal for evaluations of early perseveration preceding the development of motor dysfunction in mice.

It was also found that the TDP-43^{Q331Klow} mutants exhibited significantly increased omissions during the 4- and 8-month time points. The TDP-43^{G348C} mutants also exhibited a significant increase in omissions; however, this increase was constrained to the 8-month time point. These observed increases in omissions by TDP-43 mutants highlight the possibility of a decreased capacity to maintain prolonged attentional focus in these mice. Alternatively, failure to respond to targets may evidence an increase in apathetic behaviour in the TDP-43^{Q331Klow} and TDP-43^{G348C} mutants. In addition to increased omissions in the 5-CSRTT, TDP-43^{Q331Klow} mutant mice showed longer latencies (reward collection, correct touch, and incorrect touch) in the PVD task (4-months old). This was in the face of intact locomotor performance and no evidence of hyper- or hypo- activity. Thus, we sought to test motivation/apathy in these animals directly.

4.3 Limited Evidence for Motivational impairments in TDP-43^{Q331Klow} and TDP-43^{G348C} mutant mice

To further explore motivation/apathy concerns raised during the 5-CSRTT, the PRFR task (which evaluates motivation) was used to identify whether TDP-43 mutant mice exhibit apathetic-like behaviours or have decreased motivation. However, the PRFR task did not reveal any motivation-based deficits in TDP-43^{G348C} mutant mice. The TDP-43^{Q331Klow} mutants, in contrast, were slower to collect rewards (FR3 schedule only), yet following reward collection initiated subsequent trials significantly faster as revealed by the post reinforcement pause measures (PR12 schedule only). This finding taken alone could suggest an *increase* in motivation. However, motivation measured by breakpoints was normal. Thus, there is not strong evidence to suggest that the TDP-43^{Q331Klow} mutants are more or less motivated than controls.

As TDP-43^{Q331Klow} mice exhibited evidence of perseveration, it is conceivable that perseverative responding may have increased breakpoint, thus masking a motivational impairment. Kim et al. (2020) assessed this possibility in their TDP-43^{Q331K} KI mice using rate analysis of PRFR. These authors found that the TDP-43^{Q331K} KI mice demonstrated increased responding (total responses) during PR, but decreased *rates* of PR responding, in addition to increased omissions during PR extinction (no reward). Kim et al. (2020) interpreted this pattern of results as evidence for both

perseveration and amotivation in their mice. Unfortunately, due to constraints imposed by COVID-19, I was unable to extract my data and perform this same analysis.

4.4 Evidence of Cognitive Flexibility Deficits in TDP-43 Mutant Mice

TDP-43^{Q331Klow} and TDP-43^{G348C} mutant mice exhibited significant performance deficits in the PVD task. During the acquisition phase both TDP-43^{Q331Klow} and TDP-43^{G348C} mutant lines required more sessions to acquire the task and meet performance criterion. This suggests that learning impairments may be present in the TDP-43^{Q331Klow} and TDP-43^{G348C} mice. Furthermore, TDP-43^{Q331Klow} and TDP-43^{G348C} mutants made significantly more errors during the reversal learning phase, when the stimulus reward contingency is reversed. Impaired performance during PVD reversal is indicative of compromised cognitive flexibility in the TDP-43^{G348C} and TDP-43^{Q331Klow} mutant mice, which is a common feature of human FTD/ALS (Erkkinen et al., 2018; Kawakami et al., 2019; Tible et al., 2017; Young et al., 2018). Indeed, the orbitofrontal cortex characteristically displays early progressive degeneration followed by the dorsolateral prefrontal cortex in human FTD/ALS. Learning and cognitive flexibility deficits are primarily affected by the degeneration of these regions (Erkkinen et al., 2018; Evans et al., 2015; Kawakami et al., 2019; Young et al., 2018).

Impairments in reversal learning can be separated into early-stage performance deficits and late-stage performance deficits. Early-stage performance impairments (accuracy $\leq 50\%$) is driven by perseverative behaviour. Whereas late stage performance (accuracy $\geq 50\%$) is driven by learning the new stimulus-reward contingency (Graybeal et al., 2011). The deficits exhibited by TDP-43^{Q331Klow} mutant mice during the reversal phase appear to manifest as early as the second session and persist throughout the majority of sessions. This suggests that these mice are impaired early in reversal ($\leq 50\%$), consistent with a perseveration-induced impairment. Once TDP-43^{Q331Klow} mutants progressed into late-stage performance ($\geq 50\%$), performance deficits may still be driven by perseveration, but to a lesser degree. It must be noted, however, that TDP-43^{G348C} mice also demonstrated reduced performance in initial acquisition of the PVD task, and so both acquisition and reversal deficits could be indicative of a generalised learning impairment. Indeed, the TDP-43^{G348C} mutant mice did not exhibit a perseverative response phenotype in the

5-CSRTT task. In contrast, however, the TDP-43^{Q331Klow} mutants exhibited an early perseverative response phenotype at an identical time point of 4-months in the 5-CSRTT. Finally, the idea that these mice exhibit a generalised learning impairment is virtually ruled out by the observation that both TDP-43^{Q331Klow} and TDP-43^{G348C} mutant mouse lines exhibited intact performance in the much more difficult dPAL task (discussed below). Thus, we interpret the reversal learning impairments seen in this study as likely driven by perseveration.

Our lab, when operating at University Cambridge investigated the TDP-43^{Q331K} KI model using the same PVD (visual discrimination/reversal learning; VDR) task used here (Kim et al., 2020). The TDP-43^{Q331K} KI mice demonstrated task acquisition impairments in a manner similar to the TDP-43^{Q331Klow} mutants here (Kim et al., 2020). Furthermore, they revealed a very similar pattern cognitive inflexibility in their TDP-43^{Q331K} KI model. Specifically, their data indicate that the TDP-43^{Q331K} KIs exhibit stimulus-bound, perseveration-related reversal learning deficits (Kim et al., 2020), similar to mice in the present study. Both TDP-43^{Q331K(low/KI)} mutant variants present with similar pathology to the TDP-43^{Q331K} KI model in that they lack TDP-43 mislocalization and aggregation (White et al., 2018). Additionally, at least in the TDP-43^{Q331Klow} transgenic mice, the deficits precede the development of motor impairment (TDP^{Q331K} KI lack motor dysfunction; Kim et al., 2020; White et al., 2018). This provides further evidence that TDP-43 neurodegeneration and cognitive dysfunction in mice can occur in the absence of mislocalization and aggregation.

4.5 TDP-43 Mutant Mice Do Not Exhibit Any Apparent Deficits in the dPAL Task

Both TDP-43^{Q331Klow} and TDP-43^{G348C} mutant mouse lines exhibited highly consistent visuospatial memory performance in the dPAL task, with neither mutant line showing any significant visuospatial impairments. Both TDP-43^{Q331Klow} and TDP-43^{G348C} mutant mouse lines were able to achieve ~80% accuracy by task completion, which is the normative performance ceiling of mice in the dPAL task. This finding was largely expected due to the relatively spared visuospatial performance observed in human FTD/ALS pathology (Erkkinen et al., 2018; Kawakami et al., 2019). This is consistent with the observation that in FTD/ALS the hippocampus, perirhinal cortex, parahippocampal cortex and visual cortex -- areas important for

visuospatial learning -- degenerate only in the latest and most severe stages of FTD/ALS (Kawakami et al., 2019).

4.6 Investigation Limitations

This investigation, although informative, has a few limitations. The first was the use of only male mice. The importance of understanding the dynamics of neurodegenerative diseases such as FTD/ALS within the context of both male and female sexes is necessary, and future experiments should include both sexes. For this preliminary study, however, males were chosen as males are more affected by ALS, with higher risk for the disease compared to females (Longinetti & Fang, 2019).

Secondly, there is some variability present in the reward collection-, correct touch-, incorrect touch- and perseverative response latency data of both TDP-43^{Q331Klow} and TDP-43^{G348C} mutant lines. Among the mutants exhibiting the highest variability, it is possible that these same mutants experience the earliest and perhaps most severe impairment. However, this is merely speculative and requires subsequent analysis for a conclusive determination. Certainly, it would also be interesting to observe the severity of TDP-43 pathology in these mice for the possibility of deficits corresponding with pathological TDP-43 progression. With respect to the 5-CSRTT, only a single cohort of TDP-43^{G348C} mutants were examined. It is likely that the variation observed throughout these experiments would have been reduced by the higher n values originally planned. Unfortunately, due to the global pandemic ceasing experiments, issues concerning variability could not be further investigated.

Lastly, biochemical and histopathological confirmation of TDP-43 pathology in TDP-43^{Q331Klow} and TDP-43^{G348C} mutants unfortunately was not completed. The global pandemic created unforeseen circumstances, and brain and spinal tissue sample analysis was no longer possible. However, both TDP-43^{Q331Klow} and TDP-43^{G348C} transgenic mouse models of FTD/ALS have been extensively described previously by the Cleveland and Julien groups respectively (Arnold et al., 2013a, 2013b; Swarup et al., 2011), and our mice are likely similar.

4.7 Future Directions – Can Cognitive Deficits be Linked to Specific Pathological TDP-43 Events?

The results of this investigation provide some exciting insights into early cognitive deficits in FTD/ALS mutant mouse models. However, there is another limitation to this investigation that can be improved by future investigations; namely, the omission of an overexpressing WT-TDP-43 mouse line. This omission makes it difficult to assess the relative contribution of overexpression in TDP-43 pathology-related cognitive deficits. This limitation is worsened by the lack of a mutant TDP-43 line without overexpression (knock-in). The combination of these two limitations removes the capacity to effectively delineate whether cognitive deficits result from TDP-43 mutations or overexpression. However, the robust and highly similar TDP-43^{Q331K}(low/KI) data presented here and in a separate investigation using a KI model (Kim et al. 2020) suggest that overexpression may not be required for neurodegeneration and/or cognitive dysfunction.

Recently it has also been suggested that pathological TDP-43 aggregates may actually represent a penultimate or final stage of FTD/ALS pathology, where relevant cellular machinery has already been overwhelmed and is incapable of preventing or reversing TDP-43 phase transitions (J. R. Mann et al., 2019). It should be possible to investigate cognitive alterations resulting from phase transitions in TDP-43^{Q331K} KI (no overexpression), TDP-43^{Q331Klow} (0.5-fold increase) and TDP-43^{G348C} or ^{Q331K} (3-fold increase with TDP-43 aggregation) mice using automated touchscreens. We have already shown here cognitive deficits in 4-month-old (TDP-43^{G348C} and TDP-43^{Q331Klow}) mice preceding late-stage ALS phenotypes (TDP-43 mislocalization, aggregation and motor dysfunction; Arnold et al., 2013a; Swarup et al., 2011). Additionally, because TDP-43^{G348C} pathological aggregation and ubiquitination progressively worsens over time (e.g., 6mo, 10mo), in such a study cognitive deficits could be correlated with TDP-43 pathology (Swarup et al., 2011).

An optogenetic approach could be the most informative method for investigating cognitive dysfunction preceding aggregation in the TDP-43 mouse lines. A Cry2 (blue-light receptor) has been used previously in human cell lines and zebrafish investigations to drive TDP-43 oligomerization and phase transitions (Asakawa et al., 2020; J. R. Mann et al., 2019; Shin et al.,

2017). Further, the Asakawa group developed an optogenetic oligomerization construct by using a point mutation (E490G) to modify zebrafish Cry2, and then fuse Cry2 to the c-terminal (prion-like low-complexity domain) of TDP-43^{A315T} (tdp43-Cry2-olig). Blue-light stimulation of the tdp43-Cry2-olig construct triggers substantial clustering under exposure to blue light (Asakawa et al., 2020). Spatiotemporal control of TDP-43^{Q331K}(low/KI) and TDP-43^{G348C} oligomerization and phase transitions could facilitate investigation of upstream TDP-43 mechanisms by correlating cognitive dysfunction with the presence or absence of pathological events (e.g., mislocalization, aggregation, SG recruitment). This could prove to be extremely informative in determining the pathomechanism(s) or event(s) which result in FTD/ALS cognitive dysfunction and motor degeneration. At the time of writing, automated touchscreen systems are already capable of evaluating mice using integrated optogenetic equipment, and inciting TDP-43 oligomerization and phase transitions in mice should be feasible with the development of a Cry2-oligomerization construct in TDP-43 mice (Asakawa et al., 2020; Dumont et al., 2020; J. R. Mann et al., 2019; Shin et al., 2017). Certainly, adopting this approach may prove useful in addressing the limitations of this study and provide a more comprehensive understanding of human FTD/ALS pathomechanisms and cognitive aspects.

4.8 Final Conclusions

We explored the possibility of huTDP-43 transgene (G348C & Q331K)-mediated early cognitive deficits in mouse models of FTD/ALS. We demonstrated that human ALS-linked TDP-43^{Q331K^{low}} and TDP-43^{G348C} mutant mouse models exhibit highly similar cognitive changes, revealed by automated touchscreens with validated tasks. The cognitive flexibility deficits revealed by the PVD task, and exhibited in both the TDP-43^{Q331K^{low}} and TDP-43^{G348C} mouse lines, recapitulates principal features of BPSD (dysexecutive function and perseveration) in human FTD/ALS (Erkkinen et al., 2018; Tible et al., 2017; Young et al., 2018). A potential early perseverative response phenotype was also revealed in the TDP-43^{Q331K^{low}} mutant mouse line across two unique touchscreen tasks (5-CSRTT & PVD). Both of these findings are similar to those reported by another study using a knock-in model, providing additional evidence in support of the findings presented here (Kim et al., 2020). Furthermore, these deficits of executive function precede FTD/ALS-induced motor impairments in TDP-43 mutant mice. Collectively,

these results highlight that the combination of TDP-43 mouse models and touchscreen tests may potentially be useful tools for understanding and developing FTD/ALS cognitive therapies.

References

- Arai, T., Hasegawa, M., Akiyama, H., Ikeda, K., Nonaka, T., Mori, H., Mann, D., Tsuchiya, K., Yoshida, M., Hashizume, Y., & Oda, T. (2006). TDP-43 is a component of ubiquitin-positive tau-negative inclusions in frontotemporal lobar degeneration and amyotrophic lateral sclerosis. *Biochemical and Biophysical Research Communications*, *351*(3), 602–611. <https://doi.org/10.1016/j.bbrc.2006.10.093>
- Arnold, E. S., Ling, S.-C., Huelga, S. C., Lagier-Tourenne, C., Polymenidou, M., Ditsworth, D., Kordasiewicz, H. B., McAlonis-Downes, M., Platoshyn, O., Parone, P. A., Da Cruz, S., Clutario, K. M., Swing, D., Tessarollo, L., Marsala, M., Shaw, C. E., Yeo, G. W., & Cleveland, D. W. (2013a). ALS-linked TDP-43 mutations produce aberrant RNA splicing and adult-onset motor neuron disease without aggregation or loss of nuclear TDP-43. *Proceedings of the National Academy of Sciences of the United States of America*, *110*(8), E736-745. <https://doi.org/10.1073/pnas.1222809110>
- Arnold, E. S., Ling, S.-C., Huelga, S. C., Lagier-Tourenne, C., Polymenidou, M., Ditsworth, D., Kordasiewicz, H. B., McAlonis-Downes, M., Platoshyn, O., Parone, P. A., Da Cruz, S., Clutario, K. M., Swing, D., Tessarollo, L., Marsala, M., Shaw, C. E., Yeo, G. W., & Cleveland, D. W. (2013b). Supporting Information; ALS-linked TDP-43 mutations produce aberrant RNA splicing and adult-onset motor neuron disease without aggregation or loss of nuclear TDP-43. *Proceedings of the National Academy of Sciences*, *110*(8), E736–E745. <https://doi.org/10.1073/pnas.1222809110>
- Asakawa, K., Handa, H., & Kawakami, K. (2020). Optogenetic modulation of TDP-43 oligomerization accelerates ALS-related pathologies in the spinal motor neurons. *Nature Communications*, *11*(1), 1004. <https://doi.org/10.1038/s41467-020-14815-x>

- Austin, J. A., Wright, G. S. A., Watanabe, S., Grossmann, J. G., Antonyuk, S. V., Yamanaka, K., & Hasnain, S. S. (2014). Disease causing mutants of TDP-43 nucleic acid binding domains are resistant to aggregation and have increased stability and half-life. *Proceedings of the National Academy of Sciences*, *111*(11), 4309–4314.
<https://doi.org/10.1073/pnas.1317317111>
- Banks, G. T., Kuta, A., Isaacs, A. M., & Fisher, E. M. C. (2008). TDP-43 is a culprit in human neurodegeneration, and not just an innocent bystander. *Mammalian Genome*, *19*(5), 299–305. <https://doi.org/10.1007/s00335-008-9117-x>
- Barber, R., Snowden, J. S., & Craufurd, D. (1995). Frontotemporal dementia and Alzheimer's disease: Retrospective differentiation using information from informants. *Journal of Neurology, Neurosurgery, and Psychiatry*, *59*(1), 61–70.
- Barson, F. P., Kinsella, G. J., Ong, B., & Mathers, S. E. (2000). A neuropsychological investigation of dementia in motor neurone disease (MND). *Journal of the Neurological Sciences*, *180*(1–2), 107–113.
- Barulli, M. R., Fontana, A., Panza, F., Copetti, M., Bruno, S., Tursi, M., Iurillo, A., Tortelli, R., Capozzo, R., Simone, I. L., & Logroscino, G. (2015). Frontal assessment battery for detecting executive dysfunction in amyotrophic lateral sclerosis without dementia: A retrospective observational study. *BMJ Open*, *5*(9), e007069.
<https://doi.org/10.1136/bmjopen-2014-007069>
- Beraldo, F. H., Palmer, D., Memar, S., Wasserman, D. I., Lee, W.-J. V., Liang, S., Creighton, S. D., Kolisnyk, B., Cowan, M. F., Mels, J., Masood, T. S., Fodor, C., Al-Onaizi, M. A., Bartha, R., Gee, T., Saksida, L. M., Bussey, T. J., Strother, S. S., Prado, V. F., ... Prado, M. A. (2019).

MouseBytes, an open-access high-throughput pipeline and database for rodent touchscreen-based cognitive assessment. *ELife*, *8*, e49630.

<https://doi.org/10.7554/eLife.49630>

Boeynaems, S., Alberti, S., Fawzi, N. L., Mittag, T., Polymenidou, M., Rousseau, F., Schymkowitz, J., Shorter, J., Wolozin, B., Van Den Bosch, L., Tompa, P., & Fuxreiter, M. (2018). Protein Phase Separation: A New Phase in Cell Biology. *Trends in Cell Biology*, *28*(6), 420–435.

<https://doi.org/10.1016/j.tcb.2018.02.004>

Bozzo, F., Mirra, A., & Carrì, M. T. (2017). Oxidative stress and mitochondrial damage in the pathogenesis of ALS: New perspectives. *Neuroscience Letters*, *636*, 3–8.

<https://doi.org/10.1016/j.neulet.2016.04.065>

Bussey, T. J., Padain, T. L., Skillings, E. A., Winters, B. D., Morton, A. J., & Saksida, L. M. (2008). The touchscreen cognitive testing method for rodents: How to get the best out of your rat. *Learning & Memory*, *15*(7), 516–523. <https://doi.org/10.1101/lm.987808>

Cassel, J. A., & Reitz, A. B. (2013). Ubiquilin-2 (UBQLN2) binds with high affinity to the C-terminal region of TDP-43 and modulates TDP-43 levels in H4 cells: Characterization of inhibition by nucleic acids and 4-aminoquinolines. *Biochimica et Biophysica Acta (BBA) - Proteins and Proteomics*, *1834*(6), 964–971.

<https://doi.org/10.1016/j.bbapap.2013.03.020>

Chambers, L. W., Bancej, C., & McDowell, I. (2016). *Prevalence and Monetary Costs of Dementia in Canada*. 70.

- Chen, S., Sayana, P., Zhang, X., & Le, W. (2013). Genetics of amyotrophic lateral sclerosis: An update. *Molecular Neurodegeneration*, *8*(1), 28. <https://doi.org/10.1186/1750-1326-8-28>
- Chiò, A., Mazzini, L., D'Alfonso, S., Corrado, L., Canosa, A., Moglia, C., Manera, U., Bersano, E., Brunetti, M., Barberis, M., Veldink, J. H., van den Berg, L. H., Pearce, N., Sproviero, W., McLaughlin, R., Vajda, A., Hardiman, O., Rooney, J., Mora, G., ... Al-Chalabi, A. (2018). The multistep hypothesis of ALS revisited: The role of genetic mutations. *Neurology*, *91*(7), e635–e642. <https://doi.org/10.1212/WNL.0000000000005996>
- Crabbe, J. C., Wahlsten, D., & Dudek, B. C. (1999). Genetics of mouse behavior: Interactions with laboratory environment. *Science (New York, N.Y.)*, *284*(5420), 1670–1672.
- D'Angelo, M. A., Raices, M., Panowski, S. H., & Hetzer, M. W. (2009). Age-Dependent Deterioration of Nuclear Pore Complexes Causes a Loss of Nuclear Integrity in Postmitotic Cells. *Cell*, *136*(2), 284–295. <https://doi.org/10.1016/j.cell.2008.11.037>
- Dhar, S. K., Zhang, J., Gal, J., Xu, Y., Miao, L., Lynn, B. C., Zhu, H., Kasarskis, E. J., & St. Clair, D. K. (2014). Fused in Sarcoma Is a Novel Regulator of Manganese Superoxide Dismutase Gene Transcription. *Antioxidants & Redox Signaling*, *20*(10), 1550–1566. <https://doi.org/10.1089/ars.2012.4984>
- Dumont, J. R., Salewski, R., & Beraldo, F. (2020). Critical Mass: The Rise of a Touchscreen Technology Community for Rodent Cognitive Testing. *Genes, Brain and Behavior*. <https://doi.org/10.1111/gbb.12650>
- Elamin, M., Phukan, J., Bede, P., Jordan, N., Byrne, S., Pender, N., & Hardiman, O. (2011). Executive dysfunction is a negative prognostic indicator in patients with ALS without

dementia. *Neurology*, 76(14), 1263–1269.

<https://doi.org/10.1212/WNL.0b013e318214359f>

Erkkinen, M. G., Kim, M.-O., & Geschwind, M. D. (2018). Clinical Neurology and Epidemiology of the Major Neurodegenerative Diseases. *Cold Spring Harbor Perspectives in Biology*, 10(4), a033118. <https://doi.org/10.1101/cshperspect.a033118>

Evans, J., Olm, C., McCluskey, L., Elman, L., Boller, A., Moran, E., Rascovsky, K., Bisbing, T., McMillan, C. T., & Grossman, M. (2015). Impaired cognitive flexibility in amyotrophic lateral sclerosis. *Cognitive and Behavioral Neurology: Official Journal of the Society for Behavioral and Cognitive Neurology*, 28(1), 17–26.

<https://doi.org/10.1097/WNN.0000000000000049>

Ferrari, R., Kapogiannis, D., Huey, E. D., & Momeni, P. (2011). FTD and ALS: A tale of two diseases. *Current Alzheimer Research*, 8(3), 273–294.

Gao, J., Wang, L., Huntley, M. L., Perry, G., & Wang, X. (2018). Pathomechanisms of TDP-43 in neurodegeneration. *Journal of Neurochemistry*, 146(1), 7–20.

<https://doi.org/10.1111/jnc.14327>

Gao, J., Wang, L., Yan, T., Perry, G., & Wang, X. (2019). TDP-43 proteinopathy and mitochondrial abnormalities in neurodegeneration. *Molecular and Cellular Neuroscience*, 100, 103396.

<https://doi.org/10.1016/j.mcn.2019.103396>

Gaskin, J., Gomes, J., Darshan, S., & Krewski, D. (2017). Burden of neurological conditions in Canada. *NeuroToxicology*, 61, 2–10. <https://doi.org/10.1016/j.neuro.2016.05.001>

Gasset-Rosa, F., Lu, S., Yu, H., Chen, C., Melamed, Z., Guo, L., Shorter, J., Da Cruz, S., &

Cleveland, D. W. (2019). Cytoplasmic TDP-43 De-mixing Independent of Stress Granules

- Drives Inhibition of Nuclear Import, Loss of Nuclear TDP-43, and Cell Death. *Neuron*, 102(2), 339-357.e7. <https://doi.org/10.1016/j.neuron.2019.02.038>
- Giordana, M. T., Ferrero, P., Grifoni, S., Pellerino, A., Naldi, A., & Montuschi, A. (2011). Dementia and cognitive impairment in amyotrophic lateral sclerosis: A review. *Neurological Sciences*, 32(1), 9–16. <https://doi.org/10.1007/s10072-010-0439-6>
- Giribaldi, F., Milanese, M., Bonifacino, T., Anna Rossi, P. I., Di Prisco, S., Pittaluga, A., Tacchetti, C., Puliti, A., Usai, C., & Bonanno, G. (2013). Group I metabotropic glutamate autoreceptors induce abnormal glutamate exocytosis in a mouse model of amyotrophic lateral sclerosis. *Neuropharmacology*, 66, 253–263. <https://doi.org/10.1016/j.neuropharm.2012.05.018>
- Gomes, E., & Shorter, J. (2019). The molecular language of membraneless organelles. *Journal of Biological Chemistry*, 294(18), 7115–7127. <https://doi.org/10.1074/jbc.TM118.001192>
- Graybeal, C., Bachu, M., Mozhui, K., Saksida, L. M., Bussey, T. J., Sagalyn, E., Williams, R. W., & Holmes, A. (2014). Strains and stressors: An analysis of touchscreen learning in genetically diverse mouse strains. *PloS One*, 9(2), e87745. <https://doi.org/10.1371/journal.pone.0087745>
- Graybeal, C., Feyder, M., Schulman, E., Saksida, L. M., Bussey, T. J., Brigman, J. L., & Holmes, A. (2011). Paradoxical reversal learning enhancement by stress or prefrontal cortical damage: Rescue with BDNF. *Nature Neuroscience*, 14(12), 1507–1509. <https://doi.org/10.1038/nn.2954>
- Hansson, O., Lehmann, S., Otto, M., Zetterberg, H., & Lewczuk, P. (2019). Advantages and disadvantages of the use of the CSF Amyloid β (A β) 42/40 ratio in the diagnosis of

Alzheimer's Disease. *Alzheimer's Research & Therapy*, 11(1), 34.

<https://doi.org/10.1186/s13195-019-0485-0>

Hardiman, O. (2010). Amyotrophic Lateral Sclerosis. In John Wiley & Sons, Ltd (Ed.),

Encyclopedia of Life Sciences (p. a0000014.pub2). John Wiley & Sons, Ltd.

<https://doi.org/10.1002/9780470015902.a0000014.pub2>

Harrison, A. F., & Shorter, J. (2017). RNA-binding proteins with prion-like domains in health and disease. *Biochemical Journal*, 474(8), 1417–1438. <https://doi.org/10.1042/BCJ20160499>

Heath, C. J., O'Callaghan, C., Mason, S. L., Phillips, B. U., Saksida, L. M., Robbins, T. W., Barker, R.

A., Bussey, T. J., & Sahakian, B. J. (2019). A Touchscreen Motivation Assessment

Evaluated in Huntington's Disease Patients and R6/1 Model Mice. *Frontiers in*

Neurology, 10, 858. <https://doi.org/10.3389/fneur.2019.00858>

Heath, C. J., Phillips, B. U., Bussey, T. J., & Saksida, L. M. (2016). Measuring Motivation and

Reward-Related Decision Making in the Rodent Operant Touchscreen System: Mouse

Touchscreen FR/PR and ERC Protocol. In C. R. Gerfen, A. Holmes, D. Sibley, P. Skolnick, &

S. Wray (Eds.), *Current Protocols in Neuroscience* (p. 8.34.1-8.34.20). John Wiley & Sons,

Inc. <https://doi.org/10.1002/0471142301.ns0834s74>

Heyburn, L., & Moussa, C. E.-H. (2017). TDP-43 in the spectrum of MND-FTLD pathologies.

Molecular and Cellular Neuroscience, 83, 46–54.

<https://doi.org/10.1016/j.mcn.2017.07.001>

Hofmann, J. W., Seeley, W. W., & Huang, E. J. (2019). RNA Binding Proteins and the

Pathogenesis of Frontotemporal Lobar Degeneration. *Annual Review of Pathology:*

Mechanisms of Disease, 14(1), 469–495. <https://doi.org/10.1146/annurev-pathmechdis-012418-012955>

Hogan, D. B., Jetté, N., Fiest, K. M., Roberts, J. I., Pearson, D., Smith, E. E., Roach, P., Kirk, A., Pringsheim, T., & Maxwell, C. J. (2016). The Prevalence and Incidence of Frontotemporal Dementia: A Systematic Review. *Canadian Journal of Neurological Sciences / Journal Canadien Des Sciences Neurologiques*, 43(S1), S96–S109. <https://doi.org/10.1017/cjn.2016.25>

Horner, A. E., Heath, C. J., Hvoslef-Eide, M., Kent, B. A., Kim, C. H., Nilsson, S. R. O., Alsiö, J., Oomen, C. A., Holmes, A., Saksida, L. M., & Bussey, T. J. (2013). The touchscreen operant platform for testing learning and memory in rats and mice. *Nature Protocols*, 8(10), 1961–1984. <https://doi.org/10.1038/nprot.2013.122>

Igaz, L. M., Kwong, L. K., Lee, E. B., Chen-Plotkin, A., Swanson, E., Unger, T., Malunda, J., Xu, Y., Winton, M. J., Trojanowski, J. Q., & Lee, V. M.-Y. (2011). Dysregulation of the ALS-associated gene TDP-43 leads to neuronal death and degeneration in mice. *The Journal of Clinical Investigation*, 121(2), 726–738. <https://doi.org/10.1172/JCI44867>

Iguchi, Y., Katsuno, M., Niwa, J., Takagi, S., Ishigaki, S., Ikenaka, K., Kawai, K., Watanabe, H., Yamanaka, K., Takahashi, R., Misawa, H., Sasaki, S., Tanaka, F., & Sobue, G. (2013). Loss of TDP-43 causes age-dependent progressive motor neuron degeneration. *Brain*, 136(5), 1371–1382. <https://doi.org/10.1093/brain/awt029>

Janickova, H., Prado, V. F., Prado, M. A. M., El Mestikawy, S., & Bernard, V. (2017). Vesicular acetylcholine transporter (VACHT) over-expression induces major modifications of

- striatal cholinergic interneuron morphology and function. *Journal of Neurochemistry*, 142(6), 857–875. <https://doi.org/10.1111/jnc.14105>
- Janickova, H., Rosborough, K., Al-Onaizi, M., Kljakic, O., Guzman, M. S., Gros, R., Prado, M. A. M., & Prado, V. F. (2017). Deletion of the vesicular acetylcholine transporter from pedunculo pontine/laterodorsal tegmental neurons modifies gait. *Journal of Neurochemistry*, 140(5), 787–798. <https://doi.org/10.1111/jnc.13910>
- Kabashi, E., Bercier, V., Lissouba, A., Liao, M., Brustein, E., Rouleau, G. A., & Drapeau, P. (2011). FUS and TARDBP but Not SOD1 Interact in Genetic Models of Amyotrophic Lateral Sclerosis. *PLoS Genetics*, 7(8), e1002214. <https://doi.org/10.1371/journal.pgen.1002214>
- Kasper, E., Schuster, C., Machts, J., Bittner, D., Vielhaber, S., Benecke, R., Teipel, S., & Prudlo, J. (2015). Dysexecutive functioning in ALS patients and its clinical implications. *Amyotrophic Lateral Sclerosis & Frontotemporal Degeneration*, 16(3–4), 160–171. <https://doi.org/10.3109/21678421.2015.1026267>
- Kawakami, I., Arai, T., & Hasegawa, M. (2019). The basis of clinicopathological heterogeneity in TDP-43 proteinopathy. *Acta Neuropathologica*, 138(5), 751–770. <https://doi.org/10.1007/s00401-019-02077-x>
- Kim, E., White, M. A., Phillips, B. U., Lopez-Cruz, L., Kim, H., Heath, C. J., Lee, J. E., Saksida, L. M., Sreedharan, J., & Bussey, T. J. (2020). Coexistence of perseveration and apathy in the TDP-43Q331K knock-in mouse model of ALS-FTD. *Translational Psychiatry, In Press*, 29.
- Lee, J. H., Cho, S. Y., & Kim, E. (2020). Translational cognitive neuroscience of dementia with touchscreen operant chambers. *Genes, Brain and Behavior*. <https://doi.org/10.1111/gbb.12664>

- Ling, S.-C., Polymenidou, M., & Cleveland, D. W. (2013). Converging Mechanisms in ALS and FTD: Disrupted RNA and Protein Homeostasis. *Neuron*, *79*(3), 416–438.
<https://doi.org/10.1016/j.neuron.2013.07.033>
- Lomen-Hoerth, C., Murphy, J., Langmore, S., Kramer, J. H., Olney, R. K., & Miller, B. (2003). Are amyotrophic lateral sclerosis patients cognitively normal? *Neurology*, *60*(7), 1094–1097.
- Longinetti, E., & Fang, F. (2019). Epidemiology of amyotrophic lateral sclerosis: An update of recent literature. *Current Opinion in Neurology*, *32*(5), 771–776.
<https://doi.org/10.1097/WCO.0000000000000730>
- Machts, J., Bittner, V., Kasper, E., Schuster, C., Prudlo, J., Abdulla, S., Kollwe, K., Petri, S., Dengler, R., Heinze, H.-J., Vielhaber, S., Schoenfeld, M. A., & Bittner, D. M. (2014). Memory deficits in amyotrophic lateral sclerosis are not exclusively caused by executive dysfunction: A comparative neuropsychological study of amnesic mild cognitive impairment. *BMC Neuroscience*, *15*, 83. <https://doi.org/10.1186/1471-2202-15-83>
- Mackenzie, I. R. A. (2007). The Neuropathology of FTD Associated With ALS: *Alzheimer Disease & Associated Disorders*, *21*(4), S44–S49.
<https://doi.org/10.1097/WAD.0b013e31815c3486>
- Mackenzie, I. R. A., & H. Feldman, H. (2005). Ubiquitin Immunohistochemistry Suggests Classic Motor Neuron Disease, Motor Neuron Disease With Dementia, and Frontotemporal Dementia of the Motor Neuron Disease Type Represent a Clinicopathologic Spectrum: *Journal of Neuropathology and Experimental Neurology*, *64*(8), 730–739.
<https://doi.org/10.1097/01.jnen.0000174335.27708.0a>

- Mackenzie, I. R., & Neumann, M. (2017). Reappraisal of TDP-43 pathology in FTL-D-U subtypes. *Acta Neuropathologica*, *134*(1), 79–96. <https://doi.org/10.1007/s00401-017-1716-8>
- Mann, D. M. A., & Snowden, J. S. (2017). Frontotemporal lobar degeneration: Pathogenesis, pathology and pathways to phenotype: Frontotemporal lobar degeneration. *Brain Pathology*, *27*(6), 723–736. <https://doi.org/10.1111/bpa.12486>
- Mann, J. R., Gleixner, A. M., Mauna, J. C., Gomes, E., DeChellis-Marks, M. R., Needham, P. G., Copley, K. E., Hurtle, B., Portz, B., Pyles, N. J., Guo, L., Calder, C. B., Wills, Z. P., Pandey, U. B., Kofler, J. K., Brodsky, J. L., Thathiah, A., Shorter, J., & Donnelly, C. J. (2019). RNA Binding Antagonizes Neurotoxic Phase Transitions of TDP-43. *Neuron*, *102*(2), 321-338.e8. <https://doi.org/10.1016/j.neuron.2019.01.048>
- Mantovan, M. C., Baggio, L., Dalla Barba, G., Smith, P., Pegoraro, E., Soraru', G., Bonometto, P., & Angelini, C. (2003). Memory deficits and retrieval processes in ALS. *European Journal of Neurology*, *10*(3), 221–227.
- Massman, P. J., Sims, J., Cooke, N., Haverkamp, L. J., Appel, V., & Appel, S. H. (1996). Prevalence and correlates of neuropsychological deficits in amyotrophic lateral sclerosis. *Journal of Neurology, Neurosurgery & Psychiatry*, *61*(5), 450–455. <https://doi.org/10.1136/jnnp.61.5.450>
- Mathis, S., Goizet, C., Soulages, A., Vallat, J.-M., & Masson, G. L. (2019). Genetics of amyotrophic lateral sclerosis: A review. *Journal of the Neurological Sciences*, *399*, 217–226. <https://doi.org/10.1016/j.jns.2019.02.030>
- Mels, J. (2018). Assessing Cognition In A Mouse Model of Alzheimer's Disease. *Electronic Thesis and Dissertation Repository*. 5720, 164.

- Morton, A. J., Skillings, E., Bussey, T. J., & Saksida, L. M. (2006). Measuring cognitive deficits in disabled mice using an automated interactive touchscreen system. *Nature Methods*, 3(10), 767. <https://doi.org/10.1038/nmeth1006-767>
- Nag, S., Yu, L., Wilson, R. S., Chen, E.-Y., Bennett, D. A., & Schneider, J. A. (2017). TDP-43 pathology and memory impairment in elders without pathologic diagnoses of AD or FTLD. *Neurology*, 88(7), 653–660. <https://doi.org/10.1212/WNL.0000000000003610>
- Nithianantharajah, J., McKechnie, A. G., Stewart, T. J., Johnstone, M., Blackwood, D. H., St Clair, D., Grant, S. G. N., Bussey, T. J., & Saksida, L. M. (2015). Bridging the translational divide: Identical cognitive touchscreen testing in mice and humans carrying mutations in a disease-relevant homologous gene. *Scientific Reports*, 5, 14613. <https://doi.org/10.1038/srep14613>
- Olney, R. K., Murphy, J., Forshew, D., Garwood, E., Miller, B. L., Langmore, S., Kohn, M. A., & Lomen-Hoerth, C. (2005). The effects of executive and behavioral dysfunction on the course of ALS. *Neurology*, 65(11), 1774–1777. <https://doi.org/10.1212/01.wnl.0000188759.87240.8b>
- Onyike, C. U., & Diehl-Schmid, J. (2013). The epidemiology of frontotemporal dementia. *International Review of Psychiatry*, 25(2), 130–137. <https://doi.org/10.3109/09540261.2013.776523>
- Parker, S. J., Meyerowitz, J., James, J. L., Liddell, J. R., Crouch, P. J., Kanninen, K. M., & White, A. R. (2012). Endogenous TDP-43 localized to stress granules can subsequently form protein aggregates. *Neurochemistry International*, 60(4), 415–424. <https://doi.org/10.1016/j.neuint.2012.01.019>

- Picher-Martel, V., Renaud, L., Bareil, C., & Julien, J.-P. (2019). Neuronal Expression of UBQLN2P497H Exacerbates TDP-43 Pathology in TDP-43G348C Mice through Interaction with Ubiquitin. *Molecular Neurobiology*, *56*(7), 4680–4696.
<https://doi.org/10.1007/s12035-018-1411-3>
- Prnp-TARDBP*Q331K Jax Stock #017930*. (2020, July 1). [The Jackson Laboratory].
<https://www.jax.org/strain/017930>
- Rabinovici, G. D., & Miller, B. L. (2010). Frontotemporal lobar degeneration: Epidemiology, pathophysiology, diagnosis and management. *CNS Drugs*, *24*(5), 375–398.
<https://doi.org/10.2165/11533100-000000000-00000>
- Radakovic, R., Stephenson, L., Colville, S., Swingler, R., Chandran, S., & Abrahams, S. (2016). Multidimensional apathy in ALS: Validation of the Dimensional Apathy Scale. *Journal of Neurology, Neurosurgery, and Psychiatry*, *87*(6), 663–669. <https://doi.org/10.1136/jnnp-2015-310772>
- Rascovsky, K., Hodges, J. R., Knopman, D., Mendez, M. F., Kramer, J. H., Neuhaus, J., van Swieten, J. C., Seelaar, H., Dopper, E. G. P., Onyike, C. U., Hillis, A. E., Josephs, K. A., Boeve, B. F., Kertesz, A., Seeley, W. W., Rankin, K. P., Johnson, J. K., Gorno-Tempini, M.-L., Rosen, H., ... Miller, B. L. (2011). Sensitivity of revised diagnostic criteria for the behavioural variant of frontotemporal dementia. *Brain*, *134*(9), 2456–2477.
<https://doi.org/10.1093/brain/awr179>
- Renton, A. E., Chiò, A., & Traynor, B. J. (2014). State of play in amyotrophic lateral sclerosis genetics. *Nature Neuroscience*, *17*(1), 17–23. <https://doi.org/10.1038/nn.3584>

- Ringholz, G. M., Appel, S. H., Bradshaw, M., Cooke, N. A., Mosnik, D. M., & Schulz, P. E. (2005). Prevalence and patterns of cognitive impairment in sporadic ALS. *Neurology*, *65*(4), 586–590. <https://doi.org/10.1212/01.wnl.0000172911.39167.b6>
- Romberg, C., Bussey, T. J., & Saksida, L. M. (2013). Paying more attention to attention: Towards more comprehensive cognitive translation using mouse models of Alzheimer's disease. *Brain Research Bulletin*, *92*, 49–55. <https://doi.org/10.1016/j.brainresbull.2012.02.007>
- Shin, Y., Berry, J., Pannucci, N., Haataja, M. P., Toettcher, J. E., & Brangwynne, C. P. (2017). Spatiotemporal Control of Intracellular Phase Transitions Using Light-Activated optoDroplets. *Cell*, *168*(1–2), 159–171.e14. <https://doi.org/10.1016/j.cell.2016.11.054>
- Slegers, K., Cruts, M., & Van Broeckhoven, C. (2010). Molecular Pathways of Frontotemporal Lobar Degeneration. *Annual Review of Neuroscience*, *33*(1), 71–88. <https://doi.org/10.1146/annurev-neuro-060909-153144>
- Sreedharan, J., Blair, I. P., Tripathi, V. B., Hu, X., Vance, C., Rogelj, B., Ackerley, S., Durnall, J. C., Williams, K. L., Buratti, E., Baralle, F., de Belleruche, J., Mitchell, J. D., Leigh, P. N., Al-Chalabi, A., Miller, C. C., Nicholson, G., & Shaw, C. E. (2008). TDP-43 mutations in familial and sporadic amyotrophic lateral sclerosis. *Science (New York, N.Y.)*, *319*(5870), 1668–1672. <https://doi.org/10.1126/science.1154584>
- Stallings, N. R., Puttapparthi, K., Luther, C. M., Burns, D. K., & Elliott, J. L. (2010). Progressive motor weakness in transgenic mice expressing human TDP-43. *Neurobiology of Disease*, *40*(2), 404–414. <https://doi.org/10.1016/j.nbd.2010.06.017>
- Stojkovic, T., Stefanova, E., Pekmezovic, T., Peric, S., & Stevic, Z. (2016). Executive dysfunction and survival in patients with amyotrophic lateral sclerosis: Preliminary report from a

Serbian centre for motor neuron disease. *Amyotrophic Lateral Sclerosis & Frontotemporal Degeneration*, 17(7–8), 543–547.

<https://doi.org/10.1080/21678421.2016.1211148>

Strong, M. J., Lomen-Hoerth, C., Caselli, R. J., Bigio, E. H., & Yang, W. (2003). Cognitive impairment, frontotemporal dementia, and the motor neuron diseases. *Annals of Neurology*, 54 Suppl 5, S20-23. <https://doi.org/10.1002/ana.10574>

Swarup, V., & Julien, J.-P. (2011). ALS pathogenesis: Recent insights from genetics and mouse models. *Progress in Neuro-Psychopharmacology & Biological Psychiatry*, 35(2), 363–369. <https://doi.org/10.1016/j.pnpbp.2010.08.006>

Swarup, V., Phaneuf, D., Bareil, C., Robertson, J., Rouleau, G. A., Kriz, J., & Julien, J.-P. (2011). Pathological hallmarks of amyotrophic lateral sclerosis/frontotemporal lobar degeneration in transgenic mice produced with TDP-43 genomic fragments. *Brain: A Journal of Neurology*, 134(Pt 9), 2610–2626. <https://doi.org/10.1093/brain/awr159>

Talbot, P. R., Goulding, P. J., Lloyd, J. J., Snowden, J. S., Neary, D., & Testa, H. J. (1995). Interrelation between “classic” motor neuron disease and frontotemporal dementia: Neuropsychological and single photon emission computed tomography study. *Journal of Neurology, Neurosurgery & Psychiatry*, 58(5), 541–547. <https://doi.org/10.1136/jnnp.58.5.541>

Tible, O. P., Riese, F., Savaskan, E., & von Gunten, A. (2017). Best practice in the management of behavioural and psychological symptoms of dementia. *Therapeutic Advances in Neurological Disorders*, 10(8), 297–309. <https://doi.org/10.1177/1756285617712979>

- Van den Broeck, L., Sierksma, A., Hansquine, P., Thonnard, D., Callaerts-Vegh, Z., & D'Hooge, R. (2020). Comparison between touchscreen operant chambers and water maze to detect early prefrontal dysfunction in mice. *Genes, Brain and Behavior*.
<https://doi.org/10.1111/gbb.12695>
- Van Langenhove, T., van der Zee, J., & Van Broeckhoven, C. (2012). The molecular basis of the frontotemporal lobar degeneration-amyotrophic lateral sclerosis spectrum. *Annals of Medicine*, 44(8), 817–828. <https://doi.org/10.3109/07853890.2012.665471>
- Van Mossevelde, S., Engelborghs, S., van der Zee, J., & Van Broeckhoven, C. (2018). Genotype–phenotype links in frontotemporal lobar degeneration. *Nature Reviews Neurology*, 14(6), 363–378. <https://doi.org/10.1038/s41582-018-0009-8>
- Wang, W., Arakawa, H., Wang, L., Okolo, O., Siedlak, S. L., Jiang, Y., Gao, J., Xie, F., Petersen, R. B., & Wang, X. (2017). Motor-Coordination and Cognitive Dysfunction Caused by Mutant TDP-43 Could Be Reversed by Inhibiting Its Mitochondrial Localization. *Molecular Therapy: The Journal of the American Society of Gene Therapy*, 25(1), 127–139.
<https://doi.org/10.1016/j.ymthe.2016.10.013>
- Watermeyer, T. J., Brown, R. G., Sidle, K. C. L., Oliver, D. J., Allen, C., Karlsson, J., Ellis, C. M., Shaw, C. E., Al-Chalabi, A., & Goldstein, L. H. (2015). Executive dysfunction predicts social cognition impairment in amyotrophic lateral sclerosis. *Journal of Neurology*, 262(7), 1681–1690. <https://doi.org/10.1007/s00415-015-7761-0>
- Wegorzewska, I., Bell, S., Cairns, N. J., Miller, T. M., & Baloh, R. H. (2009). TDP-43 mutant transgenic mice develop features of ALS and frontotemporal lobar degeneration.

Proceedings of the National Academy of Sciences of the United States of America,
106(44), 18809–18814. <https://doi.org/10.1073/pnas.0908767106>

White, M. A., Kim, E., Duffy, A., Adalbert, R., Phillips, B. U., Peters, O. M., Stephenson, J., Yang, S., Massenzio, F., Lin, Z., Andrews, S., Segonds-Pichon, A., Metterville, J., Saksida, L. M., Mead, R., Ribchester, R. R., Barhomi, Y., Serre, T., Coleman, M. P., ... Sreedharan, J. (2018). TDP-43 gains function due to perturbed autoregulation in a Tardbp knock-in mouse model of ALS-FTD. *Nature Neuroscience*, 21(4), 552–563.
<https://doi.org/10.1038/s41593-018-0113-5>

Wils, H., Kleinberger, G., Janssens, J., Pereson, S., Joris, G., Cuijt, I., Smits, V., Ceuterick-de Groote, C., Van Broeckhoven, C., & Kumar-Singh, S. (2010). TDP-43 transgenic mice develop spastic paralysis and neuronal inclusions characteristic of ALS and frontotemporal lobar degeneration. *Proceedings of the National Academy of Sciences*, 107(8), 3858–3863. <https://doi.org/10.1073/pnas.0912417107>

Wilson, R. S., Yu, L., Trojanowski, J. Q., Chen, E.-Y., Boyle, P. A., Bennett, D. A., & Schneider, J. A. (2013). TDP-43 pathology, cognitive decline, and dementia in old age. *JAMA Neurology*, 70(11), 1418–1424. <https://doi.org/10.1001/jamaneurol.2013.3961>

Wolozin, B. (2019). The Evolution of Phase-Separated TDP-43 in Stress. *Neuron*, 102(2), 265–267. <https://doi.org/10.1016/j.neuron.2019.03.041>

Woolley, S. C., & Strong, M. J. (2015). Frontotemporal Dysfunction and Dementia in Amyotrophic Lateral Sclerosis. *Neurologic Clinics*, 33(4), 787–805.
<https://doi.org/10.1016/j.ncl.2015.07.011>

- Xu, Y.-F., Gendron, T. F., Zhang, Y.-J., Lin, W.-L., D'Alton, S., Sheng, H., Casey, M. C., Tong, J., Knight, J., Yu, X., Rademakers, R., Boylan, K., Hutton, M., McGowan, E., Dickson, D. W., Lewis, J., & Petrucelli, L. (2010). Wild-type human TDP-43 expression causes TDP-43 phosphorylation, mitochondrial aggregation, motor deficits, and early mortality in transgenic mice. *The Journal of Neuroscience: The Official Journal of the Society for Neuroscience*, *30*(32), 10851–10859. <https://doi.org/10.1523/JNEUROSCI.1630-10.2010>
- Xu, Y.-F., Zhang, Y.-J., Lin, W.-L., Cao, X., Stetler, C., Dickson, D. W., Lewis, J., & Petrucelli, L. (2011). Expression of mutant TDP-43 induces neuronal dysfunction in transgenic mice. *Molecular Neurodegeneration*, *6*, 73. <https://doi.org/10.1186/1750-1326-6-73>
- Young, J. J., Lavakumar, M., Tampi, D., Balachandran, S., & Tampi, R. R. (2018). Frontotemporal dementia: Latest evidence and clinical implications. *Therapeutic Advances in Psychopharmacology*, *8*(1), 33–48. <https://doi.org/10.1177/2045125317739818>
- Zakzanis, K. K. (1998). Neurocognitive deficit in fronto-temporal dementia. *Neuropsychiatry, Neuropsychology, and Behavioral Neurology*, *11*(3), 127–135.
- Zamboni, G., Huey, E. D., Krueger, F., Nichelli, P. F., & Grafman, J. (2008). Apathy and disinhibition in frontotemporal dementia: Insights into their neural correlates. *Neurology*, *71*(10), 736–742. <https://doi.org/10.1212/01.wnl.0000324920.96835.95>

Curriculum Vitae

Keon Coleman

Education

Juris Doctor – Single J.D. Program **2020 – Present**

Windsor University

Windsor, Ontario

Master’s of Science – Neuroscience

2018 – Present

Western University

London, Ontario

- **Neuroscience Research Project:** Investigating Cognitive Impairment in TDP-43 Mouse Models of FTD-ALS Using Automated Touchscreens
- **Research Project Supervisor:** Dr. Timothy Bussey & Flavio Beraldo, Western University

Honours Bachelor of Arts – Psychology, Minor – Neuroscience

2013 – 2017

University of Guelph

Guelph, Ontario

- **Neuroscience Research Project:** Investigating the Role of Cholinergic Activity in Mice for Multi-Sensory Object Perception
- **Research Project Supervisor:** Dr. Boyer Winters, University of Guelph

Honors

University of Guelph

Guelph, Ontario

- Dean’s List, College of Arts and Sciences

2017

Research Experience

Investigating Cognitive Impairment in TDP-43 Mouse Models of FTD/ALS Using

Automated Touchscreens

2018 – Present

Western University,

London, Ontario

Multi-Sensory Integration Neuroscience Research Project

2016 – 2017

University of Guelph,

Guelph, Ontario

Research Assistant to Krista Mitchnick, PhD

University of Guelph,

2016 – 2017

Guelph, Ontario

Conference Talks

Coleman, K., Lim, M-P., Cowan, M. F., Prado, V. F., Prado, M. A. M., Bussey, T. J., Beraldo. F. H (2019, June). Automated Touchscreen Tasks Reveal Early Cognitive Dysfunction in Parkinson's Disease Mouse Models of Alpha-Synucleinopathy. Presented at International Touchscreen Symposium, BrainsCAN Rodent Cognition Core Western University.

Coleman, K., Franco, R. D., Cowan, M. F., Joviano, J., Rylett, J. R., Prado, V. F., Saksida, L. M., Prado, M. A. M., Bussey, T. J., Beraldo. F. H (2019, June). Investigating Cognitive Impairment in TDP-43 Mouse Models of FTD/ALS Using Automated Touchscreens. Presented at International Touchscreen Symposium, BrainsCAN Rodent Cognition Core Western University.

Poster Presentations

Coleman, K., Franco, R. D., Cowan, M. F., Joviano, J., Rylett, J. R., Prado, V. F., Saksida, L. M., Prado, M. A. M., Bussey, T. J., Beraldo. F. H (2019, May). Investigating Cognitive Impairment in TDP-43 Mouse Models of FTD/ALS Using Automated Touchscreens. Presented at Canadian ALS Forum, London Health Research Day, Southern Ontario Neuroscience Association.

Work Experience**Proctor - Psychology**

Western University

2018 – 2020

London, Ontario